Dissertation

submitted to the

Combined Faculties for the Natural Sciences and for Mathematics

of the Ruperto-Carola University of Heidelberg, Germany

for the degree of

Doctor of Natural Sciences

presented by

Diplom-biotechnologin Elodie Kleinmann

born in: Strasbourg, France

Oral-examination: March 2nd 2009

Evaluation of cytokine-transducing parvoviral vectors for glioma therapy

Referees: **Dr. Anne Régnier-Vigouroux**

                         Prof. Dr. Lutz Gissmann

ACKNOLEDGMENTS

SUMMARY

Malignant gliomas are the most frequent primary brain tumors in adults and have a poor prognosis, despite advances in the conventional treatment involving neurosurgery, followed by radiation- and chemotherapy. Hence, there is a great need for the development of novel therapeutic approaches. Gene therapy based on viral vectors represents an interesting alternative or adjuvant to conventional cancer therapies. The oncotropic and oncolytic properties of rodent autonomous parvoviruses, together with their low pathogenicity make them particularly attractive candidates as viral vectors for cancer gene therapy.

Gliomas are highly vascularized tumors that induce a strong immunosuppressive environment. Therefore, our laboratory has recently investigated the antitumor effects of parvoviral vectors delivering human interferon inducible protein-10 (hIP-10) and mouse tumor necrosis factor-α (mTNF-α), cytokines known to have both immunostimulatory and antiangiogenic properties, in a syngeneic mouse glioma model. These recombinant viruses strongly inhibited the growth of murine GL261 glioma cells grafted subcutaneously in immunocompetent mice. Complete tumor regression was observed when glioma cells were coinfected with both vectors, demonstrating synergistic antitumor effects (Enderlin et al., 2008).

In the present study, the mechanisms sustaining subcutaneous tumor inhibition by TNF-α- and IP-10-encoding parvoviral vectors were investigated. Parvoviral-transduced TNF-α increased the mRNA expression and protein secretion of endogenous IP-10 in GL261 cells *in vitro*. When both viruses were used in combination, the IP-10 levels may thus reach a critical threshold that could account for the synergistic antitumor effects observed *in vivo*. The analysis of the cellular immune response upon peritumoral injections of recombinant parvoviruses in established subcutaneous GL261 tumors showed a decreased infiltration of CD4^{+} and CD8^{+} T lymphocytes compared to PBS-treated tumors. More strikingly, the infiltration of CD4^{+} T lymphocytes was dramatically decreased in tumors treated with cytokine-encoding vectors and inversely correlated with the tumor growth *in vivo*. We hypothesize that the antitumor effects could be due to a decrease of CD4^{+} T regulatory cells, known to suppress immune responses. In agreement with this, we could show that *in vitro* infection of GL261 cells with cytokine-

encoding vectors led to a decrease of TGF-β that strongly correlated with the infiltration of CD4$^+$ T cells.

Next, the antitumor effects of parvoviral vectors transducing mTNF-α and hIP-10 were investigated on GL261 implanted intracranially in syngeneic C57BL/6 mice. The tumor growth and survival of mice implanted with GL261 cells *in vitro* infected with parvoviral vectors were monitored. Wild-type parvovirus and the vector devoid of transgene had only a slight antitumor effect, similarly to the results obtained subcutaneously. In contrast, in the intracranial setting, TNF-α-, but not IP-10-encoding vector significantly delayed the tumor growth of GL261 glioma and prolonged the survival of tumor-bearing mice. No synergy between TNF-α and IP-10 could be observed in this setting. Immunohistochemical analysis on brain tumor samples showed that parvoviral infection induced a moderate infiltration of CD4$^+$ and CD8$^+$ T lymphocytes. The TNF-α-transducing parvoviral vector decreased tumor microvascularization as well as the infiltration of CD68$^+$ macrophages/microglia, and these effects are likely responsible for the antitumor effects observed.

The monocyte chemotactic protein (MCP)-2 and -3 are known to be potent immunoactive cytokines, recruiting a broad range of leukocytes. Parvoviral vectors delivering MCP-3 were shown to inhibit the tumor growth in several animal tumor models. This prompted us to compare the effects of parvoviruses delivering MCP-2 and MCP-3 in the GL261 intracranial glioma model to those obtained with parvoviral vectors transducing TNF-α and IP-10. No effects on tumor growth and animal survival could be observed, suggesting a possible processing of MCP-2 and MCP-3 by GL261 cells, leading to their inactivation.

ZUSAMMENFASSUNG

Maligne Gliome sind die am häufigsten bei Erwachsenen auftretenden Hirntumor. Trotz großer Fortschritte in der konventionellen Behandlung, die aus Neurochirurgie, gefolgt von Strahlen- und Chemotherapie besteht, haben maligne Gliome eine sehr schlechte Prognose. Daher bedarf es dringend einer Entwicklung neuer therapeutischer Ansätze. Die virale Gentherapie stellt eine interessante Alternative oder auch Adjuvans zur konventionellen Krebstherapie dar. Die autonomen Nagetierparvoviren sind aufgrund ihrer onkotropischen und onkolytischen Eigenschaften, sowie ihrer niedrigen Pathogenität besonders attraktive Kandidaten für die Entwicklung viraler Vektoren für die Gentherapie gegen Krebs.

Gliome sind hochvaskularisierte Tumore, die ein stark immunsuppressives Milieu erzeugen. Daher wurde in unserem Labor vor kurzem die antitumoralen Effekte parvoviraler Vektoren, die das humane Interferon-γ-induzierte Protein-10 (hIP-10) und den murinen Tumornekrosefaktor-α (mTNF-α) transduzieren, in einem syngenen, murinen Gliom-Modell untersucht. IP-10 und TNF-α sind Zytokine, die für ihre immunostimulatorischen und antiangiogenischen Eigenschaften bekannt sind. Diese rekombinanten Viren konnten das Wachstum von murinen GL261-Gliomzellen, die subkutan in immunkompetente Mäuse appliziert wurden, signifikant hemmen. Die Koinfektion der Gliomzellen mit beiden Vektoren führte zu einer kompletten Tumorregression, was auf einen synergistischen antitumoralen Effekt schließen lässt (Enderlin et al., 2008).

In der vorliegenden Arbeit wurden die Mechanismen, die zu einer Hemmung des Tumorwachstums durch TNF-α- und IP-10-kodierende parvovirale Vektoren führten, untersucht. Parvoviral transduziertes TNF-α verstärkte die mRNA-Expression und Proteinsekretion von endogenem IP-10 in GL261-Zellen *in vitro*. Die Kombination von beiden Viren könnte auf diese Weise in IP-10-Mengen resultieren, die oberhalb eines kritischen Schwellenwertes liegen und so zu den *in vivo* beobachteten synergistischen antitumoralen Effekten führen. Die Analyse der zellulären Immunantwort nach peritumoraler Applikation der rekombinanten Parvoviren in etablierte, subkutane GL261 Tumore zeigte eine verringerte Tumorinfiltration von CD4^{+} und CD8^{+} T-Lymphozyten im Vergleich zu PBS behandelten Tumoren. Auffallend war die drastisch verringerte Tumorinfiltration von CD4^{+} T-Lymphozyten durch die Behandlung mit den Zytokin-

kodierenden Vektoren, die mit dem Tumorwachstum *in vivo* umgekehrt korrelierte. Wir vermuten, dass die antitumoralen Effekte auf einer Verringerung der CD4$^+$ regulatorischen T-Zellen beruhen, welche eine Suppression von Immunantworten verursachen. Zudem konnten wir zeigen, dass die *in vitro* Infektion von GL261-Zellen mit Zytokin-kodierenden Vektoren zu einer Verringerung an TGF-β führte, welche stark mit der Infiltration von CD4$^+$ T-Lymphozyten korrelierte.

Desweiteren wurden die antitumoralen Effekte der mTNF-α- und hIP-10-transduzierenden parvoviralen Vektoren auf GL261-Zellen untersucht, die intrakranial in syngene C57BL/6 Mäuse implantiert wurden. Hierzu wurden das Tumorwachstum der mit parvoviralen Vektoren präinfizierten GL261-Zellen sowie die Überlebensrate der behandelten Mäuse beobachtet. Wildtyp Parvovirus und der virale Vektor ohne Transgen zeigten nur einen schwachen antitumoralen Effekt. Dies gleicht den Resultaten aus dem subkutanen Tumorversuch. Im Gegensatz hierzu, konnte TNF-α-, jedoch nicht IP-10-kodierende parvovirale Vektoren im intrakranial Tierversuch zu einer signifikanten Verzögerung des Tumorwachstums der GL261 Gliome sowie zu einem verlängerten Überleben der tumortragenden Mäuse führen. Zudem wurde kein synergistischer Effekt zwischen TNF-α und IP-10 beobachtet. Immunohistochemische Untersuchungen der Hirntumorproben zeigten, dass die parvovirale Infektion zu einer mäßigen Infiltration von CD4$^+$ und CD8$^+$ T-Lymphozyten führte. Der TNF-α-transduzierende parvovirale Vektor verringerte die Vaskularisierung des Tumors und die Infiltration von CD68$^+$ Makrophagen/Mikroglia. Dies scheint für die beobachteten antitumoralen Effekte verantwortlich zu sein.

Die Monozyten chemotaktisches Proteine (MCP)-2 und -3 sind potente immunaktive Zytokine, die eine Vielzahl an Leukozyten rekrutieren. Es konnte gezeigt werden, dass MCP-3-transduzierende parvovirale Vektoren das Tumorwachstum in verschiedenen Tiermodellen hemmen. Dies veranlasste uns die Effekte von MCP-2- und MCP-3-transduzierenden vektoren im intrakranialen GL261-Gliom-Modell mit denen von TNF-α und IP-10 zu vergleichen. Es konnten jedoch keine Effekte auf Tumorwachstum und Überlebensrate beobachtet werden. Wir vermuten, dass MCP-2 und MCP-3 in den GL261-Zellen prozessiert werden, was zu ihrer Inaktivierung führt.

TABLE OF CONTENTS

TABLE OF CONTENTS

1. INTRODUCTION

1.1. Gliomas

Gliomas are primary tumors of the central nervous system (CNS), originating from glial cells or their precursors. They are classified according to the glial cell types that predominate in the tumor mass as astrocytomas, oligodendrogliomas, mixed oligoastrocytomas and ependymomas. Gliomas are graded by the World Health Organization (WHO) on a scale from I to IV, based on the degree of malignancy, as determined by histopathological and genetic features. Astrocytomas are the most frequent intracranial neoplasm and account for more than 75% of all gliomas (CBTRUS, 2004). They are graded as pilocytic astrocytomas (grade I, non malignant), diffuse astrocytomas (grade II, non malignant), anaplastic astrocytomas (grade III, malignant) and glioblastoma multiforme (GBM) (grade IV, malignant) (Louis et al., 2007). GBM is the most aggressive and most prevalent type of glioma (Louis et al., 2002). It accounts for 20% of all primary brain tumors and occurs at a frequency of about 5 cases per 100 000 people (CBTRUS, 2004). GBMs typically affect adults and are preferentially located in the cerebral hemispheres. They are further subdivided into primary and secondary subtypes, based on the clinical presentation. Whereas primary GBMs develop de novo without antecedent history, secondary GBMs show evidence of malignant progression from previously diagnosed lower grade tumors (Kleihues and Ohgaki, 1999). Despite their distinct clinical histories, primary and secondary GBM have indistinguishable histopathologies and their prognosis is not significantly different.

The main histopathological features of GBMs include aggressive growth, highly infiltrative properties, potent immunosuppression, and prominent vascularization (Brandes et al., 2008). These properties together with their anatomic location make malignant gliomas very challenging tumors to treat. Despite recent advances in the conventional treatment, involving surgery followed by adjuvant radio-and chemotherapy, the prognosis of patient with malignant gliomas remain poor, especially for GBM, with a median survival of less than a year after diagnosis (Stupp et al., 2005a). Thus, there is a great need for new therapeutics and gene therapy is emerging as a promising alternative to supplement the conventional therapies.

1.2. Glioma therapy

1.2.1. Conventional treatment strategies

The current standard treatment for gliomas involves surgical resection followed by adjuvant radiation therapy and chemotherapy.

1.2.1.1 Surgery

Surgery is commonly the initial therapeutic modality for newly diagnosed gliomas (Hsieh and Lesniak, 2005; Stupp et al., 2005b). The aim is to achieve maximum resection without causing any neurological defects. Despite improved surgical techniques, complete resection of the tumor is often hampered by the absence of defined tumor edges or localization of the tumor in critical areas of the brain. Even after apparent complete removal, there are almost invariably residual tumor cells infiltrated beyond the tumor margin defined and local recurrence is almost inevitable. Yet, tumor resection, even partial, relieves the increased intracranial pressure and improves the response to post-operative adjuvant treatments through disruption of the blood brain barrier (BBB). Biopsies are performed for inoperable tumors, providing histological confirmation of the diagnosis, required prior to alternative radiation or chemotherapy.

1.2.1.2 Radiotherapy

Post-operative radiation therapy has been shown to prolong the median survival of patients with glioblastomas and is the standard adjuvant therapy for high-grade gliomas after resection or biopsy (Fiveash and Spencer, 2003; Laperriere et al., 2002). The current treatment protocol involves conventional fractionated external-beam radiotherapy to total a dose of 60 Gy delivered in 30 daily fractions of 2 Gy. To limit irradiation of normal brain tissue, radiations are directed to a localized volume including the tumor bed and a 2-5 cm margin, where recurrence occurs in most of the cases (Brada, 2006). The main limitation to brain tumor radiotherapy is the radiation tolerance of normal brain tissue. Therefore, new techniques were developed to deliver more precise and higher dose of radiation, such as hyper-fractionation, stereotactic surgery or radiation sensitizers. However, until now, these alternative radiotherapies failed to demonstrate a survival benefit compared with conventional fractionated radiation therapy (Brada, 2006; Laperriere et al., 2002).

1.2.1.3 Chemotherapy

Despite treatment of malignant gliomas with surgery followed by radiotherapy, most of the tumors recur and therefore additional therapies are required. Chemotherapy is currently a standard modality of treatment for gliomas, used either during or after radiotherapy. The most commonly used agents for glioma therapy are alkalyting agents including nitrosoureas (carmustine, lomustine), platinium-based drugs (cisplatin, carboplatin) and more recently temozolomide (Lonardi et al., 2005). The main limitations of chemotherapy are the blood-brain barrier and the development of chemorestistant cells within the tumor. The latter can be overcome through combination of multiple types of antitumoral drugs. The most common drug combination is the nitrosourea-based regime of procarbazine, lomustine, and vincristine (Stupp et al., 2005a). Nitrosoureas were long considered as the standard chemotherapy approach for malignant gliomas. However, their toxicity is not negligible and clinical studies have failed to demonstrate significant evidence of their benefits on patient survival (Lonardi et al., 2005; Stupp et al., 2005a). In contrast, concomitant and adjuvant chemotherapy with temozolomide was recently shown to increase patient survival with minimal additional toxicity, and has therefore become the standard treatment for newly diagnosed glioblastoma (Stupp et al., 2005a).

Even after surgery followed by adjuvant radio- and chemotherapies, local recurrence occurs in more than 80% of the patients (Lonardi et al., 2005). The prognosis of patients with malignant gliomas remains poor, with a median survival of approximately one year after initial diagnosis (Stupp et al., 2005a).

1.2.2. Gene therapy of glioma

Gene therapy is defined as the transfer of engineered genetic material into cells for therapeutic purpose. Malignant gliomas remain mostly refractory to conventional therapies and therefore represent attractive targets for gene therapy. Moreover, their localization in an anatomically restricted area should allow local delivery of gene therapy vehicles without the risk of severe systemic toxicity.

Currently there are two main approaches for gene transfer in the CNS, referred as *in vivo* and *ex vivo* strategies. In the *in vivo* approach, the genetic material is directly delivered into the target cells, either by systemic or local delivery into the brain. In the *ex*

vivo approach, the target cells are first removed from the patient, genetically modified by gene transfer in the laboratory, and subsequently re-implanted into the host.

1.2.2.1 Gene therapy approaches

Several gene therapy strategies were developed for malignant gliomas, including direct killing of tumor cells by correction of genetic defects, suicide genes, suppression of angiogenesis and immunotherapy.

1.2.2.1.1 Correction of genetic defects

This strategy, also referred to as replacement gene strategy, intends to transfer specific genes that are mutated or deleted in patients, such as tumor suppressor genes. Inactivation of p53, Rb and p16 suppressor genes is commonly found in glioma tumors, leading to a loss of cell cycle control. In this context, adenoviral vectors encoding wild-type p53, p16 or Rb were evaluated in preclinical studies and were shown to inhibit glioma tumor growth both *in vitro* and *in vivo* (Chintala et al., 1997; Fueyo et al., 2000; Kock et al., 1996). Adenoviral vectors delivering p53 were further evaluated in a phase I clinical study in patients with glioblastoma. Although p53 transfer was observed in tumor cells, the effect was limited to a short distance from the injection site (Lang et al., 2003).

1.2.2.1.2 Suicide genes: prodrug activating enzymes

This approach involves the gene transfer of an enzyme which converts a prodrug, normally innocuous, into a toxic compound leading to cell death. Most of the gene therapy trials for malignant gliomas have been based on the delivery of the herpes simplex virus - thymidine kinase (HSV-TK) followed by systemic administration of the prodrug ganciclovir (GVC). The HSV-TK enzyme activates GCV, which in turns inhibits DNA synthesis and leads to cell death. Retroviral as well as adenoviral vectors encoding HSV-TK were tested both in preclinical and clinical studies of gliomas (reviewed in Aghi and Chiocca, 2006). Adenoviral vectors were found to be more effective compared to retroviral vectors and this could be assigned to the higher transduction efficiency of adenoviral vectors in human glioma cells (Sandmair et al., 2000). Furthermore, there is a risk of insertional mutagenesis with retroviruses. However, the survival increase with adenoviral vectors was in most clinical trials non-significant compared with the standard treatment (Aghi and Chiocca, 2006).

1.2.2.1.3 Suppression of angiogenesis

Malignant gliomas are among the most highly vascularized tumors and thus angiogenesis represents an attractive therapeutic target. Two main strategies have been tested, namely the inhibition of endogenous angiogenic factors, and the delivery of natural antiangiogenic agents. Vascular endothelial growth factor (VEGF) and its receptors seem to be the central signaling pathway in glioma angiogenesis, but other pathways were also identified, involving for instance fibroblast growth factor (FGF) or epidermal growth factor (EGF). Inhibition of these pathways in glioma resulted in a reduced tumor vascularization and tumor growth in animal models (Tuettenberg et al., 2006). Several antiangiogenic molecules have also shown antitumor effect in preclinical studies including angiostatin (Ma et al., 2002), endostatin (Peroulis et al., 2002) and platelet factor-4 (Bikfalvi, 2004). The results of preclinical studies are very encouraging and several clinical trials in glioma patients are ongoing using antiangiogenic molecules. Up to now, the most widely antiangiogenic molecules evaluated in clinical trials for malignant gliomas have been thalidomide, known to inhibit VEGF- and FGF-mediated angiogenesis and interferon (IFN)-α and -β, known to suppress FGF expression. However, both drugs gave variable results and induced severe side effects (Tuettenberg et al., 2006).

1.2.2.1.4 Immunotherapy

This strategy aims to stimulate the immune system to mount an effective immune response against glioma cells. Gliomas create a very immunosuppressive environment and commonly escape recognition by the immune system. Thus, immunotherapy represents an attractive strategy for glioma treatment. Several approaches have been tested in preclinical and clinical studies, including the transfer of immunostimulatory cytokines, and the *ex vivo* manipulation of immune cells. The transfer of several cytokines was shown to result in significant antitumor responses in animals models including interleukin-2, -4, -12 (IL-2, IL-4, IL-12), and granulocyte macrophage-colony stimulating factor (GM-CSF) (Benitez et al., 2008; Okada and Pollack, 2004). These cytokines mainly aim to enhance the activation of T lymphocytes. Another promising approach consists in the *ex vivo* manipulation of effector cells such as T lymphocytes or especially dendritic cells (DC), normally absent from the brain parenchyma (Barzon et al., 2006).

1.2.2.2 Gene transfer vectors

To deliver the genes of interest into tumor cells, various viral and non-viral vectors were developed. Viral vectors are considered up to now as the most effective gene delivery system and are predominantly used in gene therapy trials. Most vectors are produced by replacement of one or more genes necessary for viral replication by the transgenes and are thus replication deficient.

The main viral and non-viral vectors used for gene therapy purposes in malignant gliomas have been retroviral vectors and adenoviral vectors, although liposomes were also tested. Most clinical trials have been performed using retroviral and adenoviral vectors delivering the suicide gene HSV-TK, and adenoviral vectors encoding p53 (Andreansky et al., 1996).

Although the different gene transfer methods tested in gliomas have generally been proven to be safe and well tolerated, the clinical responses were rather disappointing compared to the preclinical results. This has been mainly assigned to the inefficient transduction of tumor cells and lack of selectivity of the vectors. Thus, continuous efforts in vector engineering are required to increase the selectivity and efficiency of tumor cell transduction.

1.2.3. Oncolytic virotherapy

Oncolytic viruses are replicating viruses able to selectively infect and lyses tumor cells, either naturally or through appropriate engineering. They are either used as direct killing agent or modified to be used as gene transfer vector, thus allowing highly selective delivery in tumor cells.

Oncolytic viruses engineered from HSV type 1 (HSV-1) and adenovirus have been most intensively studied for glioma therapy, although naturally tumor-selective viruses like Newcastle disease, reovirus, poliovirus, vesicular stomatis virus and vaccinia virus are also under consideration.

Oncolytic viruses derived from HSV-1 used in clinical trials for malignant gliomas include G207 and HSV1716. Both mutants harbor deletion in the neurovirulence gene γ34.5 and are thus replication-defective in neurons but replicate efficiently in transformed cells (Harrow et al., 2004; Markert et al., 2000; Papanastassiou et al., 2002; Rampling et al., 2000). G207 and HSV1716 were tested in phase I clinical studies

in patients with malignant gliomas and gave promising results without any associated toxicity (Heise et al., 1997).

Oncolytic virotherapy of malignant glioma with oncolytic adenoviruses was conducted using ONYX-015. ONYX-015 is an adenovirus mutant deleted in the E1B gene that preferentially replicates in p53 deficient cells, thus being more selective for cancer cells (Chiocca et al., 2004). The potential efficacy and safety was evaluated in a phase I clinical trial in patient with recurrent gliomas. Although no serious side effects were observed, no significant antitumor effect could be demonstrated (Berns, 1996).

Autonomous parvoviruses are emerging as promising oncolytic viruses for cancer therapy. Indeed, they are endowed with intrinsic oncolytic but also oncotropic and oncosuppressive properties. Moreover, they show low pathogenicity in adult animals and prevalent cytotoxicity in transformed cells (Cornelis et al., 2004a).

1.3. Autonomous parvoviruses

Parvoviruses (latin *parvus* = small) are, with a diameter of approximately 20–25 nm, among the smallest, non enveloped icosahedral viruses, containing a linear single-stranded DNA genome of 4 to 6 kb and belong to the *Parvoviridae* family (Berns, 1996).

1.3.1. Taxonomy of Parvoviruses

The *Parvoviridae* family is divided into two subfamilies on the basis of their host range: the *Parvovirinae* infecting birds and mammals, and the *Densovirinae* infecting insects and other arthropods (see Figure 1-1). The *Parvovirinae* subfamily is further divided in five genera: *Parvovirus*, *Dependovirus*, *Erythrovirus*, *Amdovirus* and *Bocavirus* and includes the known human viruses such as B19 (*Erythrovirus*) and the adeno-associated viruses (AAV, *Dependovirus*). The erythrovirus B19, as well as the recently identified Human Bocavirus (HuBoca) are until now the only known human pathogenic members of the *Parvoviridea* (Anderson, 2007; Anderson et al., 1983).

Dependoviruses, with the exception of the goose (GPV) and duck parvoviruses (DPV), are so called because they require the assistance of a helper virus, adenovirus, herpes virus or vaccinia virus, for efficient replication (Berns et al., 2000; Kerr et al., 2006). In contrast, other members of the *Parvovirinae* are able to replicate independently and are commonly described as autonomous parvoviruses (Kerr et al., 2006).

Family	Subfamily	Genus	Species	Host
Parvoviridae	*Parvovirinae*	*Parvovirus*	MVM, H-1 PV, FPV, KRV, LuIIIV, MPV-1, PPV	Vertebrates
		Dependovirus	AAV, AAAV, BAAV, DPV, GPV	Vertebrates
		Erythrovirus	B19	Vertebrates
		Amdovirus	AMDV	Vertebrates
		Bocavirus	BPV-1, CnMV, HuBoca	Vertebrates
	Densovirinae	*Densovirus*	JcDNV, GmDNV	Invertebrates
		Iteravirus	BmDNV, CeDNV	Invertebrates
		Brevidensovirus	AaeDNV, AalDNV	Invertebrates
		Pefudensovirus	PfDNV	Invertebrates

Figure 1-1: Taxonomy of the *Parvoviridae* family

MVM: *Minute Virus of Mice*; H-1 PV: *H-1 parvovirus*; FPV: *Feline panleukopenia virus*; KRV: *Kilham rat virus*; LuIIIV: *LuIII virus*; MPV-1: *Mouse parvovirus 1*; PPV: *Porcine parvovirus*; AAV: *Adeno-associated virus*; AAAV: *Avian adeno-associated virus*; BAAV: *Bovine adeno-associated virus*; DPV: *Duck parvovirus*; GPV: *Goose parvovirus*; B19: *B19 virus*; AMDV: *Aleutian mink disease virus*; BPV-1: *Bovine parvovirus type 1*; CnMV: *Canine minute virus*; HuBoca: *Human bocavirus*; JcDNV: *Junonia coenia densovirus*; GmDNV: *Galleria mellonella densovirus*; BmDNV: *Bombyx mori densovirus*; CeDNV: *Casphalia extranea densovirus*; AaeDNV: *aedes aegypti densovirus*; AalDNV: *Aedes albopictus densovirus*; PfDNV: *Periplaneta fuliginosa densovirus*. (Adapted from Kerr et al., 2006)

The *Parvovirus* genus contains three distinct subgroups based on host range: *Feline panleukopenia virus* (FPV), *Porcine parvovirus* (PPV), and rodent viruses species including a mouse virus group with *Minute Virus of Mice* (MVM), and *Mouse parvovirus 1* (MPV-1), as well as a rat virus group with *H-1 virus* (H-1 PV), *Kilham rat virus* (KRV), and *LuIII virus* (LuIIIV).

MVM comprises two strains, the immunosuppressive (MVMi) strain and the prototype (MVMp) strain, used in this study. Although they are very similar, with only 3% divergence in their genome (Sahli et al., 1985), both strains display different *in vitro* tropism and *in vivo* pathogenicity. Whereas MVMp replicates *in vitro* preferentially in mouse fibroblast cell lines, MVMi replication is restricted to mouse T lymphocytes and hematopoietic precursors (Segovia et al., 1991). The two strains are therefore also commonly named fibrotropic or prototype (MVMp) and lymphohematotropic (MVMi). *In vivo*, MVMp infection of newborn mice is asymptomatic, while MVMi infection leads to severe growth retardation or death (Kimsey et al., 1986).

In this study, the parvoviral vectors used are based on the MVM prototype strain MVMp and are referred as MVMp-based vectors.

1.3.2. Organization of the parvoviral genome

Parvoviruses are composed of a small, linear, single-stranded DNA genome (minus strand) of approximately 5 kb, flanked at both ends by palindromic hairpins (Berns, 1996). The genomic organization of MVM together with the corresponding transcripts and proteins are illustrated in Figure 1-2.
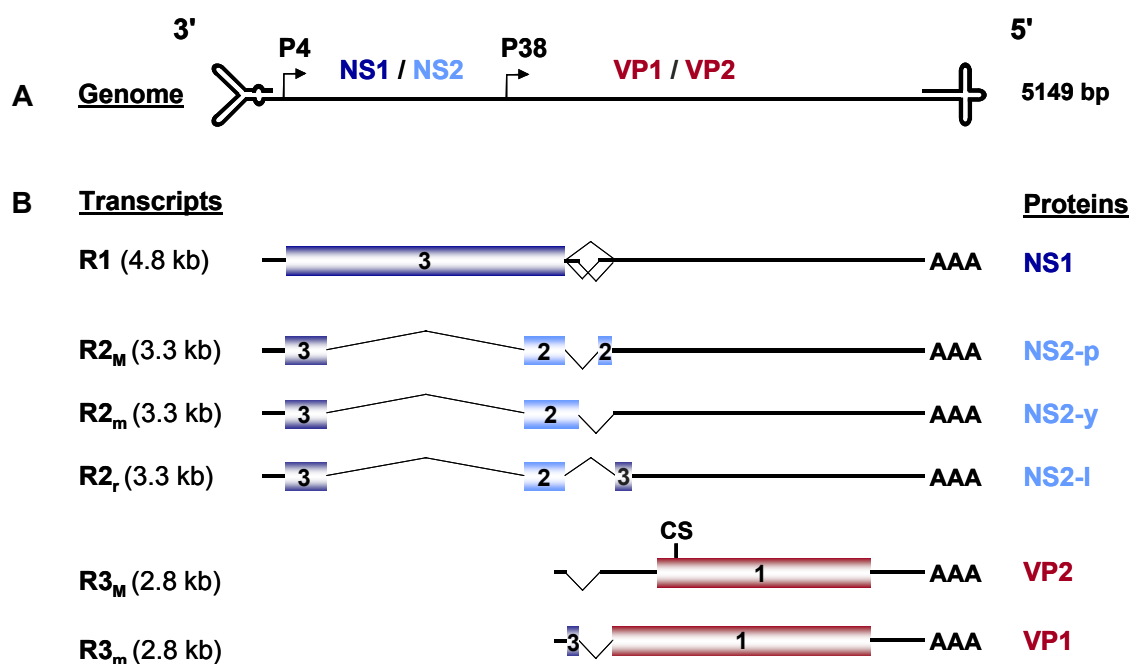
Figure 1-2: Genomic organization and transcription map of MVM

A. Line diagram of the MVM genome showing the coding sequence and terminal hairpins. The position of the early promoter P4, driving the expression of the viral non-structural proteins (NS 1/2) and of the late promoter P38, driving the expression of the viral capsid proteins (VP 1/2) is indicated by the arrows. **B.** Schematic representation of MVM transcripts and corresponding proteins. The three transcripts classes (R1, R2, R3) are represented with their frequency (M: major, m: minor, r: rare) and size. The encoded proteins are listed on the right of each transcript. The large (1 and 3) and small (2) open reading frames are depicted together with their respective splicing sites (vertical caret), as well as Poly (A) tail (AAA), and eventual cleavage site (CS).

The viral genome contains two large overlapping transcription units (Bodendorf et al., 1999) controlled by two distinct promoters: the early promoter P4 and the late promoter P38, driving respectively the expression of viral non-structural (NS) and capsid (VP) proteins (Pintel et al., 1983). Three major mRNA species, R1, R2 and R3 are produced, all terminating at a single common polyadenylation site at the right end of the genome (Clemens and Pintel, 1987). Transcription of the left unit, under the control of P4, produces two classes of mRNAs transcripts, R1 and R2, which are alternatively spliced. While R1 encodes the non-structural proteins NS1, the $R2_M$, $R2_m$ and $R2_r$ splice

variants code respectively for the NS2-p, -y, and -l isoforms. Transcription of right unit, under the control of P38, produces one mRNA transcript R3, and its two splice variants $R3_M$ and $R3_m$ code for the viral proteins VP1 and VP2. VP3 is produced by proteolytic cleavage of VP2. While the viral P4 promoter has a strong and constitutive activity, P38 promoter activity is conditional and depends on NS1 for its transactivation (Rhode, 1985).

1.3.3. Parvoviral Proteins

1.3.3.1 Non-structural proteins

NS1 is a 83 kDa nuclear phosphoprotein, involved in viral DNA replication, transactivation of the P38 promoter and parvoviral-mediated cytotoxicity (Li and Rhode, 1990). NS1 is essential for the viral replication and exerts its functions through helicase, adenosine triphosphatase (ATPase), nickase, endonuclease activities and site-specific DNA binding properties (Cotmore et al., 1995; Wilson et al., 1991). NS1 binding sites are reiterated at multiple sites throughout the viral genome, including the viral DNA replication origins and the transactivating region (TAR) upstream of the P38 promoter. Upon binding to the TAR region, NS1, endowed with a transcriptional activation domain, upregulates transcription from the P38 promoter, and thus stimulates the expression of viral capsid genes (Rhode, 1985). Besides its functions in viral replication and transcription, NS1 exerts cytotoxic properties and is considered as the major mediator of parvovirus-induced cytotoxicity (Caillet-Fauquet et al., 1990; Li and Rhode, 1990). However, the mechanisms of NS1-mediated cytotoxicity remain elusive. NS1 oligomerization, as well as phosphorylation were shown to be essential for both the replicative and cytotoxic functions of NS1 (Corbau et al., 2000; Li and Rhode, 1990; Nuesch et al., 1998).

NS2 is a 25 kDa phosphoprotein, predominantly cytoplasmic, present in three different isoforms (p, y, l). While MVM NS2 is required for a productive infection in its natural host, it seems to be non-essential in cells from other species (Naeger et al., 1990). In murine cells, NS2 appears to influence various steps of the parvovirus life-cycle including synthesis of DNA replication forms, capsid assembly (Cotmore et al., 1997) and efficient nuclear egress of progeny virions (Eichwald et al., 2002). NS2 might also be implied in parvoviral cytotoxicity (Brandenburger et al., 1990). The mechanism of

action of NS2 remains unclear. NS2 was shown to interact with different proteins, including proteins of the 14-3-3 family (Brockhaus et al., 1996), the survival motor neuron protein (SMN) (Young et al., 2002) and the chromosome region maintenance protein 1 (CRM1) (Bodendorf et al., 1999). The interaction between NS2 and CRM1 was shown to be essential for active nuclear export of NS2 and viral egress from the nucleus (Eichwald et al., 2002; Miller and Pintel, 2002). Up to now, no distinct function could be attributed to the different NS2 isoforms.

Recently, a novel non-structural protein was identified in the genus *Parvovirus*, termed SAT, for small alternatively translated protein. The SAT protein is translated from a small open reading frame (ORF) located at the 5' end of the VP2 ORF, highly conserved in the genome of all members of the *Parvovirus* genus. The SAT protein is a late non-structural protein, expressed from the VP2 mRNA. The role of the SAT protein remains elusive but its localization in the endoplasmic reticulum (ER) in *porcine parvovirus* suggests that SAT could mediate immune evasion by blocking major histocompatibility complex (MHC) type I processing or induce cell death pathways through ER stress as previously shown for other viral proteins localized in the ER (Zadori et al., 2005).

1.3.3.2 Viral capsid proteins

Parvoviral capsid proteins include VP1 (83 kDa), VP2 (64 kDa) and VP3 (60 kDa). While VP1 and VP2 constitute the majority of capsid proteins, both in empty and full capsid, VP3 is only found in DNA-containing capsids (Cotmore and Tattersall, 1987). Viral capsid proteins VP1 and VP2 are both endowed with unusual nuclear import signals and are translocated as oligomeres via nuclear pore complexes into the nucleus, where capsid assembly occurs (Lombardo et al., 2002). Besides its nuclear import signal, VP2 harbors also a nuclear export signal, required for the nuclear export of full particles (Maroto et al., 2004). While VP2 is sufficient for empty capsid assembly and virus binding to the host cell receptor, VP1 is required for a productive infection (Tullis et al., 1993). This is possibly owing to N-terminal VP1 phospholipase A_2 (PLA_2) activity, required for the transport of virions and/or viral DNA from the late endosomes to the nucleus (Zadori et al., 2001).

1.3.4. Parvoviral Life cycle

Parvoviral infection begins with adsorption of the virus particle to specific cell surface receptors. Some cellular receptors of parvoviruses have been identified, including the erythrocyte P antigen globoside for B19 (Brown et al., 1993) and transferring receptors for the related canine (CPV) and feline (FPV) parvoviruses (Parker et al., 2001). The cellular receptors of MVM and H-1 remain unknown, but their sensitivity to neuraminidase and trypsin treatment favors N-acetyl neuraminic (sialyl) containing glycoproteins (Cotmore and Tattersall, 1987). Upon adsorption, parvoviruses are internalized by receptor-mediated endocytosis, most likely through clathrin-mediated endocytosis (Vihinen-Ranta et al., 2004), as shown for CPV (Suikkanen et al., 2002). The viral particles are then transported via several endosomal compartments, early toward late, to perinuclear compartments (Cotmore and Tattersall, 2007; Ros et al., 2002). The endosomal acidification was shown to be essential for MVMp infection (Ros et al., 2002), inducing major rearrangements of the viral capsid necessary for nuclear entry in particular the externalization of the VP1 N-terminal sequence, and the cleavage of an exposed VP2 N-terminal sequence (Mani et al., 2006). The mechanisms implied in the transfer of viral DNA and/or viral particles from the endosomal compartments to the nucleus remain unclear but evidence suggests the implication of N-terminal VP1 PLA$_2$ activity (Zadori et al., 2001). In the nucleus, the viral single-stranded DNA is converted into a double-stranded monomeric replicative form, using the right-end palindromic hairpin as template to initiate DNA replication by the host cell polymerase (Berns, 1996). The conversion depends strictly on cellular factors transiently expressed during the S phase of the cell cycle such as cyclin A (Bashir et al., 2001). Thus, autonomous parvoviruses can only replicate in proliferating cells. Infection of resting cells leads to a latent infection, delayed until the host cells enter the S phase (Deleu et al., 1999). The monomeric replicative form is further amplified in multimeric intermediates and serves as template for the synthesis of viral mRNAs and progeny single-stranded DNA, which is then encapsidated in newly assembled capsids (Berns, 1996; Cotmore and Tattersall, 1987). The viral life cycle ends in permissive cells with the release of progeny virions, usually associated with cell death. The parvoviral life cycle is schematically represented in Figure 1-3.
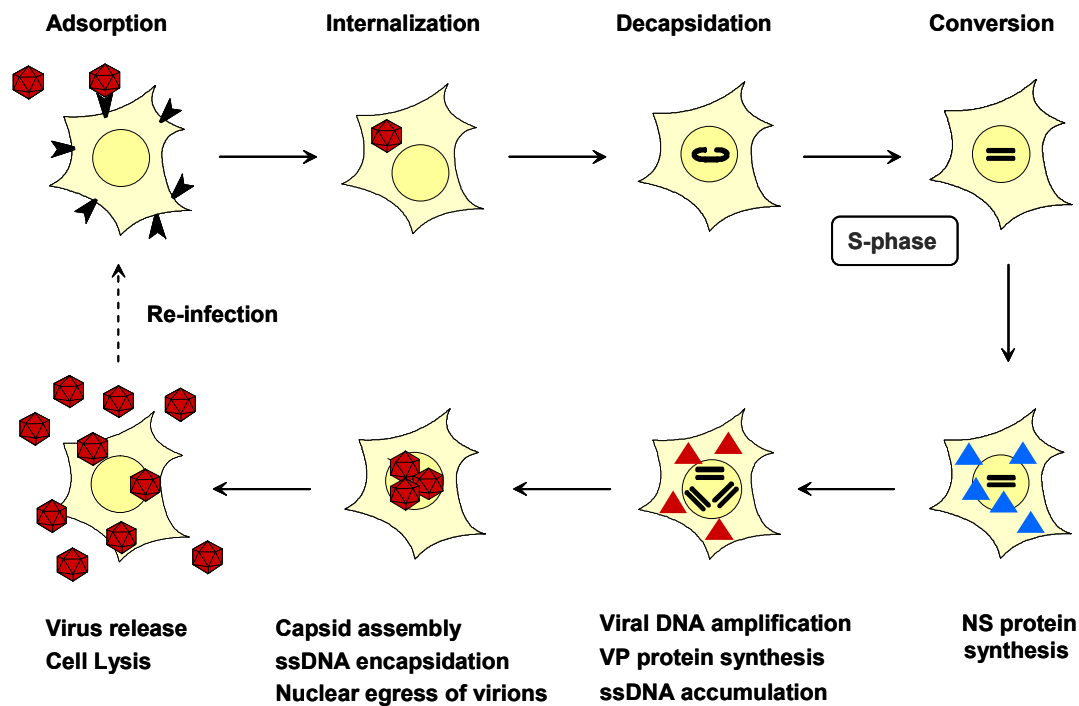
Figure 1-3: The parvoviral life cycle

1.3.5. Oncosuppressive properties of rodent parvoviruses

Originally isolated from tumor cells or tumor-bearing animals, rodent parvoviruses were first identified as potential cancerogen agents (Kilham and Olivier, 1959; Toolan et al., 1962). On the contrary, they were later shown to prevent the formation of spontaneous, virally or chemically induced tumors in laboratory animals *in vivo*, a phenomenon known as oncosuppression (Dupressoir et al., 1989; Rommelaere and Cornelis, 1991; Toolan et al., 1982). In addition, antitumor effects of rodent parvoviruses could also be demonstrated both in established tumors or virus-infected tumor cells grafted in mice (Faisst et al., 1998; Haag et al., 2000).

Tumor cells as well as *in vitro* transformed cells with oncogens or carcinogens were shown to sustain an increased viral DNA replication and gene expression, in comparison to their normal counterparts (Cornelis et al., 1988; Salome et al., 1990). The preferential replication of parvoviruses in transformed cells is referred to as oncotropism (Rommelaere and Cornelis, 1991). Cell transformation appears to provide beneficial environment for parvoviral replication. Indeed, it induces a dysregulation of the cell cycle, leading to proliferation but also to the activation of oncogenes, and was shown to stimulate all the steps of the virus life cycle depending on the cells.

Rodent parvoviruses were also shown *in vitro* to preferentially kill transformed cells, compared to the normal parental cells (Rommelaere and Cornelis, 1991). This phenomenon is known as oncolysis and has been assigned, at least in part, to the cytotoxic NS1 protein (Caillet-Fauquet et al., 1990; Li and Rhode, 1990).

1.3.6. Low pathogenicity of rodent parvoviruses

The pathology of rodent parvoviruses in their natural host depends both on the virus strain and on the age of the animal. H-1 or MVMi infection of fetuses and neonates leads to acute, lethal diseases, while the infection of adult animals remains fully asymptomatic. Other rodent parvoviruses, like MVMp, or MPV-1 seem to be non pathogen in both neonates and adults (Ball-Goodrich et al., 1998; Jacoby et al., 1996; Siegl, 1984).

In regards to the potential use of rodent parvoviruses as anti-cancer agents, their possible pathological effects in human are of importance. No correlation could be established between any human disease and serological evidence of prior infection with parvovirus H-1 (Siegl, 1984). In two limited phase I clinical trials, *in vivo* injections of H-1 in few patients with advanced disseminated cancers lead to viremia followed by seroconversion, without causing any pathological side effects (Le Cesne et al., 1993; Toolan et al., 1965). Yet, there is a need to accumulate data concerning the safety of rodent parvoviruses for human therapy.

1.3.7. Parvoviral vectors based on rodent parvoviruses

As mentioned, the oncolytic, oncotropic, and oncosuppressive properties of rodent parvoviruses, together with their low pathogenicity make them attractive candidates for cancer therapy. However, their frequent isolation from tumors demonstrates that wild-type (wt) parvoviruses are not always able to eradicate tumors. Therefore, in order to increase the antitumor properties of wt parvoviruses, recombinant parvoviruses were constructed so as to deliver transgenes in the tumors able to stimulate the immune system.

Up to now, recombinant rodent parvoviral vectors have been engineered from the MVMp, H-1 and LuIII infectious clones. Two main types of constructs were used, namely complete coding replacement vectors and capsid replacement vectors.

In the first type, based on LuIIIV, all the viral coding regions between the telomeric origin of replication were removed and replaced by a transgene (Maxwell et al., 1993; Maxwell et al., 1996). These vectors allow high encoding capacity (up to 4 kb). They retain the cis-acting elements but lack viral non-structural proteins and are thus deficient for viral DNA replication.

In contrast, capsid replacement vectors enable the expression of transgenes while maintaining the parvoviruses intrinsic properties and were thus used in this study. Based on MVMp and H-1, these vectors retain the expression of the non-structural proteins, under the control of the parvoviral early promoter P4, whereas the capsid genes, driven by the late promoter P38, have been replaced by a therapeutic transgene (Brandenburger et al., 1999; Kestler et al., 1999; Russell et al., 1992). These vectors were shown to retain the oncotropic properties of the wild-type viruses *in vitro* and represent therefore selective gene delivery vectors for cancer gene therapy (Dupont et al., 2000; Dupont et al., 1994; Russell et al., 1992). Furthermore, they retain the non-coding terminal sequences. This, together with the expression of NS1, allows viral DNA replication and high levels of transgene expression through transactivation of the P38 promoter (Kestler et al., 1999). Due to the deletion of the capsid genes, these vectors are no longer able to produce capsid proteins and hence, progeny virions. They are viral DNA-replication competent, since they retain the NS genes, but propagation deficient.

Recombinant parvoviruses are produced by co-transfection of the recombinant parvoviral vector plasmid together with a helper plasmid, providing the parvoviral capsid proteins. One major problem encountered during the production was the contamination of recombinant virus stocks with replication-dependent viruses (RCV), produced by homologous recombination between the vector and helper constructs (Dupont et al., 1994; Kestler et al., 1999; Russell et al., 1992). To reduce the probability of recombination, several strategies were developed including the decrease of homology between the two constructs (Dupont et al., 2001; Wrzesinski et al., 2003), pseudotyping (Wrzesinski et al., 2003), or the use of split helper constructs (Brown et al., 2002).

The MVMp-based capsid replacement vectors used in this study are so-called chimeric recombinant vectors (see Figure 1-4). Taking advantage of the similarity between the MVM and H-1 genomes, viral sequences were exchanged up- and downstream of the transgenes between both viruses. This strategy resulted in a dramatic decrease of RCV contamination without affecting virus titers (Wrzesinski et al., 2003).

Another limitation of capsid replacement vectors is their low cloning capacity. Indeed, while removal of up to 800 bp in the 5' VP sequence did not affect the virus yields, larger deletions lead to a dramatic reduction of the virus titers (Kestler et al., 1999). The choice of transgenes in parvoviral-based therapy is therefore restricted by their respective size. However, most immunostimulatory genes used for cancer gene therapy have a small size, compatible with the limited size of parvoviral vectors. Therapeutic transgenes used so far in H-1 and MVMp-derived vectors include genes encoding toxins, co-stimulatory factors, cytokines/chemokines and antigens from bacterial origin (reviewed in Cornelis et al., 2004b).
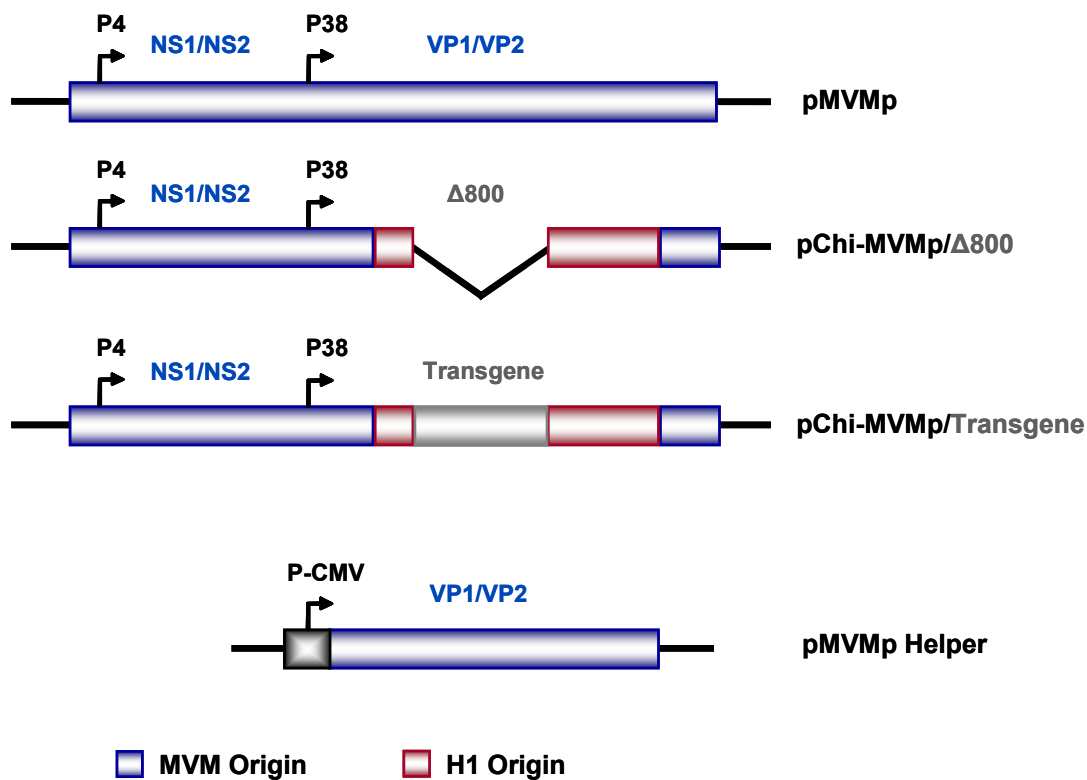
Figure 1-4: Schematic representation of pMVMp and recombinant parvoviruses

In order to increase the antitumor properties of wt MVMp, recombinant parvoviral MVMp-based vectors were developed. Based on the wt pMVMp infectious clone, part of the VP-coding sequence were deleted (800 bp), producing the so-called control empty vector (pChi-MVMp/Δ800) and replaced by various transgenes (pChi-MVMp/Transgene). Recombinant viruses are produced by co-transfection of the recombinant parvoviral vector plasmid together with a helper plasmid (pMVMp Helper), providing the parvoviral capsid proteins in trans, driven by the human cytomegalovirus (CMV) promoter. To reduce the probability of homologous recombination between the vector and helper constructs, viral sequences were exchanged up- and downstream of the transgenes between the close related MVMp (blue) and H-1 (red) viruses, producing so-called chimeric recombinant vectors.

1.3.8. Antitumor effects of recombinant parvoviruses *in vivo*

The anti-neoplastic effects of recombinant parvoviruses transducing various cytokines and chemokines as well as the co-stimulatory factor B7.1 were evaluated by monitoring the formation and growth of tumors after implantation of human or mouse tumor cells in recipient mice (see Table 1-1).

Tumor cells [1]	Virus	Transgene [2]	Mice [3]	Infection [4]	Antitumor effect [5]	Ref [6]
HeLa	H-1	IL-2	nude	*ex vivo*	+	1
HeLa	H-1	MCP-1	nude	*ex vivo*	-	1
HeLa	H-1	MCP-3	nude	*ex vivo*	+	2
K1735	MVMp	IL-2	syn	*ex vivo*	+	3
K1735	MVMp	MCP-3	syn	*in vivo*	+	4
B78/H-1	MVMp	MCP-3	syn	*ex vivo / in vivo*	+	4
H5V	MVMp	IP-10	syn	*in vivo*	+	5
H5V	MVMp	IL-2	syn	*in vivo*	-	5
EL4	MVMi	B7.1	syn	*in vivo*	+	6

Table 1-1: Antitumor effects of recombinant parvoviral vectors *in vivo*

1: HeLa: human cervical carcinoma; K1735: mouse melanoma; B78/H-1: mouse melanoma; H5V: mouse endothelioma; EVL4: mouse thymoma.

2: IL-2: interleukin-2; MCP-1 and MCP-3: monocyte chemotactic protein 1 and 3; IP-10: interferon-γ inducible protein 10; B7.1: costimulatory molecule B7.1.

3: H-1-derived vectors were used against human tumor cells grafted in immunosuppressed (nude) mice, whereas MVMp-derived vectors were against mouse tumor cells injected in syngeneic (syn) mice.

4: *ex vivo*: tumors cells infected prior to subcutaneous grafting; *in vivo*: established tumors treated with peritumoral injections of virus.

5: Antitumor effects include longer life expectancy, prevention of tumor appearance, inhibition of tumor growth, and regression of established tumors. +: enhanced effect of the transgene-delivering vector compared to a control virus (wild-type, empty vector or vector carrying a reporter gene); -: no improvement of the antitumor effect with the transgene-delivering vector over a control virus.

6: The numbers correspond to the following references: (1) Haag et al., 2000;(2) Wetzel et al., 2001; (3) El Bakkouri et al., 2005; (4) Wetzel et al., 2007; (5) Giese et al., 2002; (6) Palmer and Tattersall, 2000.

(Adapted from Kerr et al., 2006)

Altogether these studies show that H-1 and MVMp-based vectors transducing IL-2, monocyte chemotactic protein (MCP) -3, Interferon-γ inducible protein 10 (IP-10), and B7.1 induce significant antineoplastic effects in several mouse tumor models. Furthermore, these studies argue for the safety of parvoviral based-therapy as relatively low doses of parvoviral vectors were sufficient to achieve a therapeutic effect and no harmful side effects could be detected, even after repeated virus injections (Giese et al., 2002; Lang et al., 2006; Wetzel et al., 2007).

The antitumor effects observed could be assigned largely to the virus-mediated transgene expression. Indeed, therapeutic vectors had greater antitumor effects than the respective control viruses including wild-type viruses, empty vectors or recombinants expressing a reporter gene (Giese et al., 2002; Haag et al., 2000; Wetzel et al., 2001; Wetzel et al., 2007). In these studies, parvoviral vectors were inoculated either to tumor cells prior to implantation (*ex vivo*) or to established tumors (*in vivo*). The antitumor effects of parvoviral vectors were generally lower *in vivo* than *ex vivo* (Wetzel et al., 2007). This can be ascribed to poor intratumoral virus spread, virus uptake by non-tumoral cells, and generation of neutralizing antibodies at later stages.

1.3.9. Rationale for the use of rodent parvoviruses in glioma therapy

The properties of parvoviruses outlined above and especially their oncotropic properties make them attractive candidates as antitumor agents in glioma therapy. Indeed, the adult brain is composed of post-mitotic neurons and low proliferative glial cells, and should therefore not be prone to parvoviral infection, as the parvoviral life cycle is strictly dependent on host cell proliferation. In accordance with this, rodent parvovirus replication was reported in fetal but not adult brain (Cotmore and Tattersall, 1987).

In this context, several pre-clinical studies investigated the permissiveness of glioma cells for rodent parvoviruses H-1 and MVMp infection. The permissiveness for H-1 infection was analyzed in established glioma cell lines of rat and human origin as well as in short-term and low-passage cultures of malignant brain tumors. H-1 was found to infect all the cells tested and to induce a dose-dependent killing (Herrero et al., 2004). MVMp was shown to infect and to efficiently kill *in vitro* mouse glioma cells but also several rat and human gliomas cells lines (Dupont et al., 2000; Wollmann et al., 2005). In the rat system, a MVMp-based vector carrying a reporter gene showed preferential transduction and killing in rat C6 glioma cells, whereas no killing and no or low levels of transgene expression could be detected in normal rat neurons and astrocytes respectively (Dupont et al., 2000). Similarly to rat astrocytes, normal mouse astrocytes were shown to sustain an abortive viral life cycle and to express limited amounts of viral proteins upon MVMp infection, whereas microglia did not (Abschuetz et al., 2006).

Together, these data show that H-1 or MVMp are able to efficiently infect and kill most malignant glioma cells, without deleterious effects on normal brain cells *in vitro*. Thus, these preclinical studies suggest that glioma cells may represent a good target for rodent parvoviral-mediated gene therapy.

1.4. Candidate transgenes

As described above, gliomas are highly vascularized tumors, known to grow in a very immunosuppressive environment. Thus, antiangiogenic and immunostimulatory cytokines represent attractive candidates as antitumor agent for glioma gene therapy.

In this context, the antitumor effects of MVMp-based parvoviral vectors transducing such cytokines/chemokines were evaluated in a mouse glioblastoma model.

1.4.1. Tumor necrosis Factor-α

Tumor necrosis Factor-α (TNF-α) was first isolated from the serum of mice treated with bacterial endotoxin, and shown to cause hemorrhagic necrosis of mice tumors (Carswell et al., 1975). Since then, TNF-α was shown to be a multifunctional cytokine involved in apoptosis, cell survival, inflammation, and immunity. TNF-α is mainly produced by activated macrophages, natural killer (NK) cells, and T lymphocytes. TNF-α expression was also reported in a variety of other cell types, including, DCs, fibroblatsts, astrocytes, endothelial cells, smooth muscle cells, and tumor cells (Oppenheimer and Feldmann, 2000).

TNF-α is synthesized as a 26 kDa membrane-bound propeptide (pro-TNF), and is released upon cleavage of its pro-domain by the TNF-converting enzyme. In its soluble form, TNF-α is biologically active as a homotrimer of 17 kDa subunits (Bemelmans et al., 1996).

TNF-α signals through two distinct cell receptors, referred to as TNFR-1 and TNFR-2. While TNFR-1 is expressed on all cell types, TNFR-2 expression is restricted to endothelial and immune cells (Aggarwal, 2003). The major difference between the two receptors is the presence of a death domain in TNFR-1, absent in TNFR-2. Through this domain, TNFR-1 is able to induce apoptotic cell death and belongs to the death receptor family (Ashkenazi and Dixit, 1998). Besides the induction of apoptosis, TNFR-1 has also the ability to transduce cell survival signals. Both TNFR-1 survival and death pathways are well defined but their regulation remains elusive (Muppidi et al., 2004). TNFR-1 signaling activates multiple signal transduction pathways including Nuclear Factor kappa B (NF-κB) and Jun kinase (JNK) survival pathways as well as the apoptosis pathway. TNFR-2 was also shown to activate both NF-κB and JNK (Chen and Goeddel, 2002; Wajant et al., 2003).

TNF-α acts on many cells types and has a broad range of activities. TNF-α is above all a potent pro-inflammatory cytokine, inducing the release of inflammatory cytokines such as IL-6 or IL-8. It also induces the activation of many professional cells of the immune system including macrophages, lymphocytes, and NK cells (Waterston and Bower, 2004). In addition, TNF-α is also reported to induce the maturation of DCs which in turn activate the adaptative immune response (Trevejo et al., 2001; Yanagawa et al., 2002). While TNF-α is involved in the clearance of viral, bacterial, fungal, or parasitic infection, it has also been shown to be involved in the pathogenesis of many human diseases, including autoimmunity, allergy, and septic shock (Oppenheimer and Feldmann, 2000). The role of TNF-α in cancer is controversial and both tumor promoting as well as antitumor activities are discussed. Indeed, TNF-α was shown to promote tumor formation, growth, invasion, and metastasis. On the other hand, TNF-α was shown to have antineoplastic effects such as induction of apoptosis, disruption of tumor vasculature, stimulation of antitumor immunity, and synergism with chemotherapeutic drugs (Balkwill, 2006; Mocellin and Nitti, 2008; Mocellin et al., 2005). It is worth mentioning that systemic administration of TNF-α in clinical trials resulted in minimal tumor response with severe toxicity (reviewed in Creagan et al., 1998; Lejeune et al., 1998; Van Horssen et al., 2006). In contrast, local delivery of high concentration of TNF-α could be maintained safely, in particular for the treatment of melanoma (Lejeune et al., 1994; Lejeune et al., 2006; Manusama et al., 1996).

1.4.2. Chemokines

Chemokines (chemotactic cytokines) represent a large family of structurally and functionally related small (8-15 kDa) proteins that induce directional cellular migration. Chemokines establish concentration gradients along which responding cells migrate, thus promoting the accumulation of cells at the source of chemokine production. Chemokines and their receptors have been involved in development, homeostasis, and angiogenesis but also in autoimmune and infectious diseases, as well as tumor growth and metastasis (Horuk, 1998; Rossi and Zlotnik, 2000).

Until now, the chemokine superfamily consists of approximately fifty members (Laing and Secombes, 2004; Zlotnik et al., 2006) and twenty receptors (Zlotnik and Yoshie, 2000). Chemokines are structurally subdivided into four subfamilies, CXC (α), CC (β), CX_3C (δ) and C (γ), according to the position of two highly conserved N-terminal cysteine residues (Murphy, 2002; Zlotnik et al., 2006). Functionally, chemokines are

divided into homeostatic and inflammatory proteins. Homeostatic chemokines are constitutively expressed, and generally involved in the development and homeostasis of the hematopoietic and immune systems as well as in immune surveillance. In contrast, inflammatory chemokines are inducible, produced only in response to physiological stress including inflammation or infection, and induce leukocyte recruitment to the injured or infected site (Luster, 1998; Zlotnik and Yoshie, 2000). The CXC subfamily is further functionally divided in ELR+ and ELR- chemokines, depending on the presence or absence of the ELR (glutamic acid - leucine - arginine) motif preceding the CXC domain. Whereas ELR+ chemokines are strong angiogenic factors, able to simulate endothelial cell chemotaxis, ELR- are potent angiostatic factors (Strieter et al., 1995).

Chemokines signal through G-protein coupled, seven transmembrane receptors, which are divided into four subfamilies, CXCR, CCR, CX_3CR and XCR, based on their chemokine subclass specificity (Murphy, 2002). Most receptors can respond to several chemokines and similarly most chemokines can bind to more than one receptor, although these interactions are typically class restricted (Rossi and Zlotnik, 2000).

Upon signaling, chemokines receptors induce inhibition of adenylcyclase and activation of phospholipase C, leading to release of intracellular calcium. Downstream of the G proteins, several signal transduction molecules were shown to be activated by chemokines including GTPases like Rho, Rac and Cdc42, or pathways of major kinases like mitogen-activated protein kinase (MAPK) and phosphatidyl inositol-3 kinase (PI3K) (reviewed in Balkwill, 1998; Thelen, 2001). After signaling, chemokine receptors are usually internalized and cells become thus refractory to further stimulation with the same or other ligands.

1.4.3. Interferon-γ inducible protein 10

Interferon-γ (IFN-γ) inducible protein 10, commonly designated as IP-10 or CXCL10 is a 10 kDa protein, member of the ELR- CXC chemokine subfamily. IP-10 binds to a unique chemokine receptor, CXCR3, shared with two other ELR- CXC ligands, namely monokine induced by IFN-γ (Mig or CXCL9) and IFN-inducible T-cell α-chemoattractant (I-TAC or CXCL11) (Cole et al., 1998; Loetscher et al., 1996).

Human IP-10 was originally isolated from U937 monocytic leukemia cells as an interferon-γ inducible mRNA (Luster et al., 1985). Later, IP-10 was found to be synergistically induced by IFN-γ and TNF-α in several cells types (Majumder et al.,

1996), but also slightly by TNF-α alone (Sheng et al., 2005) or lipopolysaccharide (LPS) (Ohomori and Hamilton, 1992).

IP-10 has multiple biological functions including T cell development, recruitment of immune cells, adhesion of T cells to endothelial cells, and inhibition of angiogenesis.

IP-10 is a potent chemoattractant for NK cells (Taub et al., 1995), NKT cells (Kim et al., 2002), plasmoid dendritic cells (Penna et al., 2001), monocytes and stimulated T cells (Loetscher et al., 1996; Taub et al., 1993). Both the activation status and the phenotype of T cells were shown to be determinant for IP-10 chemotaxis. Indeed, IP-10 promotes the migration of stimulated but not of naïve T cells (Taub et al., 1993). Furthermore, IP-10 attracts specifically activated Th1 but not Th2 lymphocytes (Bonecchi et al., 1998; Sallusto et al., 1998). In agreement with this, IP-10 has been shown to be involved in several Th1-type inflammatory diseases, such as multiple sclerosis (Salmaggi et al., 2002) or experimental autoimmune encephalomyelitis (EAE) (Ransohoff et al., 1993). In addition to the recruitment of T cells, IP-10 also promotes the adhesion of activated T cells to endothelial cells, and thus seems to play a role in the entry of T cells to sites of tissue inflammation (Taub et al., 1993). IP-10 is a highly inducible gene but it is also constitutively expressed in some organs including naïve lymphoid organs, suggesting a role for IP-10 in T cell development (Gattass et al., 1994). Besides its function as chemoattractant, IP-10, as ELR- chemokine, has been shown to be a potent inhibitor of angiogenesis *in vitro* (Angiolillo et al., 1995; Strieter et al., 1995) and *in vivo* (Sgadari et al., 1996). This seems to be mediated by direct effects on endothelial cells through inhibition of endothelial cell migration (Belperio et al., 2000; Strieter et al., 1995), proliferation (Angiolillo et al., 1995; Feldman et al., 2006; Luster et al., 1995; Strieter et al., 1995), and differentiation (Angiolillo et al., 1995). In addition, IP-10 was also recently shown to induce endothelial cell apoptosis (Feldman et al., 2006).

Owing to both its angiostatic and immunostimulatory properties, IP-10 represents an attractive candidate for cancer therapy. Indeed, IP-10 demonstrated strong antitumor effects in several mouse tumor models, used either alone (Feldman et al., 2002; Giese et al., 2002; Sun et al., 2005) or in combination with other cytokines, such as MIG (Tominaga et al., 2007), or IL-12 (Keyser et al., 2004; Narvaiza et al., 2000). The antitumor effects of IP-10 were shown to be mediated by both its immunostimulatory (Luster and Leder, 1993) and angiostatic properties (Arenberg et al., 1996; Sgadari et al., 1996).

1.4.4. Monocyte chemotactic protein-2 and -3

Monocyte chemotactic protein-2 and -3 (MCP-2, MCP-3), also known as CCL8 and CCL7, are inflammatory chemokines belonging to the CC chemokine family (Van Damme et al., 1992). MCP-2 and -3 are produced by various cell types, including tissue cells, leukocytes, and tumor cells. Their expression is induced by pro-inflammatory cytokines such as IL-1, TNF-α, and IFN-γ, but also by exogenous stimuli like LPS, bacteria, and viruses (reviewed in Van Coillie et al., 1999; Zlotnik et al., 2006). Both chemokines bind multiple CCR receptors including CCR1, CCR2, CCR3 and CCR5 (Fioretti et al., 1998). Owing to their multiple receptors, they have a broad range of target cells, including most leukocyte cell types. Indeed, they were shown to be chemotactic *in vitro* for monocyte/macrophages, basophils, neutrophils, eosinophils, T lymphocytes, NK cells, and DCs. Besides leukocyte chemotaxis, MCP-2 and -3 were reported to induce the release of specific enzymes in monocytes and T cells, allowing these cells to digest extracellular matrix components and thus to migrate into tissues. They were also reported to induce histamine release in basophils and granzyme A release from T and NK cells (reviewed in Menten et al., 2001; Van Coillie et al., 1999).

The broad range of actions of MCP-2 and -3 and especially their chemotaxis for NK cells, T cells and DCs, known to play a critical role in antitumor immunity, make them attractive candidates as antitumor agents. MCP-3 was shown to be a potent antitumor agent in several mouse tumor models, including mouse mastocytoma (Fioretti et al., 1998), human carcinoma HeLa (Wetzel et al., 2001), and mouse melanomas B78/H-1 and K1735 (Wetzel et al., 2007).

1.5. Aim of the study

Recombinant parvoviral vectors encoding TNF-α and IP-10 were recently shown in our laboratory to exert antitumor effects on mouse GL261 glioma implanted subcutaneously (Enderlin et al., 2008). In this context, the first aim of this study was to investigate the mechanisms sustaining tumor inhibition by TNF-α- and IP-10-expressing parvoviral vectors in the GL261 subcutaneous tumor model. The second aim of this work was to implement the intracranial GL261 tumor model in our laboratory, which was not established at the time this study was started, and to analyze the antitumor effects of parvoviral vectors transducing TNF-α, IP-10, compared to MCP-2 and MCP-3 on GL261

implanted intracranially in syngeneic C57BL/6 mice. The mechanisms sustaining tumor inhibition subcutaneously as well as intracranially were to be investigated by immunohistochemistry on tumor samples and included the analysis of the cellular immune infiltration, intratumoral cell proliferation and apoptosis as well as microvascularization.

2. MATERIALS

2.1. Animals

Female, 5 to 7 weeks old, C57BL/6 mice were purchased from Charles River WIGA.

2.2. Mammalian cells lines

Name	Species	Description	Reference
293T	Human	Adenovirus-transformed human embryonic kidney cells expressing SV40 large T antigen	Graham et al., 1977
A9	Mouse	Fibroblastic cells	Littlefield, 1964
GL261	Mouse	3-methylcholanthrene induced astrocytoma cells	Seligman and Shear, 1939
MLEC-PAI/Luc	Mouse	Mink lung epithelial cells transfected with luciferase under a plasminogen activator inhibitor-1 promoter	Abe et al., 1994

2.3. Bacteria strains

Name	Resistance	Origin	Reference
E. Coli SURE	Tetracyclin + Kanamycin	Stratagene	Greener, 1990
E. Coli JM 109	-	Stratagene	Yanisch-Perron et al., 1985

2.4. Plasmids

Name	Description	Size (bp)	Resistance	Origin
pChi-MVMp/Δ800	Infectious MVMp DNA clone bearing an 800 bp deletion in VP genes	6469 -	Ampicillin	Wrzesinski et al., 2003
pChi-MVMp/MCP-2	Infectious MVMp DNA clone expressing human MCP-2	6855 440	Ampicillin	T.Kayser, unpublished
pChi-MVMp/MCP-3	Infectious MVMp DNA clone expressing human MCP-3	6987 434	Ampicillin	Wetzel et al., 2007
pChi-MVMp/TNF-α	Infectious MVMp DNA clone expressing mouse TNF-α	7283 700	Ampicillin	Enderlin et al., 2008
pChi-MVMp/IP-10	Infectious MVMp DNA clone expressing human IP-10	6984 380	Ampicillin	Enderlin et al., 2008
pCMV-VP<MVMp	MVMp helper plasmid expressing VP genes under a CMV promoter	7700	Ampicillin	Wrzesinski et al., 2003

2.5. Primers

Transcript	Primer sequence 5´→3´ sense/antisense	$T_{annealing}$ (°C)	Cycles	Supplier Reference
mGAPDH	ACCACAGTCCATGCCATCAC TCCACCACCCTGTTGCTGTA	60	25	Paulukat et al., 2001
mIFN-α	TGACCTCCACCAGCAGCTCAA GACCACCTCCCAGGCACAGG	58	35	Maxim Biotech
mIFN-β	CATCAACTATAAGCAGCTCCA TTCAAGTGGAGAGCAGTTGAG	56	35	Cervantes-Barragan et al., 2007
mIP-10	TGAGCAGAGATGTCTGAATC TCGCACCTCCACATAGCTTACAG	58	25	Giese et al., 2002
MCS	ACTTCTTCTGCTGCACAGCA GGGTCAGTGTTAAAGATGTAGGTG	58	30	self designed
NS1	TGAATGGAAAAGATATCGGATGGAATAG GCCTCCGTCTCTTGGTGG	58	30	Giese et al., 2002
mTGF-β1	TCAACGGGATCAGCCCCAAA TGGTAGCCCTTGGGCTCGTG	58	35	Maxim Biotech
mTGF-β2	CCCCCGGAGGTGATTTCCAT TGGGGTTTTGCAAGCGGAAG	58	35	Maxim Biotech
mTGF-β3	CACTGTGCGCGAGTGGCTGT TCCTCCAGGTTGCGGAAGCA	58	35	Maxim Biotech

2.6. Antibiotics

Antibiotic	Working dilution	Stock concentration	Supplier
Ampicillin	75 ng/ml	75 µg/ml	Roche Applied Science
Chloramphenicol	136 µg/ml	34 mg/ml, in 75% EtOH	Roche Applied Science
Geneticin	250 µg/ml	50 mg/ml	Gibco-Invitrogen
Kanamycin	12.5 ng/ml	25 µg/ml	Roche Applied Science
Penicillin	100 U/ml	10,000 U/ml	Gibco-Invitrogen
Streptomycin	100 µg/ml	10,000 µg/ml	Gibco-Invitrogen
Tetracyclin	12.5 ng/ml	12.5 µg/ml, in 75% EtOH	Sigma

2.7. Antibodies

2.7.1. Primary antibodies

Antigen	Host	Isotype	Clonality	Dilution	Application	Supplier / Reference
33D1	Rat	IgG	Monoclonal	1:200	IHC	BD Pharmingen
CD4	Rat	IgG	Monoclonal	1:200	IHC	Abcam
CD8	Rat	IgG	Monoclonal	1:200	IHC	Abcam
CD31	Rat	IgG	Monoclonal	1:200	IHC	BD Pharmingen
CD68	Rat	IgG	Monoclonal	1:500	IHC	AbD Serotec
Ki67	Rabbit	IgG	Polyclonal	1:500	IHC	Abcam
NKG2D	Rat	IgG	Monoclonal	1:100	IHC	R&D Systems

2.7.2. Secondary antibodies

Specificity	Host	Conjugate	Dilution	Application	Supplier Reference
Rabbit IgG	Donkey	Biotin	1:100	IHC	Amersham Biosciences
Rat IgG	Goat	Biotin	1:100	IHC	Amersham Biosciences

2.8. Cytokines and growth factors

Product name	Supplier
Recombinant human IP-10	R&D systems
Recombinant human TGF-β1	PeproTech

2.9. Enzymes

Product name	Supplier
M-MLV reverse transcriptase	Promega
Rnasin ribonuclase inhibitor	Promega
RQ1 Rnase-Free Dnase I	Promega
Taq DNA polymerase	Invitrogen
Restriction endonucleases	NEB, Roche, Fermentas
Streptavidin-horseradish peroxidase complex	Amersham Biosciences

2.10. Kits

Name used in the text	Product name	Supplier
DNA labeling system	Megaprime DNA Labeling systems	Amersham Biosciences
Gel Extraction kit	QIAQuick Gel Extraction kit	Qiagen
Luciferase assay system	Luciferase assay system	Promega
Mouse IFN-α ELISA	Mouse IFN-α ELISA kit	PBL Biomedical Laboratories
Mouse IP-10 ELISA	Quantikine Mouse CXCL10/IP-10	R&D Systems
Mouse TNF-α ELISA	BD optEIA Mouse TNF-α ELISA set	BD Biosciences
Plasmid mega kit	Qiagen Plasmid mega kit	Qiagen
TUNEL assay kit	Apoptag	Qbiogene

2.11. Reagents

Name used in the text	Product name	Supplier
Agarose	Agarose NA	Pharmacia Biotech
Antiseptic cream	Bepanthen	Bayer
BSA	BSA Fraction V	Roche
Casy blue	Casy blue	Schärfe System
Casy ton	Casy ton	Schärfe System
DAB	DAB substrate	Roche
DMSO	DMSO Hybri Max	Sigma
Dnase/Rnase-free water	UltraPURE water DNAse/RNAse Free	Gibco-Invitrogen
dNTPs Mix	dNTPs Mix (PCR grade)	Invitrogen
DPBS	calcium- and magnesium-free DPBS	Gibco-Invitrogen
Guanidium thiocyanate / phenol solution	TRIzol	Invitrogen
HBSS	HBSS -CaCl$_2$ and –MgCl$_2$	Gibco-Invitrogen
Herring sperm DNA	Herring sperm DNA	Promega
Histogreen	Histoprime	Linaris
Hydrogen peroxyde	Hydrogen peroxyde	Roth
Iodixanol	OptiPrep	Axis-Shield
Isopetane	Isopentane	Roth
Ketamin	Ketavet (100 mg/ml)	Pfizer
Mounting medium	Histofluid	Marienfeld
NaCl 0.9%	0.9% NaCl solution	Braun
OCT Compound	Tissue-Tek	Sakura Finetek
Oligo (dT) primer	Oligo (dT)$_{18}$ primer	Fermentas
Paraformaldehyde	Paraformaldehyde	Roth
Rotihistol	Rotihistol	Roth
Trypan blue	Trypan blue solution	Fluka
Trypsin 0.25%	0.25% Trypsin-EDTA	Gibco-Invitrogen
Xylazin	Rompun 2%	Bayer

2.12. DNA ladders

Name used in the text	Product name	Supplier
DNA ladder	2 Log DNA ladder	NEB
	100 bp DNA ladder	NEB

2.13. Chemicals

Acids, bases, as well as organic and inorganic solutions were purchased in analytical grades from Applichem, Becton Dickinson, Bio-Rad, Calbiochem, Fluka, Gerbu, Baker, Merk, Pharmacia Biotech, Riedel-de Haen, Roth, and Sigma.

Radiochemicals used for the labeling of DNA probes (^{32}P-dCTP) were obtained from Amersham Pharmacia.

2.14. Consumables

Standard plasticware for cell culture and molecular biology was purchased from Greiner, Nunc, Satstedt, Costar, Millipore, BD Falcon, and Eppendorf.

Name used in the text	Product name	Supplier
Absorbent swabs	Sugi absorbent swabs	Kettenbach
Centrifugal buffer exchange columns	Zeba Desalt Spin Column	Pierce-Therma Scientific
Cryomolds	Cryomold 10x10x5 mm	Sakura
33 gauge beveled needle	NanoFil 33 gauge beveled	WPI
Nitrocellulose membrane filters	NC45	Schleicher & Schuell
Non absorbable nylon thread	Daclon DS 12mm EP 0.7	SMI
1 ml fine dosage syringe	Omnican-F 1ml	B/Braun
10 µl syringe	10µl NanoFil	WPI
Polyallomer centrifuge tube	Polyallomer Quick-seal	Beckman Instruments
Matrix tubes	Lysing Matrix D	Qbiogene
Superfrost microscope slide	Superfrost Plus	Menzel

2.15. Equipment

Name used in the text	Product name	Supplier
Cell counter	CASY Cell Counter & Analysis System	Schärfe System
Cell disrupter	Fast-Prep	Qbiogene
Centrifuges:		
High speed	HERMLE ZK380; Megafuge 1.0R	Hermle; Heraeus
Super speed	Sorvall RC 5C Super Speed	Thermo Scientific
Ultra speed	Optima LE-80K	Beckman Coulter
Table	MiniSpin	Eppendorf
Centrifuge rotors:		
Fixed angle	FiberLite F-10	Thermo Scientific
Fixed angle (ultra speed)	50.2 Ti	Beckman Coulter
Swinging bucket	Sorvall HB-6	Thermo Scientific
Swinging bucket	Heraus 2706D	Heraus
Clinical 1.5 T MR scanner	Magnetom Vision	Siemens
Heating pad	Solac CT8630	Solac
Horizontal electrophoresis system	Easy Cast electrophoresis system	Peqlab
Luminometer	Fluoroskan Ascent FL	Thermo Labsystems
Microinjection unit:	UltraMicroPump II Microserynge Injector	WPI
	Micro4 Microsyringe Pump Controller	WPI
Microplate reader	Multiscan EX	Thermo Labsystems
Microscopes:	leica DMIL	Leica
	Axio Imager Z1	Carl Zeiss
Microtome	HM 550	Microm
Spectrophotometer	Ultrospec 3100 pro	Amersham Biosc.
Stereotactic frame:	Stoelting Lab Standard Stereotaxic	WPI
	Stoelting Mouse/Neonatal Rat Adapter	WPI
Thermal cycler	Mastercycler epGradientS	Eppendorf
UV-transilluminators:	Image Master VDS (302 nm)	Pharmacia Biotech
	N90 (366 nm)	Konrad Benda
Water purification system	Milli-Q Biocell A10	Millipore

2.16. Softwares

Product name	Supplier
Adobe Photoshop	Adobe Systems Inc
Ascent Multiscan	Thermo Labsystems
Ascent Fluoroscan	Thermo Labsystems
AxioVision Rel. 4.7	Carl Zeiss
Endnote X	Thomson
Image Master 1D	Amersham Pharmacia Biotech
Microsoft Office	Microsoft

3. METHODS

3.1. Microbiological methods

3.1.1. Bacteria culture

All bacteria were grown in Luria Bertani (LB) medium supplemented with the appropriate antibiotics at 37°C with vigorous shaking (200 rpm). The *Escherichia Coli* (*E. Coli*) strains used in this study as well as the antibiotics applied for the selection of plasmid containing bacteria are listed below.

Strain	Use	Selective antibiotics
E. Coli SURE	Propagation of infectious recombinant DNA clones	Tet + Kan + Amp
E. Coli JM 109	Propagation of MVM helper vector	Amp

Media and additives for bacteria culture were purchased from Fluka, Gibco-Invitrogen, PAA Laboratories, and Sigma.

LB-medium: 1% (w/v) Bacto-tryptone
0.5% (w/v) Yeast extract
0.5% (w/v) NaCl
pH 7.0

3.1.2. Preparation of bacteria for plasmid isolation

For amplifying plasmid DNA, 20 ml LB-medium supplemented with the appropriate selective antibiotics were inoculated with transformed *E. Coli* SURE or *E. Coli* JM109 bacteria containing the desired plasmid. After incubation at 37°C with vigorous shaking (200 rpm) for 8 h, 5 ml of the starter culture were transferred to 250 ml LB-medium with the appropriate antibiotics. The culture was incubated at 37°C for 12-16 h until bacteria growth reached the end of the logarithmic growth phase. In the case of *E. Coli* SURE bacteria, the culture was further incubated for 5 h at 37°C in the presence of chloramphenicol to amplify plasmid replication. The bacterial cells were harvested by centrifugation at 5000 rpm for 10 min at 4°C (fixed angle rotor, super speed centrifuge)

and all traces of supernatant were removed. The cell pellet was further processed to isolate plasmid DNA or stored at -20°C.

3.1.3. Long-term storage of bacteria

For cryopreservation of bacteria, 1 ml of late logarithmic phase growing bacteria was removed from the culture before addition of chloramphenicol, mixed with 0.5 ml 50% glycerol, frozen in liquid nitrogen, and stored at -80°C.

3.2. Molecular biological methods

3.2.1. Plasmid DNA isolation and purification

Plasmid DNA isolation and purification from 2 x 250 ml bacteria culture was performed using a plasmid purification kit according to the manufacturer's instructions. Briefly, bacteria were lyzed under alkaline conditions and the plasmid DNA was bound to an anion exchange resin under low salt conditions. RNA, proteins and low molecular weight impurities were removed by a medium salt wash. Plasmid DNA was eluted in a high salt buffer and precipitated with isopropanol. Purified DNA was dissolved in Tris-EDTA (TE) buffer, quantified by spectrophotometry at 260 nm, and analyzed by restriction digestion followed by agarose gel electrophoresis. Plasmid DNA was further processed for calcium phosphate transfection or stored at -20°C.

TE buffer: 10 mM Tris-HCl, pH 8.0
               1 mM EDTA, pH 8.0

3.2.2. DNA quantification and quality assessment

The DNA concentration was determined by measuring the absorbance at 260 nm with a spectrophotometer. An absorbance of 1 unit at 260 nm corresponds to 50 µg/ml dsDNA. The purity of DNA can be estimated by the ratio of the absorbance values at 260 nm and 280 nm (A260/A280). Only pure plasmid preparations with a ratio of A260/A280 between 1.8 and 2.0 were subjected to transfection of mammalian cells. Alternatively, the concentration of a DNA fragment was estimated by gel electrophoresis by

comparing the intensity of the isolated band with a molecular weight marker of known concentration.

3.2.3. Restriction enzyme digestion of DNA

Restriction analysis was used for the characterization, identification, and isolation of DNA molecules. The treatment of plasmid DNA with restriction endonucleases produces, due to their sequence specificity, a series of precisely defined fragments which are separated according to their size by gel electrophoresis.

Restriction enzyme digestions were performed in a final volume of 20 µl according to the enzyme manufacturer's instructions, using 1 µg of plasmid DNA. Incubation periods ranged from 1 h to 2 h at 37°C depending on the enzyme used. Analysis of the fragmented plasmid DNA was done by agarose gel electrophoresis.

3.2.4. Agarose Gel electrophoresis

Separation of nucleic acids according to size was conducted for analytical as well as preparative purposes by agarose gel electrophoresis. Agarose concentrations varied between 1 and 2 % in Tris-Acetate-EDTA (TAE) buffer, depending on the expected size of the fragments. Ethidium bromide was added to the gel at a final concentration of 1 µg/ml to allow visualization of the nucleic acids under UV-light. The samples were supplemented with 10x DNA loading buffer and loaded in parallel to DNA molecular weight markers for product size and concentration estimation. The gels were run in an horizontal electrophoresis system at 5-10 V/cm in 1x TAE buffer until sufficient separation of the fragments. The gel was visualized in a UV transilluminator (302 nm), and documentation was done by photography of the visualized bands using the Image Master 1D software.

TAE buffer: 40 mM Tris-Acetat, pH 7.8
               1 mM EDTA
               pH 8.0

3.2.5. DNA gel extraction

The DNA fragment to be purified was run in an agarose gel, visualized under UV light at a wavelength of 366 nm (UV transilluminator) to avoid DNA damage, and was cut out from the gel using a scalpel. Isolation and purification of the fragment was performed with the gel extraction kit, according to the manufacturer's instructions. The purified DNA fragment was dissolved in TE buffer and stored at -20°C. Qualitative and quantitative analysis was carried out by agarose gel electrophoresis.

3.2.6. Total RNA isolation from eukaryotic cells

Total RNA was isolated from cell monolayers by guanidium thiocyanate extraction and purified by phenol/chloroform extraction according to the method described by Chomczynski and Sacchi, 1987. Monolayer cells were washed once with PBS and lyzed with a cell scraper using 1 ml of guanidium thiocyanate/phenol solution (TRIzol) per 10 cm plate. The cell lysates were transferred into matrix tubes, homogenized with rapid and vertical angular motion in a cell disrupter (time: 3x 20 s, speed: 5) at RT and transferred to eppendorf tubes. Addition of chloroform (0.2 ml per ml of TRIzol) and incubation for 3 min at RT, followed by centrifugation (15 min, 13000 rpm, 4°C, table centrifuge), separated the solution in an aqueous phase, containing RNA, and an organic phase, containing protein. The upper aqueous phase was transferred to a new tube and mixed with equal volume of isopropanol. Samples were then incubated for 10 min at RT, centrifuged (10 min, 11000 rpm, 4°C, table centrifuge) and the supernatant discarded. The RNA pellet was washed once with 75% ethanol, centrifuged again, air-dried and dissolved in 300 µl Dnase/Rnase-free water. Total RNA was stored at -80ºC.

3.2.7. Total RNA quantification and quality assessment

The RNA concentration was determined by measuring the absorbance at 260 nm with a spectrophotometer. An absorbance of 1 unit at 260 nm corresponds to 40 µg/ml ssRNA. The purity of RNA can be estimated by the ratio of the absorbance values at 260 nm and 280 nm (A260/A280), with pure RNA having a A_{260}/A_{280} ratio of 1.9 -2.1.

The integrity of total RNA was verified by agarose gel electrophoresis in the presence of ethidium bromide. For this, 1µg RNA was run on a 2% agarose gel. The 18S and 28S ribosomal RNA from eukaryotic source should appear as sharp bands. Pure RNA was further used for reverse transcriptase polymerase chain reaction (RT-PCR).

3.2.8. Reverse transcription-polymerase chain reaction (RT-PCR)

This method is a two steps process allowing the amplification of a defined piece of RNA. In the first step, called 'first strand cDNA synthesis', complementary DNA (cDNA) is made from a messenger RNA template by a RNA-dependent DNA polymerase reverse transcriptase through the process of reverse transcription (RT).

The second step consists in the amplification of the resulting cDNA through polymerase chain reaction (PCR). This method allows specific amplification of defined regions of a DNA molecule *in vitro* through enzymatic replication by a DNA-dependent DNA polymerase.

3.2.8.1 Deoxyribonuclease treatment and secondary structures removal

Prior to RT-PCR, 1 µg of total RNA was treated with 1 U Rnase free Deoxyribonuclease I (DNAse I) according to the manufacture's instructions in order to eliminate contaminating DNA.

RNA secondary structures were denatured by incubation at 70°C for 5 min, followed by direct chilling on ice for 5 min to prevent their reformation.

3.2.8.2 First strand cDNA synthesis from total RNA

Total polyA RNA was reverse transcribed by the Moloney Murine Leukaemia Virus Reverse Transcriptase, RNAse H Minus Point Mutant (M-MLV RT (H-)), a RNA-dependent DNA polymerase, using oligo(dT) primers.

The reverse transcription was performed using a thermal cycler and the reaction was set up on ice in a final volume of 25 µl as follows:

Component	Final quantity
- DNAse-treated RNA	1 µg
- M-MLV RT (H-)	200 U
- Oligo(dT) primers	0.5 µg
- dNTPs mix	0.5 mM each
- Rnasin (Rnase Inhibitor)	20 U

The reaction was mixed gently, briefly centrifuged, and incubated at 40°C for 1 h. The reverse transcriptase was subsequently inactivated by incubating at 90°C for 5 min. The

cDNA was diluted 1:8 using RNAse/DNAse free water and further used for PCR amplification or stored at -20°C.

The cDNA synthesis was verified by amplification of the housekeeping gene glyceraldehyde-3-phosphate dehydrogenase (GAPDH) via PCR.

3.2.8.3 Polymerase chain reaction (PCR) amplification of cDNA

The reverse transcribed cDNA was used as template to amplify target sequences by PCR using specific primer pairs, self-designed, or commercially purchased. For commercial primers, the PCR reaction was performed according to the manufacturer's instructions. PCR reactions with self-designed primers were set up on ice in a total volume of 25 or 50 µl as follows:

Component	Final quantity
- cDNA template	5 / 10 µl
- Taq DNA Polymerase	2 U
- Forward primer	0.5 µM
- Reverse primer	0.5 µM
- dNTPs mix	0.2 mM each
- MgCl$_2$	1.5 mM

The samples were mixed, briefly centrifuged and the PCR was performed in a thermal cycler. The PCR program was adapted to the primer pair, using the following protocol:

Step	Temperature	Time	
- Initial denaturation	94°C	3 min	
- Denaturation	94°C	30 s	
- Annealing	58-60°C	30 s	25-35 cycles
- Extension	72°C	30 s	
- Final extension	72°C	10 min	
- Storage	4°C	hold	

The primers, as well as their specific PCR conditions (annealing temperature, number of cycles) are listed in section 2.5. The amplified PCR products were analyzed in terms of size and quantity by agarose gel electrophoresis and stored at -20°C.

When semi-quantitative PCR was performed, the quantity of cDNA templates was adjusted according to their housekeeping gene signal intensity.

3.2.9. Preparation of a NS-specific radioactive labeled probe for virus titration

The replication titer of purified viruses was determined by hybridization with a NS-specific radiolabeled DNA probe to detect the viral DNA amplified within infected cells (see section 3.4.3.2). The probe was prepared according to Wrzesinski et al., 2003.

The NS-specific DNA probe was generated by double restriction digestion of 50 µg pMVMp/Δ800 plasmid with EcoRV and EcoRI in a final volume of 50 µl, generating two fragments of 703 and 5716 bp, which were separated in a 1% preparative agarose gel. The 703 bp NS-specific DNA fragment was purified by agarose gel extraction and its concentration was estimated by comparison with a DNA standard. The DNA probe was stored at – 20°C before further processing for radioactive labeling.

The NS-specific DNA fragment was radiolabeled using a DNA labeling system with ^{32}P-dCTP according to the manufacturer's instructions, and the reaction was terminated by addition of 150 µl TE buffer. The radiolabeled probe was subsequently purified from unincorporated radiolabeled dNTPs by gel filtration through a Sephadex G50 column. For this, the probe was carefully pipetted onto the column matrix and centrifuged at 2000 rpm for 10 min at RT (high speed centrifuge). The radioactivity of the purified probe was measured in a radioisotope counter using 2 µl of probe. The activity ranged typically between 30000 and 50000 CPM/µl. The labeled probe was subsequently denatured at 100°C for 10 min (heat block) and chilled on ice for 5 min before being transferred into the hybridization solution. Alternatively, the probe was frozen at -20°C before denaturation for short-term storage.

3.3. Cell biological methods

3.3.1. Maintenance of mammalian cell lines

The given cell lines were maintained in monolayer cultures in defined medium with the adequate supplements under standard conditions (37°C, 5% CO_2, 90% humidity). Sub-confluent cells were splitted 1:5 - 1:20, depending on the cellular growth, usually twice a week. For this, the medium was removed, the cells were detached with 0.25% trypsin, and resuspended in fresh complete medium. Mammalian cells were generally centrifuged at 1000 rpm for 10 min at RT (high speed centrifuge) or alternatively at 1500 rpm for 10 min at RT (table centrifuge).

The different cell lines used in this study as well as their respective media are indicated in the table below.

Cell line	Use	Media
293T	Production of recombinant viruses by co-transfection	DMEMc
A9	Production of wt MVMp Titration of wt and recombinant MVM	MEMc
GL261	Glioma tumor model	DMEMc
MLEC-PAI/Luc	TGF-β luciferase bio-assay	DMEMc + geneticin

Media and additives for cell culture were purchased from: Fluka, Gibco-Invitrogen, PAA Laboratories, and Sigma.

DMEM complete: (DMEMc)	10% FBS 100 U/ml Penicillin 100 µg/ml Streptomycin 2 mM Glutamine in DMEM	MEM complete: (MEMc)	5% FBS 100 U/ml Penicillin 100 µg/ml Streptomycin 2 mM Glutamine in MEM
DMEMc + geneticin:	250 µl/ml G418 in DMEMc		

3.3.2. Long term storage of mammalian cell lines

For cryopreservation, cells were trypsinised, collected in 15 ml tubes, pelleted by centrifugation, and resuspended at the desired density in freezing medium. The cell suspensions were aliquoted into cryovials, gradually frozen to -80°C overnight in a cell freezing box, and then transferred to a cryogenic refrigerator for long term storage in liquid nitrogen.

Freezing medium:	5% DMSO 5% Glycerol in DMEMc or MEMc

3.3.3. Thawing of mammalian cell lines

The cryo-preserved cells were quickly thawed in a water bath at 37°C and the cell suspension was added to pre-warmed medium containing all supplements. The cells were incubated overnight under standard conditions and the next day, fresh medium was provided.

3.3.4. Cell number and viability determination

3.3.4.1 Manual counting: trypan blue exclusion

This assay is based on the principle that living cells possess intact cell membranes that exclude certain dyes, such as trypan blue, eosin, or propidium, whereas dead cells do not and therefore take up the dyes. The cell suspension is simply mixed with dye and then visually examined to assess whether cells take up or exclude the dye.

An aliquot of cells was diluted in trypan blue solution, loaded onto a haemocytometer, and counted under a light microscope. For statistical significance, a minimum of 100 cells per large square were counted.

The cell concentration, total amount of viable cells, and the percentage of viability of a cell suspension were calculated as follows:

Total number of cells = cell concentration x volume of original cell suspension

Cell concentration (cells/ml) = average of viable cells per square x dilution factor x 10^4

$$Cell\ viability\ (\%) = \frac{number\ of\ viable\ cells}{total\ number\ of\ cells} x100$$

The factor 10^4 compensates for the volume of the counting chamber to obtain the amount of cells present per ml of cell suspension as the volume over the central counting area is 0.1 µl.

3.3.4.2 Automated counting: CASY cell counter and analyzer system

Automated cell counting was performed with a CASY cell counter and analyzer system. The CASY technology combines an established particle measurement technique with an additional pulse area analysis. For measurement of cell number or viability, the cell suspension is diluted in a weak electrolyte (CASY ton) and drawn through a capillary with a constant flow velocity. A low voltage field is applied to the capillary by two

platinum electrodes, resulting in a defined electrical resistance. During their passage, the cells displace a quantity of electrolyte corresponding to their volume and intact cells, considered as isolators, increase the resistance. These electric changes are proportional to the cell volume and can be used as a scale for living cells.

Depending on the cell amount, about 50 - 200 µl of cell suspension were diluted in 10 ml of CASY ton and gently mixed by inverting the solution. 400 µl of diluted cell suspension were then measured in triplets, and the number of viable and total cells as well as the viability were determined. Discrimination between vital and dead cells or cell debris was carried out by cell-type-dependent cursor setting as determined with the CASY blue solution.

3.4. Virological methods

3.4.1. Virus production

3.4.1.1 Production of wild-type parvovirus

Wild type MVMp was produced by infection of mouse A9 cells with a master stock of virus, and virions were extracted from the cells by freeze-thaw cycles in Viral Tris-EDTA (VTE) buffer as described by Kestler et al., 1999. The EDTA present in VTE complexes the calcium ions needed for the binding to the receptor and therefore leads to the release of the virus from the cell membrane. In addition, freeze-thaw cycles help destroying the cells. For large scale production, 21 x 10 cm cell culture dishes were seeded with A9 cells and incubated overnight so that they reached 90 - 95% confluency before infection. The cells were infected at a multiplicity of infection (MOI) of 3 x 10^{-3} plaque forming units/cell (PFU/cell), trypsinised 4 h post-infection and transferred to 15 cm dishes. The cells were further incubated for 4 to 5 days, until the cytopathic effects were visible. A9 cells were then detached from the plate with a cell scraper and pooled together with their media into 50 ml tubes. Cells were pelleted by centrifugation at 2500 rpm for 10 min at RT (swinging bucket rotor, high speed centrifuge), washed with PBS, and centrifuged again. The cell pellets were then resuspended each in 5 ml VTE and lyzed by three subsequent freeze-thawing cycles (-20°C/RT). Cell debris were pelleted by centrifugation at 2500 rpm for 10 min at RT (swinging bucket rotor, high

speed centrifuge), whereas supernatants, containing recombinant viruses were collected in 50 ml tubes and stored at 4°C. Pelleted cells were resuspended again in 5 ml VTE and viruses were extracted as described above. The supernatants were pooled to a final volume of 20 ml virus-containing crude extract, and further processed for purification or stored at 4°C.

VTE buffer: 50 mM Tris-HCl, pH 8.7
              0.5 mM EDTA, pH 8.0

3.4.1.2 Production of recombinant MVM parvoviruses

Recombinant viruses were produced in 293T cells by calcium phosphate co-transfection of parvoviral vector DNA and helper plasmid, as described by Haag et al., 2000; Kestler et al., 1999. On the day before transfection, 30 x 10 cm culture dishes were seeded with 2×10^6 293T cells and incubated overnight so that they reached 90 - 95% confluency before the transfection. Per dish, 6 µg recombinant vector DNA and 12 µg of capsid protein-providing helper plasmid pBK-CMV/VP were suspended in a 250 mM $CaCl_2$ solution. In parallel, a separate tube containing an equal volume of HBSS 2x, pH 7.05 was prepared. Following, the DNA/$CaCl_2$ solution was added drop-wise to the HBSS solution under delicate mixing. The mixture was allowed to precipitate for 15 - 20 min and then spread equally onto the 293T cells. Three days post-transfection, virions were extracted from the cells as described for wild-type MVMp and further processed for purification or stored at 4°C.

HBSS, 2x: 280 mM NaCl
            50 mM HEPES
            12 mM D-Glucose
            10 mM KCl
            1.5 mM Na_2HPO_4
            pH 7.05

3.4.2. Purification and buffer exchange of virus stocks

3.4.2.1 Virus purification through iodixanol density gradient centrifugation

Virus purification was performed through an iodixanol discontinuous density gradient ultracentrifugation, adapted from Zolotukhin et al., 1999. The gradient is formed by under-layering and displacing the less dense cell lysate with solutions of increasing iodixanol concentration, buffered in PBS supplemented with 1 mM $MgCl_2$ and 2.5 M KCl (PBS-MK). For each gradient, 20 ml of the virus-containing clarified lysate were transferred into a 40 ml polyallomer centrifuge tube using a Pasteur pipette. Successively, 7 ml of 15%, 5 ml of 25%, 4 ml of 40%, and 4 ml of 60% iodixanol solutions were under-layered. To prevent aggregation of virus particles with proteins from the cell lysates, NaCl was added to the 15% iodixanol solution to a final concentration of 1 M. In addition, phenol red was added to the upper 25% and lower 60% density steps to a final concentration of 0.01 µg/ml to distinguish the different phases. Tubes were sealed and ultra-centrifuged at 50000 rpm for 2.5 h at 10°C (fixed angle rotor). The centrifuge tube was then ventilated with a syringe needle at the top and the 40% layer, containing full virus particles, was recovered under sterile conditions by inserting a syringe needle below the 60% to 40% density interphase and collecting a total of about 4 ml. The purified viral suspension was stored at 4°C.

PBS:	136.9 mM NaCl	PBS-MK:	2.5 mM KCl
	2.7 mM KCl		1 mM $MgCl_2$
	4.9 mM KH_2PO_4		in PBS
	1.8 mM K_2HPO_4		
	pH 7.2 - 7.4		

3.4.2.2 Buffer exchange of virus suspensions

For *in vivo* virus injection, a buffer exchange of the iodixanol virus suspension to Dulbecco PBS (DPBS) was performed using centrifugal buffer exchange columns, according to the manufacturer's instructions. Viral suspensions in DPBS were short-term stored at 4°C.

3.4.3. Virus titration

3.4.3.1 Wild type infectious titer determination: Plaque assay

This method, routinely performed to titrate replication competent viruses, was used to determine the infectious titer of wt MVMp as described by Cornelis et al., 1988.

Briefly, 2.5×10^5 A9 cells per 6 cm culture dish were infected with serial dilutions (10^{-6} - 10^{-10}) of wt MVM. Dilutions were performed in duplicate and mock-infected cells were included as control. After aspiration of the inoculum, the cells were covered with 7 ml overlay medium 1 and incubated at 37°C in a CO_2 incubator. 5 days post-infection, cells were stained with 3 ml of overlay medium 2, containing neutral red and incubated overnight at 37°C. The plates were dried and the plaques scored visually.

Titers are expressed as plaque forming unit (PFU) per ml of virus suspension, and calculated as follows:

$$Titer\ (PFU/ml) = \frac{average\ number\ of\ plaques}{dilution\ x\ inoculum\ volume}$$

<u>Bacto-Agar, 1.7%</u>	1.7% (w/v) Bacto-Agar in LB-medium	<u>Overlay medium 1:</u>	3/7 Bacto-Agar 1.7% 4/7 MEMc 2x
<u>Neutral red solution:</u>	0.33% (w/v) neutral red pH 6.8 - 7.0	<u>Overlay medium 2:</u>	2/32 neutral red sol. 15/32 PBS 2x 15/32 Bacto-Agar 1.7%

3.4.3.2 Recombinant and wt infectious titer determination: Hybridization assay

This method, adapted for the titration of recombinant viruses, unable to produce progeny virions, measures the amplification of viral DNA within infected cells using a radioactive-labeled viral DNA probe as described by Kestler et al., 1999.

2.5×10^5 A9 cells per 6 cm culture dish were infected with serial dilutions (10^{-4} - 10^{-7}) of recombinant virus in supplement-free MEM. Dilutions were performed in duplicate and mock-infected cells were included as control. 48 h post-infection, the medium was aspirated and cells were washed with sterile PBS. Cells were transferred onto nitrocellulose filters by placing gently the filters on the cells and moistening them with 100 μl PBS. Cells were lyzed and their DNA denatured by applying the filters to denaturation buffer for 8 min and subsequently neutralized in neutralization buffer for 10 min. Fixation of the DNA was performed by backing filters for 2 h at 80°C. To avoid

unspecific binding of the radioactive probe, filters were pre-hybridized for at least 1 h at 65°C in hybridization solution supplemented with 0.2 ng of heat-denatured herring sperm DNA per ml hybridization solution. The denatured radioactive labeled DNA probe (see section 3.2.9) was added to the hybridization solution and hybridization was performed overnight at 65°C. The next day, the hybridization solution was discarded and membranes were washed twice in washing solution 1 for 45 min at 65°C and once in washing solution 2 for 15 min at 65°C. After air-drying, the membranes were exposed to X-ray films in an autoradiography cassette for 24 - 72h at -80°C in the presence of an amplifier screen and films were developed in a darkroom film processor. Each spot on the X-ray film represents viral DNA-replication within one cell. Alternatively, this method was also used for titration of wt MVM. In this case, the infection was stopped 28 h post-infection in order to avoid secondary infections.

Titers are expressed as replication unit (RU) per ml of virus suspension and calculated as follows:

$$Titer\ (RU/ml) = \frac{average\ number\ of\ spots\ x\ 7.5}{dilution}$$

$$Factor\ 7.5 = \frac{21.5\ cm^2\ (dish\ area)}{7.2\ cm^2\ (filter\ area)} \times \frac{1000\ \mu l}{400\ \mu l}\ \frac{(fraction\ of}{inoculum)}$$

Denaturation buffer:	1.5 M NaCl 0.5 M NaOH	Neutralization buffer:	1.5 M NaCl 1 mM EDTA 0.5 M Tris-HCl pH 7.0
SSC, 20x:	3M NaCl 300mM Tri-Na-Citrate pH 7.0	Hybridization solution:	3x SSC 1% (w/v) SDS 5 mM EDTA 10x Denhardt's
Denhardt´s, 100x:	2% (w/v) BSA 2% (w/v) Ficoll 400 2% (w/v) PVP	Washing solution 1:	3x SSC 1% (w/v) SDS
		Washing solution 2:	0.3x SSC 1% (w/v) SDS

3.4.4. Virus infection of adherent cells

To infect mammalian cell lines, a defined ratio of infectious virus particles to cell is used, termed multiplicity of infection (MOI). Depending on the titration method, the MOI is expressed as PFU/cell (plaque assay) or RU/cell (hybridization assay).

On the day before infection, the cells were seeded at the appropriate density and incubated overnight in a 37°C incubator. The culture medium was aspirated and 0.1 ml (24 well plate), 0.4 ml (6 cm dish), or 1 ml (10 cm dish) of virus inoculum was applied onto the cell monolayer. Virus dilutions with the appropriate MOI were prepared in supplement-free MEM or DMEM, depending on the cell type. Virus stocks were diluted at least 1:3 in media to avoid high concentrations of iodixanol which could affect the infection efficiency. As negative control (mock infection), virus free buffer was used as inoculum. Cells were incubated under standard conditions for 1 h and the dishes were gently rocked every 10 min to allow the inoculum to spread evenly over the whole dish. Finally, the inoculum was replaced by complete fresh medium and cells were further incubated at 37°C.

3.4.5. Assessment of progeny virion production by virus production assay

2×10^5 GL261 or A9 cells were seeded in 6 cm plates and infected at a MOI of 0.1 or 1 PFU/cell. 7 days post-infection, cells were scraped in their culture medium, transferred into 15 ml tubes, and pelleted by centrifugation at 2500 rpm for 10 min at RT (swinging bucket rotor, high speed centrifuge). The supernatant was collected in a new tube and stored at -20°C until further processing. The cell pellet was resuspended in 1 ml VTE and viruses were extracted from the cell pellet as described above (see section 3.4.1.1), performing five freeze-thaw cycles. Titration of progeny virions present in the cell pellets and supernatants respectively was performed by plaque assay (see section 3.4.3.1).

3.5. Biochemical methods

3.5.1. Quantification of TGF-β in cell supernatants: PAI/L bioassay

The amount of TGF-β present in cell supernatants was assayed using the plasminogen activator inhibitor-1 / luciferase (PAI/L) bioassay, as described by Abe et al., 1994 . This quantitative bioassay is based on the ability of TGF-β to induce PAI-1 expression, using mink lung epithelial cells (MLEC) stably transfected with a luciferase reporter gene under the control of a truncated PAI-1 promoter. Under these conditions, binding of TGF-β to the receptors of the PAI-1/Luc transfected MLEC (MLEC-PAI/Luc) results in a dose-dependent increase of luciferase activity.

Briefly, transfected MLEC cultures were plated in a 96 well plate at a density of 1.6×10^4 cells per well in complete DMEM supplemented with geneticin and allowed to attach for 3 h at 37°C in a 5% CO_2 incubator. After being washed once with production media, MLEC cells were further incubated for 14 to 18 h with 100 µl of cell supernatants to be investigated, or recombinant human TGF-β1, serially diluted in production media (0 - 4 µg/ml), to generate a standard curve. Cells were then washed twice with PBS and lyzed using 20 µl of cell lysis buffer for 30 min at RT under gentle agitation. The cell lysates were freezed at -20°C for 3 h and 20 µl cell lysates were subsequently transferred to an opaque 96 well plate. The bioassay was measured in a luminometer following the injection of 100 µl/well luciferase substrate reagent, using a luciferase assay system according to the manufacturer's instructions. Luciferase activity was reported as relative light units (RLU), converted into concentrations using the standard curve obtained with human recombinant TGF-β1 and normalized in cell number.

Only the active form of TGF-β is detected with the MLEC-PAI/Luc bioassay. Therefore, to evaluate the amount of total (active and latent) TGF-β, half of the cell supernatants were transiently acidified with 1 N HCl for 5-10 min at RT, followed by neutralization with 1 N NaOH prior addition to the MLEC cells.

Production Media:	0.1% (w/v) BSA	Cell lysis buffer:	25 nM Tris-HCl pH 7.4
	100 U/ml Penicillin		2 mM EDTA-NaOH pH 7.4
	100 µg/ml Streptomycin		10% Glycerol
	2 mM Glutamine		1% NP40
	in DMEM		2 mM DTT

3.6. Immunological methods

3.6.1. Cytokine quantification by enzyme-linked immunosorbent assays (ELISA)

The expression of cytokines *in vitro* was measured by a quantitative sandwich enzyme immunoassay, ELISA, which specifically detects and quantitates the concentration of soluble cytokines. Briefly, a capture antibody, specific for the cytokine of interest, is pre-coated onto a microplate and the plate is blocked to avoid non-specific binding. Standards, controls, and samples are distributed into the coated wells and the cytokine of interest is bound to the immobilized capture antibody. A detection antibody, horseradish peroxidase-linked specific for the cytokine is then added, followed by a

chromogenic substrate solution, which is acted upon by the bound enzyme to produce color. The reaction is stopped, and the levels of colored product are determined spectrophotometrically at 450 nm using a microplate reader. The intensity of this colored product is directly proportional to the amount of cytokine bound in the initial step. Cytokine concentrations are determined from the standard curve established from serial dilutions of a recombinant cytokine.

The levels of cytokines released in cell culture supernatants were determined with commercially available ELISA kits according to manufacture's instructions or with specific ELISA established by the laboratory of Prof. Dr. Jo Van Damme (Rega Institute, University of Leuven, Belgium) for hMCP-2, hMCP-3 and hIP-10.

Cell supernatants were harvested at the indicated time post-infection (p.i.), and stored at -80°C until analysis. The cumulative and daily cytokine production were determined. For the measurement of daily cytokine production, the medium was removed, frozen and replaced with fresh medium every day.

3.6.2. Immunohistochemistry

Immunohistochemistry was done in collaboration with the laboratory of Prof. Dr. Ralf Kinscherf, in the Centre for Biomedicine and Medical Technology Mannheim (CBTM), Medical Faculty Mannheim, University of Mannheim.

3.6.2.1 Immunohistochemical staining

Cryosections (6 µm) were cut with a microtome, mounted on Superfrost microscope slides, fixed in acetone for 10 minutes at -20°C and air-dried for 30 min.

The sections were fixed in 4% paraformaldehyde in PBS for 10 min, washed three times with PBS for 5 min and non-specific binding sites were blocked in 1% normal swine serum in PBS for 10 min. All subsequent washing steps were performed with PBS for 5 min. The primary antibody (see section 2.7.1) diluted in PBS was applied on the tissue and incubated overnight at RT in a humidified chamber. The sections were then washed twice and the endogenous peroxidase activity was blocked with 3% hydrogen peroxide in PBS for 5 min at RT. The sections were then washed three times and the corresponding secondary biotinylated antibody (see section 2.7.2) was applied to the tissue and incubated at 37°C for 30 min. After being washed twice, the sections were incubated for 30 min at 37°C with streptavidin-horse radish peroxidase (HRP) complex diluted 1:100 in PBS. After washing three times, a chromogenic substrate solution was

added, either diamino-benzidine (DAB) or histogreen, staining in brown or green, respectively, and the reaction was stopped with PBS. The sections were counterstained with hematoxylin according to Mayer's protocol for a few seconds and washed twice in water for 5 min. The sections were then dehydrated by successive incubations in 99% ethanol (twice) and rotihistol (three times, xylol replacement) and cover glasses were placed using mounting medium.

Apoptosis measurement was performed by terminal deoxynucleotidyl transferase biotin-dUTP nick end labeling (TUNEL) assay using a commercially available kit following the manufacturer's instructions. This method allows detection of free 3'-OH termini present in the DNA of apoptotic cell by enzymatic labeling.

PBS: 136.9 mM NaCl
2.7 mM KCl
4.9 mM KH2PO4
1.8 mM K2HPO4
pH 7.2 - 7.4

Paraformaldehyde, 4%: 4% (w/v) paraformaldehyde in PBS

3.6.2.2 Morphometric analyses

Cryosections were photographed using an Axio Imager Z1 microscope equipped with the AxioVision Rel 4.7 imaging software and digitalized images were processed with the same software to measure labeled nucleus, cells, or surfaces.

For the intracranial model, the whole tumor was photographed and analyzed, whereas for the subcutaneous model, 10 regions of interest per tumor were photographed and analyzed.

3.7. Animal experiments

3.7.1. Mouse handling

Animals were kept under specific pathogen-free conditions within the central animal facility at the German Cancer Research Center of Heidelberg. Mice were housed five per cage within a flexible film isolator. The temperature was maintained at 21 - 24°C and the relative humidity at 40 - 60%. All animals were housed under the same conditions with food and water ad libitum, with a 12 h regime light schedule. Animal

experimentation was performed in compliance with institutional, governmental, and EU guidelines, and in accordance with recommendations for proper care and use of laboratory animals. All mice used in experiments were females between 7 and 9 weeks of age. Individual animals were identified using ear punches. Animals were sacrificed by cervical dislocation or CO_2 inhalation.

3.7.2. Subcutaneous GL261 tumor model

3.7.2.1 Preparation of virus for injection in established subcutaneous tumors

Prior to injection in established tumors, the virus stock was diluted to desired concentration of viral particles in DPBS, or buffer exchanged to DPBS when the ratio iodixanol:DPBS was higher than 1:3 to avoid iodixanol- or phenol red-mediated side effects. Virus in DPBS was kept on ice until the injection or alternatively stored for short time at 4°C.

3.7.2.2 Subcutaneous inoculation of GL261

Subcutaneous tumors were established by injection of GL261 cell suspension into the mice right posterior flank. To transfer the tumor, the flank of the carrier was shaved and 1×10^6 cells GL261 cells were injected subcutaneously in 100µl of DPBS with a 1 ml fine dosage syringe.

3.7.2.3 Virus injection in established subcutaneous tumors

100 µl of virus suspension was applied peritumorally to avoid mechanical damage of the tumor.

3.7.2.4 Subcutaneous tumor growth monitoring

After subcutaneous tumor inoculation, the tumor growth was monitored every 2 to 3 days by measuring its dimensions using an electronic digital caliper. The tumor volume (*V*) was calculated using the formula for an ellipsoid, $V(mm^3)=(\pi/6) L \times W \times H$, where *L* is the length and *W* the width and *H* the height of the tumor.

Animals were sacrificed when the tumor volume reached 4 cm^3, one dimension exceeded 2 cm, or in case of necrosis.

3.7.2.5 Tumor embedding for immunohistochemistry

Mice were sacrificed at the indicated time by cervical dislocation and the subcutaneous tumors were resected. The tumor samples were placed in cryomolds and embedded in OCT compound for cryo-sectioning. The cryomolds were then snap frozen in liquid nitrogen-cooled isopentane and stored at -80°C.

3.7.3. Intracranial GL261 tumor model

3.7.3.1 Preparation of in vitro infected cells for intracranial injection

Three hours post-infection, virus-infected tumor cells were trypsinized, collected by centrifugation, and washed twice with calcium- and magnesium-free DPBS. The cells were then counted, resuspended in DPBS at a concentration of 2.5×10^4 cells/µl, and kept on ice until the injection.

3.7.3.2 Intracranial inoculation of GL261

Intracranial implantation of 1×10^5 *in vitro* infected GL261 cells was performed stereotactically in the left striatum.

Female 7 to 9 weeks old C57BL/6 mice were anesthetized by intraperitoneal injection of a mixture of ketamin (0.1 mg/g body weight) and xylazin (0.02 mg/g body weight) in 0.9% NaCl. The eyes of the mice were carefully covered with an antiseptic cream to avoid cornea drying. The head of the mouse was fixed in a stereotactic frame fitted with a mouse adaptor. A 1 cm midline scalp incision was made to expose the surface of the skull and a small hole was made into the left side of the skull with a 25 gauge needle at the defined location of the caudate/putamen, in the striatum, 2.5 mm lateral to the sagittal suture at the level of the bregma. The cortical surface was carefully cleared of any traces of blood using absorbent swabs. Tumor cells were delivered using a 10 µl syringe with a 33 gauge needle inserted into an automated microinjection unit. The syringe was inserted to a depth of 3.5 mm and retracted to a depth of 3 mm below the surface of the skull to create an injection canal. 1×10^5 GL261 cells suspended in 4 µl of phosphate buffer (DPBS) were stereotactically injected with an injection rate of 250 nl/min. Following injection, the needle was left in place for an additional 5 min and then slowly withdrawn to minimize any back-flow through the insertion canal. The skin was sutured with non absorbable nylon thread and the mice were placed on a heating

pad until recovery from anesthesia. Animals were monitored daily after treatment and sacrificed at the indicated time.

3.7.3.3 Intracranial tumor growth monitoring by MRI

Magnetic resonance imaging (MRI) provides high soft tissue contrast and high spatial resolution. Due to MRI as a non invasive *in vivo* imaging modality individual animals can be examined at various time points during longitudinal animal studies with little or no effect on measured animals.

After intracranial tumor inoculation, tumor growth was monitored weekly by MRI. To avoid movements during MRI measurements, mice were immobilized by inhalation anesthesia applied by a nose cone (1.5% isoflurane in oxygen). MRI measurements were performed using a 1.5 tesla whole-body MR-scanner (see Figure 3-1 B) in combination with a custom-made radio-frequency coil for excitation and signal reception (see Figure 3-1 A). Morphologic MR-imaging was carried out using a transversal T2-weighted turbo-spin echo sequence (repetition time, TR = 1,510 ms, echo time, TE = 59 ms, field of view, FOV = 50 x 50 mm^2, matrix 128, slice thickness = 1.0 mm).

Regions of interest were drawn by hand around tumor borders on every acquired two-dimensional (2D) slice, and the tumor surface was determined on the MR scan with the biggest tumor diameter (see Figure 3-1 C).

Morphologic MRI was done in collaboration with the division of Medical Physics in Radiology of the DKFZ (Prof. Dr. Dr. Semmler) by M. Batel and Dr. M. Jugold.
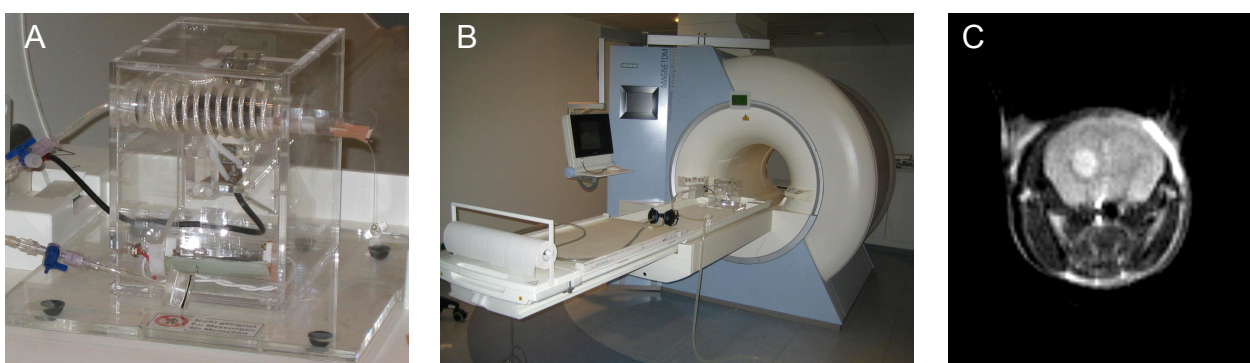
Figure 3-1: Magnetic resonance imaging of mouse glioma

Mice to be imaged were anesthetized and placed in a custom-made animal coil (**A**). Magnetic resonance imaging was performed on a clinical 1.5 T MR scanner (**B**), using a Turbo Spin Echo Sequence. Transversal sections of the brain (**C**) were obtained on which the tumor size was estimated.

3.7.3.4 Tumor embedding for immunohistochemistry

Mice were sacrificed at the indicated time by CO_2 inhalation. The brains were dissected and divided at the injection site into two coronal pieces. Tumor samples were placed in cryomolds and embedded in OCT compound for cryo-sectioning. The cryomolds were then snap frozen in liquid nitrogen-cooled isopentane and stored at -80°C.

3.7.3.5 Survival follow-up

Survival curves were constructed using the Kaplan and Meier survival rate analysis (Kaplan and Meier, 1958). For this, the percentage of surviving mice in the different groups of animals was recorded daily after glioma implantation. Moribund animals were euthanized and their death recorded as occurring on the following day. The median survival, representing the time at which half the subjects have died, was estimated for each group. In the cases where the survival curve was horizontal at 50% survival, the median survival time was calculated as the average of the two time points at which the survival curve equals 50 %.

3.8. Statistics

Statistical analyses for the intracranial tumor growth and animal survival were performed in collaboration with Dr. Lutz Edler (department of Biostatistics, DKFZ) using the nonparametric Wilkinson Rank Sum and Koziol tests (Koziol et al., 1981).
All other statistical analyses were performed using the Student *t* test.
P values < 0.05 were considered statistically significant.

4. RESULTS

Gliomas are highly vascularized solid tumors, known to induce an immunosuppressive environment. In this context, our laboratory has recently investigated the antitumor effects of parvoviral vectors delivering TNF-α and IP-10, cytokines known to have both immunostimulatory and antiangiogenic properties, in a syngeneic subcutaneous glioma tumor model. The growth of mouse glioma GL261 cells infected *in vitro* with TNF-α- or IP-10-transducing parvoviruses, grafted subcutaneously in C57BL/6 mice, was significantly delayed compared to buffer-treated cells or to cells infected with the vector devoid of transgene (Chi-MVMp/Δ800). A complete tumor regression was observed when GL261 cells were coinfected with both TNF-α- or IP-10-encoding parvoviruses. The treatment of established tumors with repeated peritumoral injection of cytokine-encoding parvoviruses also inhibited tumor growth compared to tumors treated with Chi-MVMp/Δ800, MVMp wt, or buffer-treated tumors, but to a lesser extend than in the *in vitro* setting. *In vivo*, the antitumor effects of TNF-α- and IP-10- transducing vectors or the combination of both were comparable.

This work was initiated by Enderlin M. (Enderlin, 2004) and was completed during the present work, leading to a publication in which I contributed as second author (Enderlin et al., 2008).

In this thesis, the mechanisms sustaining GL261 subcutaneous tumor inhibition were investigated. Next, the analysis of the antitumor effects of these parvoviral vectors was extended to GL261 implanted intracranially in syngeneic mice.

Monocyte chemotactic proteins MCP-2 and MCP-3 are known to be potent immunoactive cytokines, recruiting a broad range of leukocytes. Parvoviral vectors delivering MCP-3 were previously demonstrated to inhibit the tumor growth of human Hela grafted in nude mice (Wetzel et al., 2001) and mouse melanoma implanted subcutaneously in syngeneic mice (Wetzel et al., 2007). This prompted us to investigate the antitumor effects of parvoviruses delivering these chemokines in the GL261 glioma tumor model.

4.1. Production of wt and recombinant MVM parvoviruses

Wild-type (wt) MVMp was produced by infection of mouse A9 cells, the reference producer cell line, with a master-stock of virus available in the laboratory. Recombinant MVMp-derived viruses Chi-MVMp/Δ800, Chi-MVMp/TNF-α, Chi-MVMp/IP-10, Chi-MVMp/MCP-2, and Chi-MVMp/MCP-3 were produced in 293T cells by co-transfection of the corresponding recombinant MVMp DNA clones with a helper plasmid, providing the parvoviral capsid proteins in trans.

The virus stocks were purified by iodixanol gradient ultracentrifugation and titrated either by infected cell hybridization assay (recombinant and MVMp wt viruses), or by plaque assay on A9 cells (MVMp wt). The infectious titers of wt virus determined by infected cell hybridization (4×10^9 RU/ml) and plaque assay (3×10^9 PFU/ml) were comparable and typically higher than the ones of recombinant viruses which ranged between 9×10^6 and 10×10^7 RU/ml. This difference can be assigned to the capacity of wt MVMp to produce progeny virions through secondary infections during the production procedure, whereas recombinant viruses are replication defective.

4.2. Characterization of GL261 infected with wt MVMp and MVMp-based vectors *in vitro*

The recombinant parvoviruses used in this study are so-called capsid replacement vectors. While they retain the expression of parvoviral non-structural proteins (NS1 and NS2) under the control of the P4 promoter, the viral capsid proteins genes, driven by the P38 promoter, have been replaced by cDNA encoding cytokines or chemokines.

Mouse glioma GL261 cells infected *in vitro* with recombinant parvoviruses were analyzed for the expression of the transgenes. Next, the effects of both wt and recombinant MVMp infection on GL261 cellular growth were analyzed.

Recombinant viruses encoding TNF-α and IP-10 strongly inhibited the growth of GL261 mouse glioma cells grafted subcutaneously in C57BL/6 mice, especially when used in combination (Enderlin et al., 2008). Therefore, in addition to the effects of parvoviral infection using single vectors, the effects of the coinfection of these both viruses were also investigated in the following experiments.

4.2.1. Transgene expression in GL261 after infection with parvoviral vectors

High and transient expression of transgenes is a prerequisite in cytokine-mediated cancer gene therapy. Indeed, sustained expression of a cytokine could lead to chronic inflammation or autoimmunity and hence induce severe adverse reactions.

We first verified the expression of transgenes in infected GL261 at the mRNA level, together with the expression of MVMp non-structural protein NS1. Indeed, NS1, retained in parvoviral capsid replacement vectors, is involved in the amplification of the viral genome and transactivates the parvoviral P38 promoter, driving the expression of the transgene (Kestler et al., 1999). For this, 2×10^5 GL261 cells were infected with Chi-MVMp/TNF-α, Chi-MVMp/IP-10, Chi-MVMp/MCP-2, and Chi-MVMp/MCP-3 at an MOI of 3 RU per cell. GL261 cells infected with Chi-MVMp/Δ800, or MVMp wt at an MOI of 3 RU per cell, or buffer-treated (mock) served as controls. Total RNA was isolated 24 h post-infection, reverse-transcribed, and amplified by PCR using specific primers flanking the transgene in MVMp-derived vectors and for the MVMp non-structural protein NS1. Figure 4-1 shows the result of one representative experiment out of two.
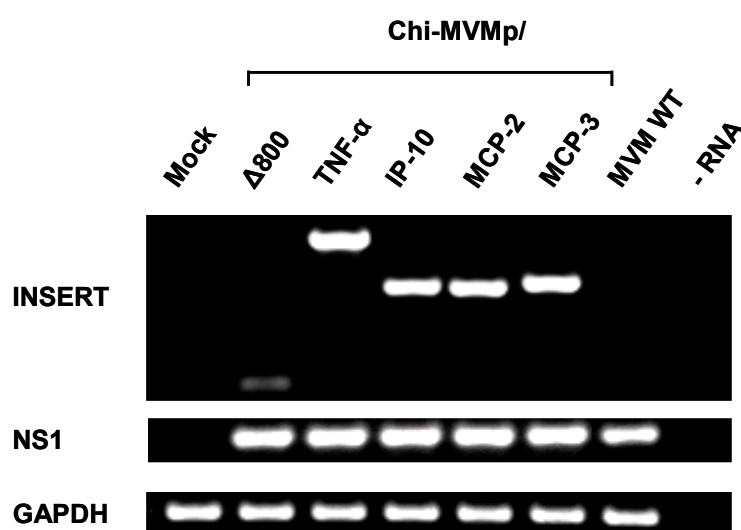

Figure 4-1: Expression of transgenes and NS1 by GL261 after infection with MVMp-derived vectors

2×10^5 GL261 cells were infected with Chi-MVMp/TNF-α, Chi-MVMp/IP-10, Chi-MVMp/MCP-2, and Chi-MVMp/MCP-3 (MOI = 3 RU/cell). Cells infected with Chi-MVMp/Δ800, MVMp wt (MOI = 3 RU/cell), or buffer-treated (mock) served as controls. Total RNA was isolated 24 h post-infection, reverse-transcribed, and amplified by PCR using specific primers for the multiple cloning site of MVMp-derived vectors and MVMp non-structural protein NS1. GADPH was used as loading control and a RT-PCR with all reagents except RNA (-RNA) was included as negative control.

The expression of the transgenes and their relative size was verified at the mRNA level by amplification of the region comprised in the multiple cloning site of MVMp-based vectors. Furthermore, the levels of NS1 mRNA in GL261 cells were similar in all infected

cells, showing similar efficiency of infection by the different vectors. The expression of GAPDH was used as control for sample loading, and as expected no amplification products were obtained when RNA was omitted from the reaction.

In order to evaluate the levels of cytokines secreted in the culture medium by GL261 cells upon infection with recombinant MVMp viruses, 2×10^5 GL261 cells were infected with Chi-MVMp/TNF-α, Chi-MVMp/IP-10, Chi-MVMp/MCP-2, or Chi-MVMp/MCP-3 at an MOI of 3 RU per cell, and the amounts of cytokines released in the culture medium were measured by ELISA at day 1 to 4 post-infection. As controls, 2×10^5 GL261 cells were also infected with Chi-MVMp/Δ800 or MVMp wt at an MOI of 3 RU per cell or buffer-treated. Figure 4-2 shows the cumulative and daily production of secreted cytokines determined in one representative experiment.
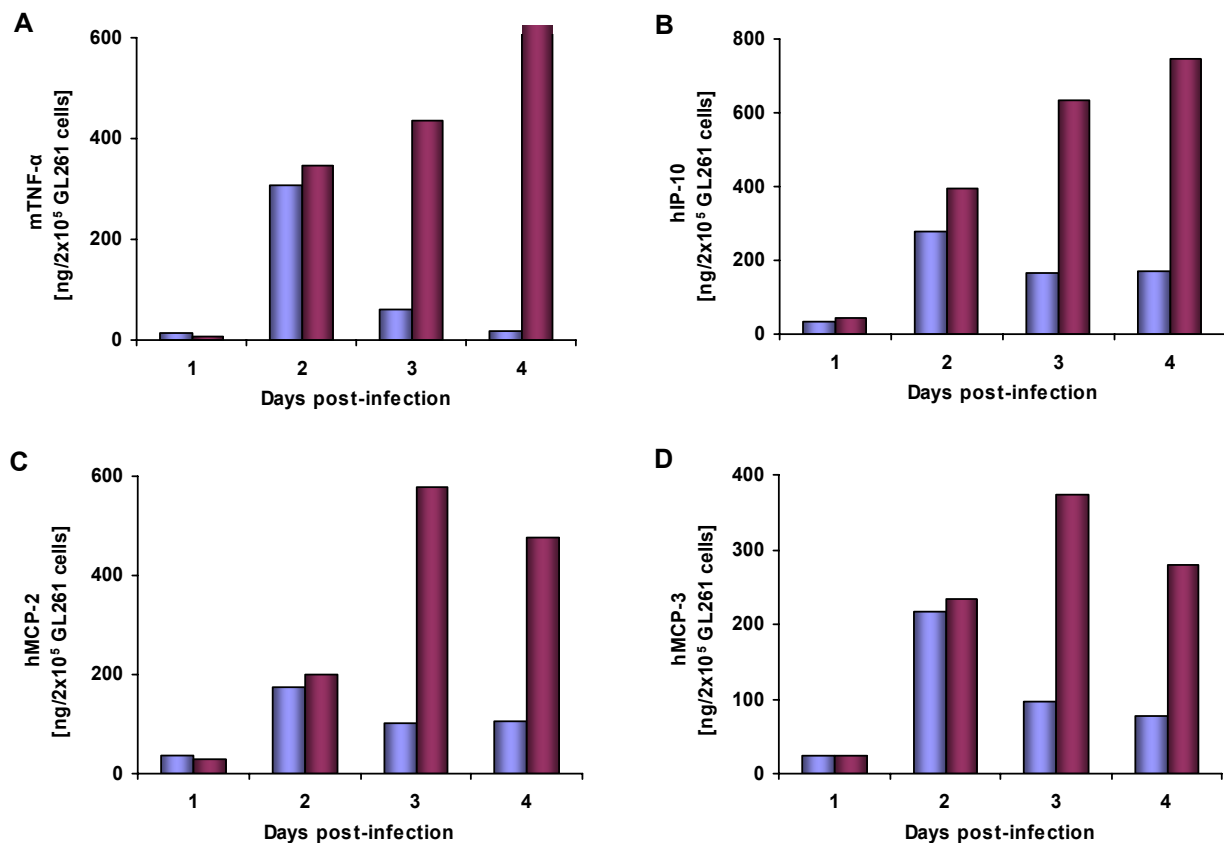
Figure 4-2: Levels of mTNF-α, hIP-10, hMCP-2, and hMCP-3 in GL261 supernatants after infection with MVM-based vectors

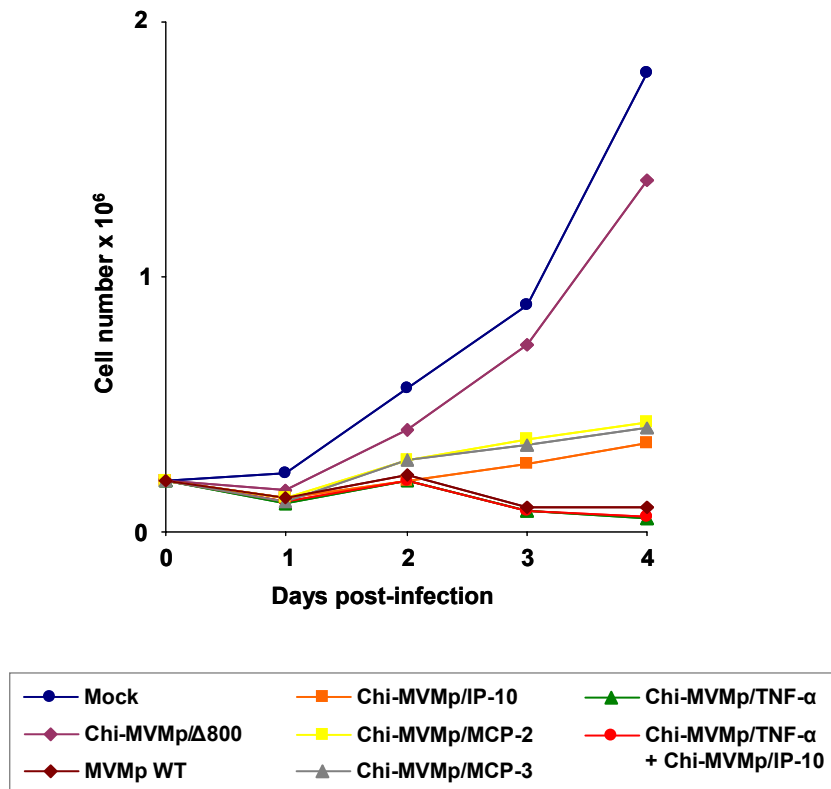2×10^5 GL261 cells were infected with Chi-MVMp/TNF-α (**A**), Chi-MVMp/IP-10 (**B**), Chi-MVMp/MCP-2 (**C**), or Chi-MVMp/MCP-3 (**D**) (MOI = 3 RU/cell). GL261 cells infected with Chi-MVMp/Δ800, MVMp wt (MOI = 3 RU/cell) or buffer-treated (mock) served as controls. Cell supernatants were harvested either daily (blue bars) or after 1 to 4 days for the accumulated (violet bars) cytokine secretion. The levels of cytokines released in the culture medium were measured by ELISA and expressed as nanograms per 2×10^5 initially infected cells. All cytokine determinations were carried out at least in duplicates. The cytokines content in cell supernatants from Chi-MVMp/Δ800-, MVMp wt-, or mock-infected cells were lower than 8 ng per 2×10^5 GL261 cells.

The daily release of cytokines delivered by parvoviral vectors increased from day 1 post-infection, peaked at day 2, and decreased thereafter, as previously observed in HeLa cells for hH-1/MCP-1 (Haag et al., 2000) or hH-1/MCP-3 (Wetzel et al., 2001). The peak production of cytokine at day 2 post-infection was observed for all vectors, ranging between 175 (MCP-2) and 276 (IP-10) ng per 2 x 10^5 initially infected GL261 cells. Transgenes accumulated in large amounts ranging from 350 ng (MCP-2) up to 750 ng (IP-10) of cytokines per 2 x 10^5 cells. The accumulation of cytokines in the cell culture medium increased and reached a plateau 4 or 5 days post-infection (data not shown), suggesting that all cytokines were stable for at least 5 days in the cell culture medium. As expected, human MCP-2, MCP-3, and IP-10 were undetectable in the supernatants of mouse GL261 cells infected with Chi-MVMp/Δ800-, MVMp wt- or mock-infected cells showing the specificity of the ELISAs for human chemokines. No mouse TNF-α secretion could be detected in the same settings indicating that GL261 cells did not constitutively express mTNF-α and that its expression was not induced after infection with these parvoviral vectors.

Taken together, these results show that parvoviral-mediated gene expression in GL261 fulfills the conditions for gene therapy as mTNF-α, hIP-10, hMCP-2, and hMCP-3 are transiently secreted in high amounts into the culture medium of GL261 cells infected with the respective vector. The cytokine yields obtained in GL261 cells with recombinant parvoviruses were much higher than those obtained with retroviral or adenoviral vectors, transducing respectively MCP-1 (Herrlinger et al., 2004) and TNF-α (Ehtesham et al., 2002), where the production was limited to pg levels.

4.2.2. Effects of wt and recombinant MVMp infection on GL261 cellular growth

In order to investigate the effects of the parvoviral infection and the transduced genes on GL261 cells, the growth of *in vitro* infected GL261 cells was monitored over 4 days. 2 x 10^5 GL261 cells were infected with MVMp wt, Chi-MVMp/TNF-α, Chi-MVMp/IP-10, Chi-MVMp/MCP-2, Chi-MVMp/MCP-3, or Chi-MVMp/Δ800 at an MOI of 3 RU per cell or buffer-treated (mock). For the coinfection with Chi-MVMp/TNF-α and Chi-MVMp/IP-10, an MOI of 1.5 RU per cell was used for each vector. The number of viable cells was determined from day 1 to 4 post-infection by the trypan blue dye exclusion method. Figure 4-3 shows the result of one representative experiment out of three.

Figure 4-3: Cellular growth of GL261 after infection with MVMp or MVMp based vectors
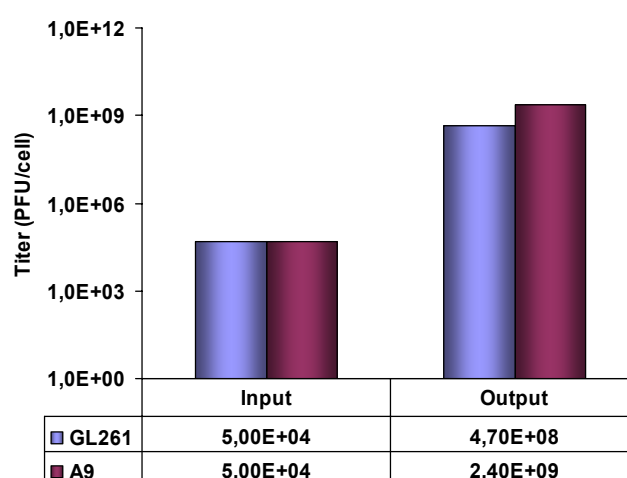
2×10^5 GL261 cells were infected with MVMp-based vectors and wt (MOI = 3RU/cell), coinfected with Chi-MVMp/TNF-α and Chi-MVMp/IP-10 (MOI = 1.5 RU/cell for each vector) or buffer-treated (mock). The number of viable cells was determined at the indicated times by the trypan blue dye exclusion method.

Buffer-treated (mock) GL261 cells grew fast, with a generation time of about 24 h. The infection with Chi-MVMp/Δ800 had only a marginal effect on the cellular growth. In contrast, infection with Chi-MVMp/IP-10, Chi-MVMp/MCP-2, and Chi-MVMp/MCP-3 displayed cytostatic effects on GL261 cells, as shown by a limited increase in the cell number. Infection of GL261 cells with MVMp wt, Chi-MVMp/TNF-α alone, or coinfection with Chi-MVMp/IP-10 had comparable cytotoxic effects, as shown by the drop in the number of living cells from day 3 post-infection. This suggests a toxicity of the accumulated transgene products in GL261 cells, especially of TNF-α. The effects observed with wt MVMp, TNF-α-, and IP-10-encoding viruses are consistent with the results previously obtained in the laboratory (Enderlin, 2004). Indeed, GL261 glioma cells were shown to be very sensitive to TNF-α *in vitro*, either recombinant or parvoviral-transduced and thus an autocrine cytotoxic effect of TNF-α, accumulated in the cell culture medium, is very likely. The cytotoxic effect of wt MVMp can be assigned to the ability of GL261 cells to produce progeny virions and to induce secondary infections, as shown in Figure 4-4.

4.2.3. Production of progeny virions by MVMp-infected GL261

Since MVMp exerted a high cytotoxicity on GL261 cells *in vitro*, we investigated whether GL261 cells were able to produce progeny virions upon MVMp infection. To this end, 2×10^5 GL261 cells were infected with MVMp wt at an MOI of 0.1 PFU per cell and the production of virions was compared to the production of the reference A9 cells. 7 days post-infection, the medium of infected cells was harvested and viruses were extracted from the cell lysates by freeze-thaw cycles. The titration of progeny virions released in the medium and intracellular was performed by plaque assay.

	Input	Output
■ GL261	5,00E+04	4,70E+08
■ A9	5,00E+04	2,40E+09

Figure 4-4: Production of progeny viruses by GL261 and A9 cells after MVMp infection

2×10^5 cells GL261 or A9 cells were infected with MVMp at a MOI of 0.1 PFU/cell and lyzed 7 days post-infection. The production of progeny viruses was then determined by plaque assay on reference A9 cells. The input represents the quantity of virus used initially to infect the cells and the output corresponds to the total amount of virus produced.

As shown in Figure 4-4, GL261 cells produced high amounts of progeny virions. Indeed, the amount of neosynthetized viruses (4.7×10^8 PFU) was much higher than the amount of inoculum used initially to infect the cells (5×10^4 PFU), and only slightly lower than with the producer A9 cell line (2.4×10^9 PFU).

The production of progeny virions is of importance as it could contribute to increased killing of MVMp wt through successive rounds of infection, in contrast to MVMp-based vectors which are replication defective. Although MVMp wt was indeed shown to mediate high cytotoxicity on GL261 cells *in vitro*, it had similar effects as the recombinant parvovirus devoid of transgene when injected in established GL261 tumors (Enderlin et al., 2008), indicating that the cytotoxicity of MVMp wt is hampered *in vivo*. This could be due to the dilution *in vivo* of factors inducing cytotoxicity *in vitro* and/or to parvovirus entry in non tumoral cells *in vivo* and hence loss of infectious viruses.

4.3. Analysis of the mechanisms sustaining tumor inhibition by TNF-α- and IP-10-expressing parvoviral vectors in the GL261 subcutaneous model

The antitumor effects of recombinant parvoviral vectors encoding TNF-α and IP-10 on mouse GL261 glioma implanted subcutaneously were recently investigated in our laboratory. The growth of GL261 infected *in vitro* with TNF-α- or IP-10-transducing parvoviruses, grafted subcutaneously in C57BL/6 mice, was significantly delayed compared to buffer-treated cells or to cells infected with the empty vector Chi-MVMp/Δ800. Complete tumor regression was observed when GL261 cells were coinfected with both TNF-α- and IP-10-transducing parvoviruses, suggesting a synergistic antitumor effect of these cytokines. In contrast, the treatment of established tumors with repeated peritumoral injections of cytokine-encoding parvoviruses viruses inhibited the tumor growth compared to wt MVMp-, Chi-MVMp/Δ800-, and PBS-treated tumors, but the effects were similar whether TNF-α, IP-10, or both cytokine-transducing vectors were used (Enderlin et al., 2008).

In this thesis, I investigated the mechanisms sustaining tumor inhibition by TNF-α- and IP-10-expressing parvoviral vectors in the GL261 subcutaneous tumor model. The synergy between TNF-α and IP-10, observed when parvovirus-infected GL261 glioma cells were implanted subcutaneously, was analyzed *in vitro*.

Next, the infiltration of leukocytes as well as proliferation and apoptosis of intratumoral cells were investigated by immunohistochemistry after peritumoral injections of recombinant parvoviruses in established tumors.

4.3.1. Analysis of the synergistic antitumor effects of TNF-α and IP-10

4.3.1.1 Increased mIP-10 RNA expression and protein secretion in GL261 cells infected with Chi-MVMp/TNF-α

The subcutaneous growth of GL261 cells *in vitro* coinfected with both TNF-α- and IP10-expressing viruses grafted subcutaneously in mice was strongly impaired, in contrast to GL261 cells infected with each of the virus independently, showing synergistic antitumor effects of TNF-α and IP-10 in this system (Enderlin et al., 2008).

TNF-α was reported to induce, in synergy with IFN-γ, the production of IP-10 in various cell types, such as keratinocytes, fibroblasts (Majumder et al., 1996), or astrocytes (Salmaggi et al., 2002). TNF-α alone was also shown to induce IP-10 expression, for instance in human neural precursors cells (Sheng et al., 2005), normal astrocytes (Salmaggi et al., 2002), and astrocytomas (Majumder et al., 1998).

To investigate whether TNF-α-encoding virus was able to induce murine IP-10 (mIP-10) expression in the GL261 model, the levels of mIP-10 transcripts were analyzed in infected GL261 cells. To this end, 2×10^5 GL261 cells were infected with Chi-MVMp/TNF-α at an MOI of 3 RU per cell, or coinfected with Chi-MVMp/TNF-α and Chi-MVMp/IP-10 at an MOI of 1.5 RU per cell for each virus. MVMp wt-, Chi-MVMp/Δ800-, and Chi-MVMp/IP-10-infected cells at an MOI of 3 RU per cell as well as buffer-treated (mock) were used as controls. Total RNA was isolated 24 h and 48 h post-infection, reverse transcribed using primers specific for mouse IP-10, and the PCR products were analyzed on agarose gel electrophoresis. Figure 4-5 shows the results obtained after 24 h post-infection. Similar results were obtained 48 h post-infection.
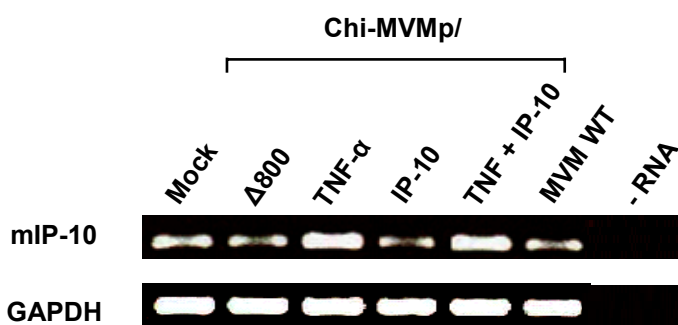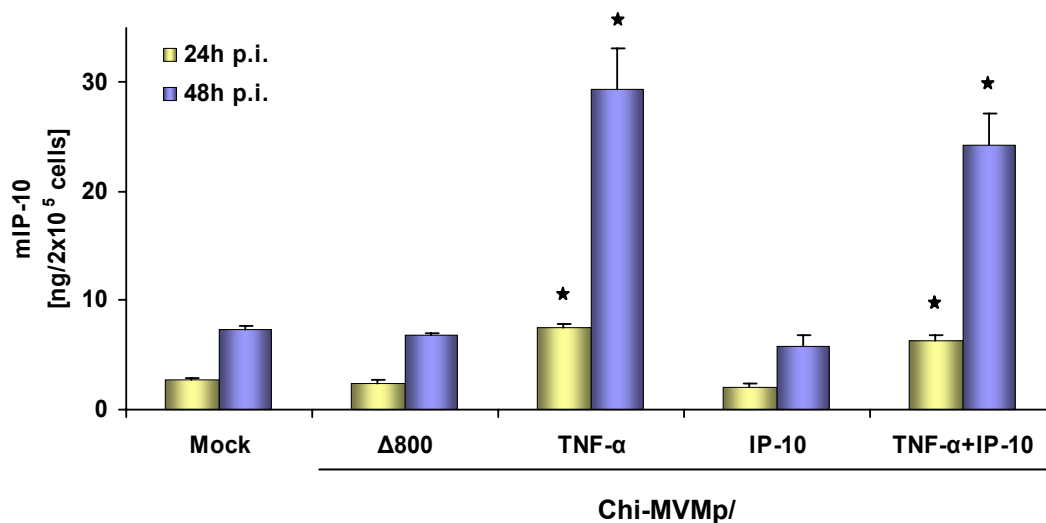

Figure 4-5: Increased mIP-10 mRNA levels after infection of GL261 cells with Chi-MVMp/TNF-α

2×10^5 GL261 cells were infected with Chi-MVMp/TNF-α (MOI = 3 RU/cell), or coinfected with Chi-MVMp/TNF-α and Chi-MVMp/IP-10 (MOI = 1.5 RU/cell for each vector). MVMp wt-, Chi-MVMp/IP-10- and Chi-MVMp/Δ800-infected cells (MOI = 3 RU/cell) as well as buffer-treated cells (mock) were used as controls. Total RNA was isolated 24 h post-infection and reverse transcription-PCR analysis was performed for the expression of mIP-10. GADPH was used as loading control and a RT-PCR with all reagents except RNA (-RNA) was included as negative control.

Similar mIP-10 mRNA expression levels were observed after infection with MVMp, Chi-MVMp/Δ800, and Chi-MVMp/IP-10, compared to buffer-treated GL261 infected cells. Thus, some mIP-10 expression is constitutive in GL261 cells and it is not increased upon parvoviral infection. In contrast, infection of GL261 cells with Chi-MVMp/TNF-α or coinfection with Chi-MVMp/TNF-α and Chi-MVMp/IP-10 resulted in a significant increase of mIP-10 mRNA levels.

The induction of mIP-10 expression in GL261 cells by TNF-α-transducing parvovirus was verified at the protein level. To this end, 2 x 10^5 GL261 cells were infected with Chi-MVMp/TNF-α at an MOI of 3 RU per cell, or coinfected with Chi-MVMp/TNF-α and Chi-MVMp/IP-10 at an MOI of 1.5 RU per cell for each virus. Chi-MVMp/Δ800-, and Chi-MVMp/IP-10-infected cells at an MOI of 3 RU per cell as well as buffer-treated (mock) were used as control. The secretion of mIP-10 in the culture medium was measured 24 and 48 h post-infection by ELISA. The results are illustrated in Figure 4-6.

**Figure 4-6: Increased mIP-10 secretion in GL261 cells after infection with Chi-MVM/TNF-α**

2 x 10^5 GL261 cells were infected with Chi-MVMp/TNF-α (MOI = 3 RU/cell), or coinfected with Chi-MVMp/TNF-α and Chi-MVMp/IP-10 (MOI = 1.5 RU/cell for each vector). Chi-MVMp/IP-10- and Chi-MVMp/Δ800-infected cells (MOI = 3 RU/cell) as well as buffer-treated cells (mock) were used as controls. Cell supernatants were harvested after 24 and 48 h and the levels of mIP-10 accumulated in the culture medium were measured by ELISA. Results are expressed as nanograms per 2 x 10^5 initially infected cells and shown as mean of triplicates from one representative experiment. Error bars represent the standard deviation. Statistical analysis was performed using Student's *t* test (*=*p*<0.01 versus mock).

As shown in Figure 4-6, the infection of GL261 cells with Chi-MVMp/Δ800 and Chi-MVMp/IP-10 resulted in mIP-10 protein levels comparable to the constitutive secretion from mock-infected GL261 cells. In contrast, statistically significant increased levels of mIP-10 were detected in the supernatants of GL261 cells infected with Chi-MVMp/TNF-α, alone or coinfected with Chi-MVMp/IP-10 compared to mock-infected cells at 24 and 48h post-infection (*p*<0.01). The difference between GL261 cells infected with Chi-MVMp/TNF-α alone or in combination with Chi-MVMp/IP-10 was not statistically significant. The increase of mIP-10 secretion by TNF-α delivering viruses was about 4 times higher than the constitutive levels secreted 48 h post-infection.

These results, together with the data obtained by RT-PCR, show that the infection of GL261 glioma cells with TNF-α-transducing parvovirus significantly increases both mIP-10 mRNA expression and protein secretion in GL261 cells *in vitro*. The levels of mIP-10 produced after 48 h (30 ng per 2 x 10^5 cells) represent up to 20 % of the levels produced after infection with Chi-MVMp-hIP-10 under the same conditions (200 ng). The expression of mouse IP-10 induced by Chi-MVMp/TNF-α combined with the expression of human IP-10 induced by Chi-MVMp/IP-10 may thus result in IP-10 amounts above a critical threshold. This could account for the synergistic antitumor effects of Chi-MVMp/TNF-α and Chi-MVMp/IP-10 observed in the GL261 subcutaneous tumor model. Indeed, TNF-α, and IP-10 may synergize to induce the production of one or more factors which, in turn, would also participate in the antitumor response.

4.3.1.2 Production of interferons in parvovirus-infected GL261 cells

As mentioned above, TNF-α was reported to induce the production of IP-10, usually in synergy with IFN-γ in various cell lines, but also more rarely in synergy with IFN-α or -β (Buttmann et al., 2007; Kato et al., 2003; Matikainen et al., 2000; Petry et al., 2006). Whereas IFN-γ is exclusively produced by lymphocytes, IFN-α, and -β, known as viral IFNs, can also be produced by most types of virally infected cells (Pestka et al., 2004). In this context, we investigated at the mRNA level, whether parvoviral infection of GL261 cells could induce the expression of IFN-α, and/or -β isoforms. For this, 2 x 10^5 GL261 cells were infected with the different parvoviral vectors at an MOI of 3 RU per cell, coinfected with Chi-MVMp/TNF-α and Chi-MVMp/IP-10 at an MOI of 1.5 RU per cell for each vector or buffer-treated cells (mock). Total RNA was isolated 24 h and 48 h post-infection and reverse transcription-PCR analysis was performed using primers specific for IFN-α or -β isoforms. The results are illustrated in Figure 4-7.
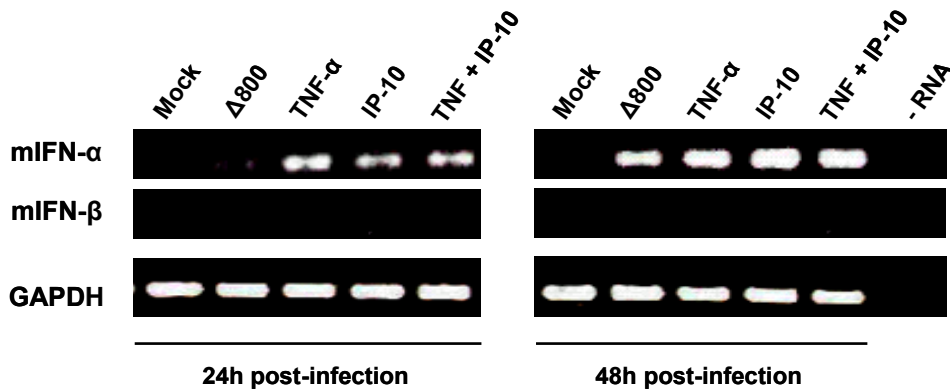
Figure 4-7: Induction of mIFN-α but not mIFN-β mRNA expression after infection with MVMp-derived vectors

2×10^5 GL261 cells were infected with Chi-MVMp/Δ800, Chi-MVMp/TNF-α, Chi-MVMp/IP-10 (MOI = 3 RU/cell), coinfected with Chi-MVMp/TNF-α and Chi-MVMp/IP-10 (MOI = 1.5 RU/cell for each vector), or buffer-treated cells (mock). Total RNA was isolated 24 h and 48 h post-infection and reverse transcription-PCR analysis was performed using primers specific for mIFN-α or -β. GADPH was used as loading control and a RT-PCR with all reagents except RNA (-RNA) was included as negative control.

Whereas no expression of IFN-β could be detected in infected or non-infected cells, the expression of IFN-α was induced 48 h post-infection in GL261 cells after parvoviral infection. The infection with all cytokine-encoding parvoviruses resulted in an increased expression of IFN-α compared to the infection with the empty vector Chi-MVMp/Δ800. The expression increased with time as shown by higher levels of mRNA 48 h post-infection irrespective of the group. No striking difference could be observed between cells infected with Chi-MVMp/TNF-α, Chi-MVMp/IP-10, or coinfected with both vectors.

At the protein level, the induction of IFN-α expression in GL261 cells after infection with parvoviral vectors was undetectable by ELISA, meaning that the IFN-α concentrations were lower than 12.5 pg/ml.

Together, these results suggest that TNF-α transduced by parvoviral vectors is sufficient to induce mIP-10 expression and secretion in the GL261 system. Whether low amounts of IFN-α, may also contribute to the induction of mIP-10 by TNF-α remains to be elucidated.

We next verified that mIP-10 expression could be induced by TNF-α alone in GL261 cells and not in the context of parvoviral infection. For this, 1×10^5 GL261 cells were treated with increasing concentrations of recombinant mouse TNF-α (0, 1, 10 or 100 ng/ml) for 24 to 48 h and the secretion of mIP-10 in the culture medium was measured by ELISA.
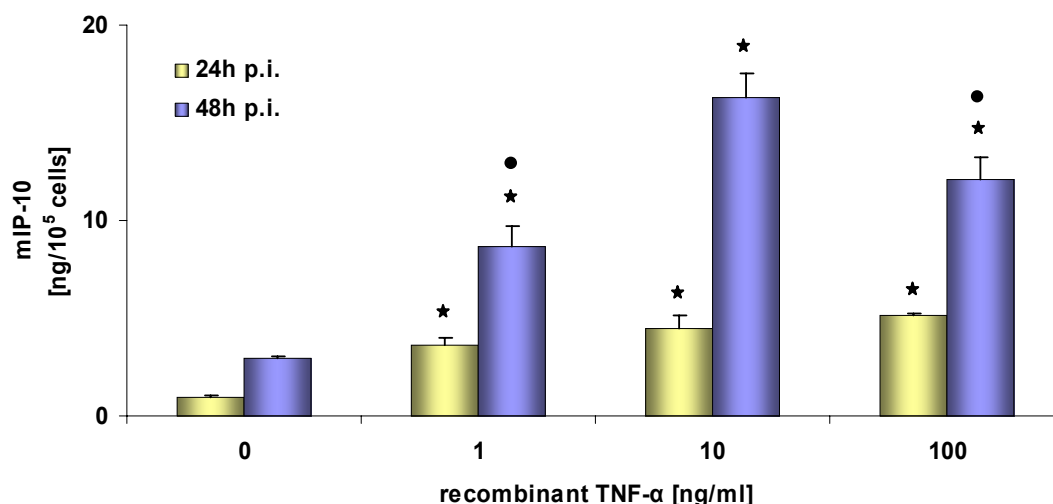
Figure 4-8: Increased mIP-10 secretion in GL261 cells treated with recombinant mTNF-α

1×10^5 GL261 cells were treated with increasing concentrations of recombinant mouse TNF-α (0 - 100 ng/ml) for 24 to 48 h, and the levels of mIP-10 released in the culture medium were measured by ELISA. Results are expressed as nanograms per 1×10^5 cells and shown as mean of triplicates. Error bars represent the standard deviation and statistical analysis was performed using Student's t test (*=$p<0.01$ versus mock; °=$p<0.05$ versus 10 ng/ml).

As shown in Figure 4-8, TNF-α alone is indeed sufficient to induce mIP-10 expression in GL261 cells. The treatment of GL261 cells with increasing concentrations of recombinant TNF-α induced, in a concentration dependent manner, statistically significantly increased levels of mIP-10 secretion in comparison to untreated cells ($p<0.01$). High concentrations of TNF-α (100 ng/ml) were toxic for GL261 cells resulting in decreased levels of mIP-10 ($p<0.05$).

TNF-α was reported to induce IP-10 by itself in various cells. The analysis of the IP-10 proximal promoter region revealed the presence of an interferon-stimulated responsive element (ISRE) and of two Nuclear Factor-kappa B (NF-κB) binding elements, κB1 and κB2, conserved among mammalian species (Ohmori and Hamilton, 1993; Yang et al., 2007). The κB motifs are recognized by members of the NF-κB/Rel homology family (Kunsch et al., 1992). Of interest, the TNF-α signaling pathway induces the activation of the NF-κB/Rel proteins. Therefore, the induction of mIP-10 by TNF-α most probably happens through positive transcriptional regulation of the mIP-10 promoter by the κB elements. Whether one or both NF-κB binding elements are involved in the induction of mIP-10 in GL261 cells and which members of the NF-κB/Rel protein family may participate remains to be elucidated.

4.3.2. Analysis of the immune cells infiltration, cell proliferation, and apoptosis in established subcutaneous GL261 tumors treated with peritumoral injections of parvoviral vectors

The treatment of established subcutaneous GL261 tumors with repeated peritumoral injections of parvoviruses transducing TNF-α, IP-10, or with both vectors was recently shown to inhibit tumor growth, while wt MVMp and the control vector Chi-MVMp/Δ800 had only marginal effects compared to buffer-treated tumors. Whereas synergistical antitumor effects were observed when GL261 cells were coinfected *in vitro* with both cytokines-encoding vectors and grafted subcutaneously, the antitumor effects were similar whether established tumors were treated with single cytokine-encoding vectors or their combination. This suggests that the synergy might be effective only in early tumor stages, before tumors become palpable. Alternatively, this could be assigned to the lower probability that tumor cells might be coinfected with both viruses *in vivo* (Enderlin et al., 2008).

To investigate the mechanisms sustaining tumor inhibition by TNF-α- and IP-10-expressing parvoviral vectors, we examined the infiltration of the major types of leukocytes involved in immune responses, including T lymphocytes, macrophages, dendritic cells, and natural killer cells. In addition, we also investigated intratumoral cell proliferation and apoptosis.

As the tumors developing from GL261 cells coinfected *in vitro* with both parvoviral vectors encoding TNF-α and IP-10 remained very small and regressed rapidly, we rather decided to analyze the antitumor mechanisms after injection of recombinant parvoviruses in established GL261 tumors. For this, 1×10^6 GL261 cells were grafted subcutaneously in C57BL/6 mice. Small tumors were treated with two peritumoral injections, at day 9 and 13 post-implantation, of Chi-MVMp/Δ800, wt MVMp, Chi-MVMp/TNF-α, Chi-MVMp/IP-10 (1×10^6 RU per injection), both Chi-MVMp/TNF-α and Chi-MVMp/IP-10 (each at 1×10^6 RU per injection), or PBS (mock) (3 mice per group). 17 days post-implantation, tumors were resected, cryofixed and tumors sections were stained with specific antibodies by immunohistochemistry. Cryosections were photographed and digitalized images were processed with an imaging software to quantify stained cells.
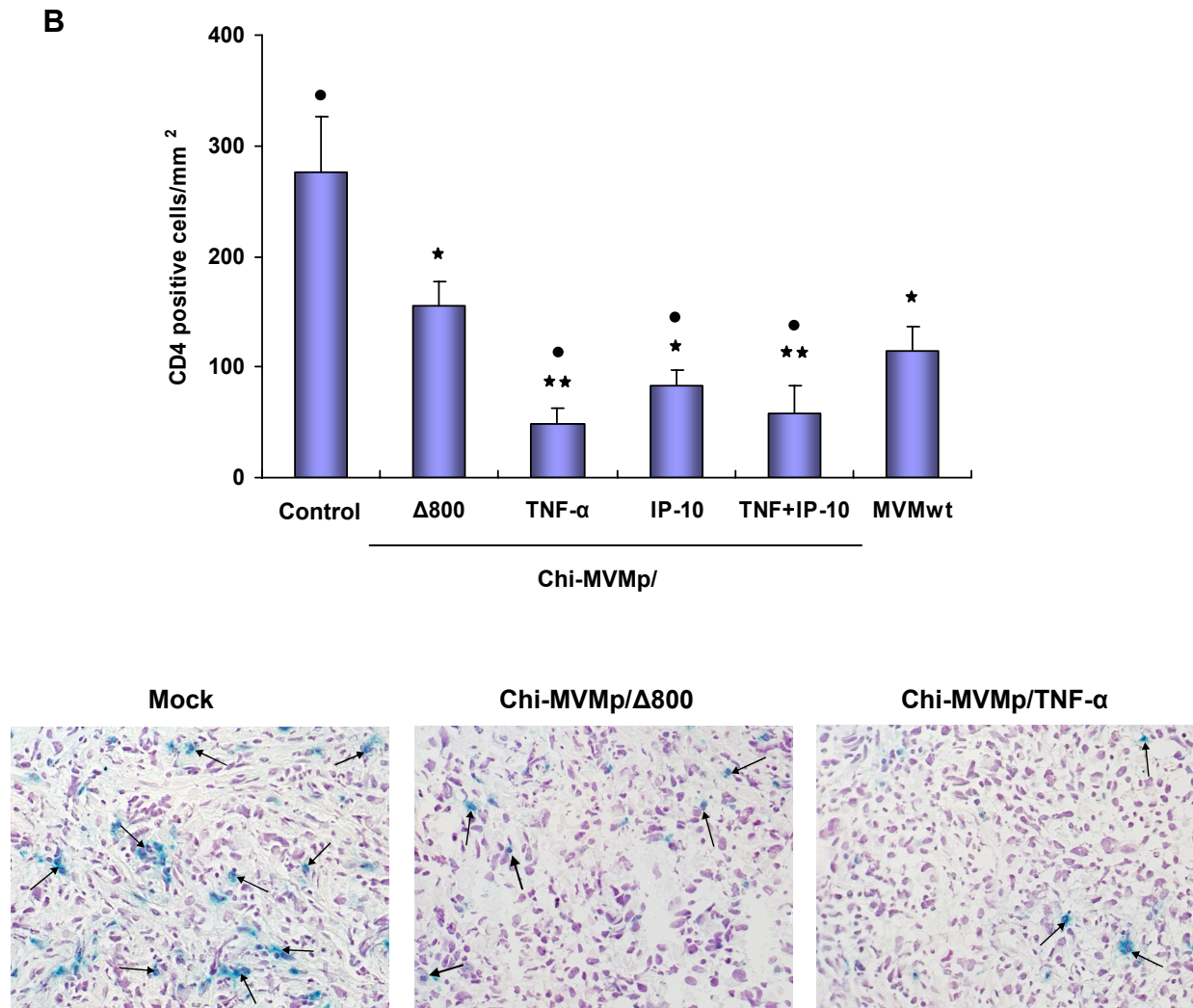
4.3.2.1 Decreased infiltration of CD8^{+} and CD4^{+} lymphocytes in subcutaneous GL261 treated with parvoviral vectors

Cellular immune responses were suggested to contribute to the antitumor effects observed when GL261 cells coinfected with both TNF-α- and IP-10-encoding vectors were grafted subcutaneously in immunocompetent mice. Indeed, when GL261 cells coinfected with both vectors were grafted in immunodeficient (nude) mice, all animals developed tumors and there was no significant difference in the tumor volume in mice implanted with coinfected cells or buffer-treated cells (Enderlin et al., 2008). Moreover, IP-10 is known as a potent chemoattractant for activated T cells (Taub et al., 1993), especially CD4^{+} Th1 helper cells, which induce the proliferation of cytotoxic CD8+ T cells (Bonecchi et al., 1998; Sallusto et al., 1998).

In this context, we analyzed the infiltration of lymphocytes in tumor samples, using antibodies against CD4 and CD8. These antibodies can detect CD4^{+} and CD8^{+} T lymphocytes, respectively, as well as NKT cells, which can be CD4^{+} or CD8^{+}. The results are summarized in Figure 4-9.

B
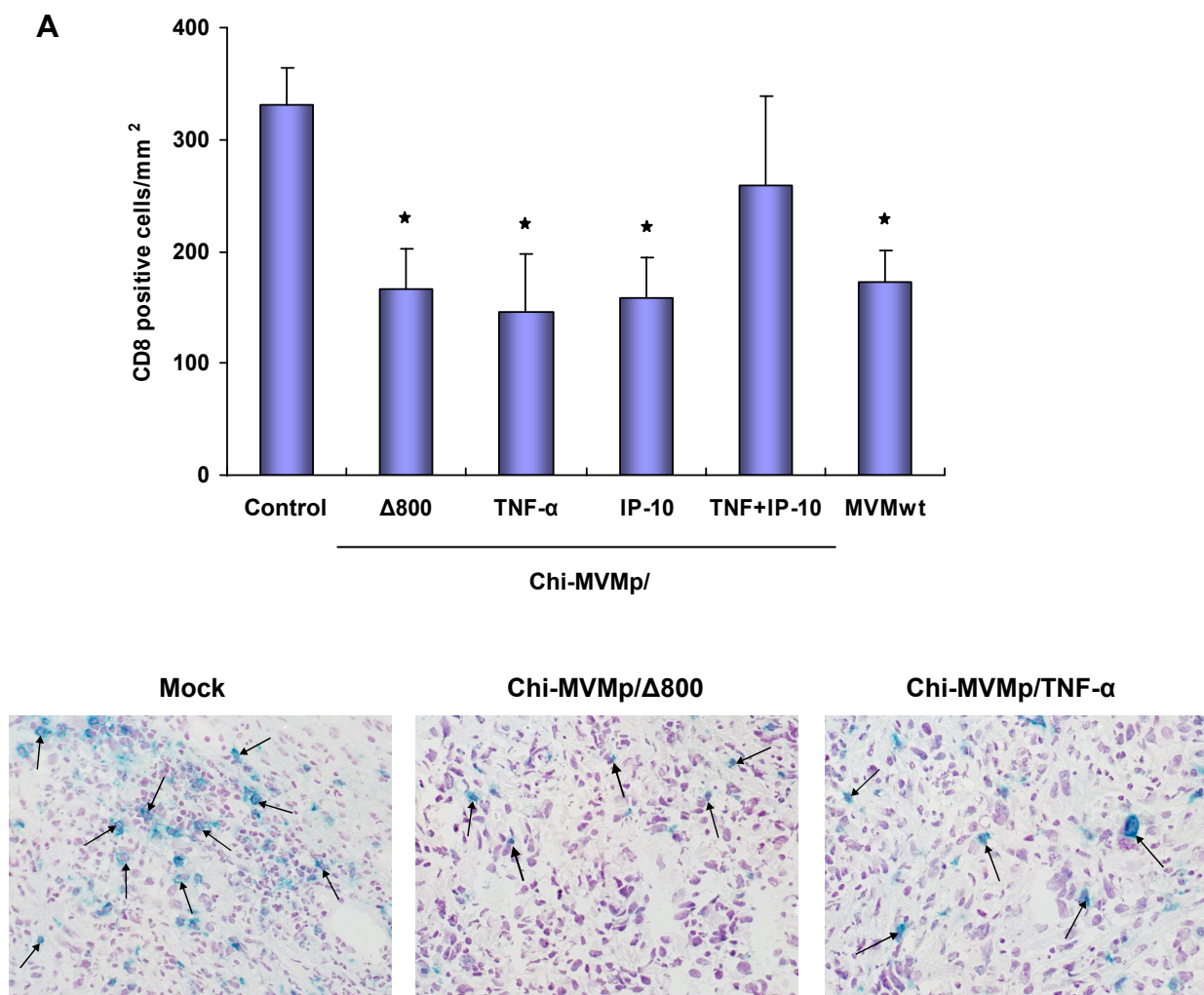
Figure 4-9: Decreased infiltration/proliferation of CD4$^+$ and CD8$^+$ T lymphocytes in subcutaneous GL261 treated with MVMp wt and derived vectors

1 x 10^6 GL261 cells were grafted subcutaneously in C57BL/6 mice. Small tumors were treated with two peritumoral injections (day 9 and 13 post-implantation) of Chi-MVMp/Δ800, wt MVMp, Chi-MVMp/TNF-α, Chi-MVMp/IP-10 (1 x 10^6 RU per injection), with both Chi-MVMp/TNF-α and Chi-MVMp/IP-10 (each at 1 x 10^6 RU per injection), or PBS (control) (3 mice per group). 17 days post-implantation, tumors were resected, cryofixed, and T lymphocytes were stained by immunohistochemistry using anti-mouse CD8$^+$ (**A**) and CD4$^+$ (**B**) rat monoclonal antibodies, and counterstained with hematoxylin. Cryosections were photographed and digitalized images were processed with an imaging software to measure CD4$^+$ and CD8$^+$ positive cells. The number of positive cells is given per mm^2 as mean value of three animals per group and the error bars represent the SEM. Statistical analysis was performed using Student's *t* test (*=$p<0.05$;**=$p<0.01$ versus mock; °=$p<0.05$ versus Chi-MVMp/Δ800). Representative picture are shown below.

Both CD8$^+$ and CD4$^+$ cells were found in all subcutaneous GL261 tumors, but surprisingly more lymphocytes were found in PBS-treated tumors (control) than in virus-treated groups. Whereas the infiltration of CD8$^+$ cells was quite similar in all virus-treated groups, the infiltration of CD4$^+$ cells varied depending on the treatment. Indeed, dramatically decreased numbers of CD4$^+$ lymphocytes were observed in tumors treated with cytokine-encoding vectors, compared to tumors treated with the empty vector or with PBS ($p<0.05$). The differences observed between Chi-MVMp/TNF-α,

Chi-MVMp/IP-10 or with both cytokine-encoding vectors groups were not statistically significant. Thus, in this setting, parvoviral-transduced IP-10 did not seem to mediate chemoattraction of T lymphocytes.

A significant tumor inhibition was observed in established subcutaneous GL261 tumors treated with parvoviral vectors encoding TNF-α, IP-10, or both, compared with the controls (Enderlin et al., 2008). Thus, the infiltration of CD4^{+} cells is inversely correlated with the tumor growth *in vivo*. Of interest, CD4^{+} cells comprise helper T cells and regulatory T cells (Tregs), which respectively stimulate or suppress immune responses. Tregs were indeed shown to be present in high numbers in GL261 subcutaneous tumors (El Andaloussi et al., 2006). Thus, we hypothesized that the treatment of GL261 tumors with cytokine-encoding vectors might inhibit the infiltration and/or proliferation of Tregs and hence promote an effective immune response.

Gliomas are known to induce an immunosuppressive environment through the secretion of several molecules including IL-10, prostaglandin E2 (PGE2), and transforming growth factor-β (TGF-β). TGF-β is known as the most immunosuppressive molecule and its role in malignant glioma biology is not restricted to immunosuppression but also affects tumor growth, invasion, migration, as well as tumor angiogenesis (Platten et al., 2001). Interestingly, TGF-β was reported to induce Tregs proliferation and infiltration (Chen and Wahl, 2003; Ghiringhelli et al., 2005; Schramm et al., 2004).

In this context, we investigated the effects of parvoviral infection and of the transgenes on the production of TGF-β in GL261 cells. The expression of the TGF-β isoforms (TGF-β1, -β2, -β3) was analyzed in virus-infected GL261 cells at the messenger RNA level. To this end, 2×10^5 GL261 cells were infected with Chi-MVMp/TNF-α, Chi-MVMp/IP-10, Chi-MVMp/Δ800, MVMp wt at an MOI of 3 RU per cell, coinfected with Chi-MVMp/TNF-α and Chi-MVMp/IP-10 at an MOI of 1.5 RU per cell for each virus, or buffer-treated (mock). Total RNA was isolated 24 h and 48 h post-infection, and reverse transcription-PCR analysis was performed using primers specific for TGF-β isoforms. Figure 4-10 shows the result of one representative experiment out of two.
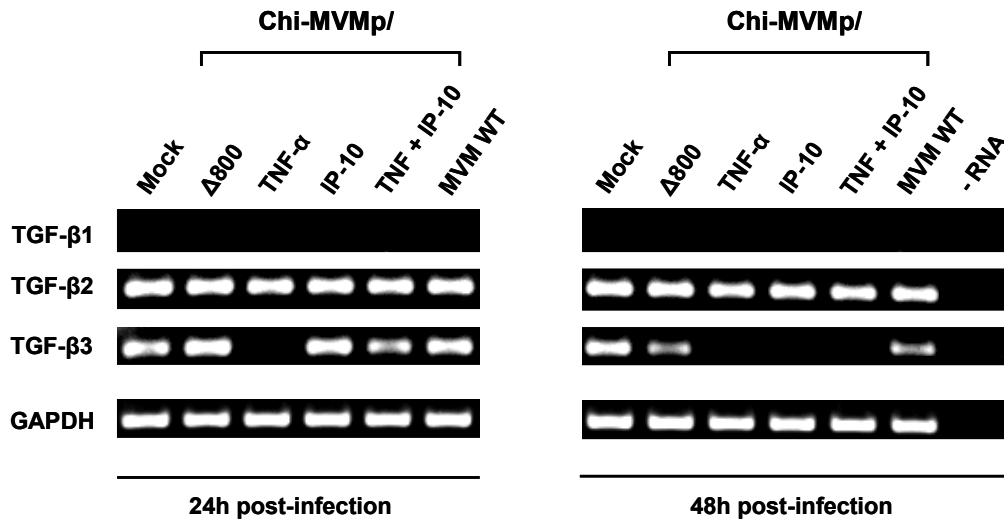
Figure 4-10: Reduced TGF-β expression by GL261 after infection with MVMp wt and derived vectors

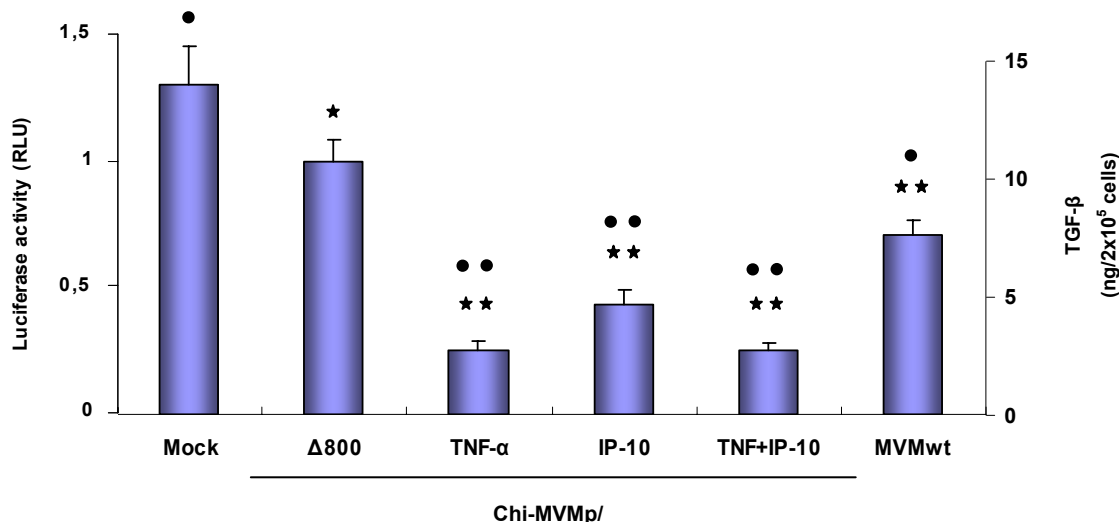2×10^5 GL261 cells were infected with Chi-MVMp/TNF-α, Chi-MVMp/IP-10, Chi-MVMp/Δ800, MVMp wt (MOI = 3 RU/cell), coinfected with Chi-MVMp/TNF-α and Chi-MVMp/IP-10 (MOI = 1.5 RU/cell for each virus), or buffer-treated (mock). Total RNA was isolated 24 h and 48 h post-infection, and RT-PCR analysis was performed for the expression of TGF-β1, -β2, and -β3 isoforms. GADPH was used as loading control and a RT-PCR with all reagents except RNA (-RNA) was included as negative control.

As shown in mock-infected cells, GL261 cells expressed both TGF-β2 and TGF-β3 isoforms, but not TGF-β1. TGF-β2 expression was not affected upon parvoviral infection or by any of the transgenes, neither at 24 h nor at 48 h post-infection. In contrast, TGF-β3 expression was found to be reduced after parvoviral infection, and more strikingly with cytokine-encoding vectors. While TGF-β3 mRNA levels remained unchanged after infection with Chi-MVMp/Δ800, MVMp wt or Chi-MVMp/IP-10 at 24 h post-infection, no TGF-β3 expression could be detected after infection with Chi-MVMp/TNF-α. Furthermore, TGF-β3 transcripts were significantly reduced after coinfection with both Chi-MVMp/TNF-α and Chi-MVMp/IP-10, suggesting an effect of parvoviral-transduced TNF-α. 48 h post-infection, TGF-β3 expression was slightly reduced by the parvoviral infection itself, as shown by reduced mRNA levels after infection with MVMp wt or Chi-MVMp/Δ800, compared with buffer-treated cells. Most strikingly, TGF-β3 expression remained undetectable, not only after infection with Chi-MVMp/TNF-α, as already seen 24 h post-infection, but also after infection with Chi-MVMp/IP-10 or coinfection of both viruses. This indicates that IP-10 could also have an effect on TGF-β3 expression, yet at later times post-infection.

In summary, while parvoviral infection has a only moderate effect on TGF-β3 expression, the infection with TNF-α- and IP-10-encoding viruses significantly decreased the accumulation of TGF-β3 mRNA, indicating a direct role of the cytokines.

In contrast, we could not detect an effect on TGF-β2 expression. One should point out that all three TGF-β isoforms bind to the same receptors, induce a similar transduction pathway and thus have similar functions per se (Graycar et al., 1989). The effects of different isoforms depend on the type and differentiation state of target cells and on the presence of other cytokines (Nathan and Sporn, 1991).

The inhibition of TGF-β in infected GL261 cells observed at the mRNA level, was confirmed at the protein level. For this, the amounts of TGF-β released in the supernatants of infected GL261 were assayed using the plasminogen activator inhibitor-1 / luciferase (PAI/Luc) bioassay, described by Abe et al., 1994. This assay is based on the ability of TGF-β to induce PAI-1 expression, using mink lung epithelial cells (MLEC) stably transfected with a luciferase reporter gene under the control of a truncated PAI-1 promoter. The assay detects all three TGF-β isoforms. To this end, GL261 cells were infected as described here-above with Chi-MVMp/TNF-α, Chi-MVMp/IP-10, Chi-MVMp/Δ800, MVMp wt, coinfected with Chi-MVMp/TNF-α and Chi-MVMp/IP-10, or buffer-treated (mock). The levels of TGF-β released in the supernatants of infected GL261 were measured using the MLEC-PAI/Luc bioassay. Figure 4-11 shows one representative experiment out of three.

Figure 4-11: Decrease of TGF-β secretion after infection with wt and recombinant MVMp in GL261

2×10^5 GL261 cells were infected with Chi-MVMp/TNF-α, Chi-MVMp/IP-10, Chi-MVMp/Δ800, MVMp wt (MOI = 3 RU/cell), coinfected with Chi-MVMp/TNF-α and Chi-MVMp/IP-10 (MOI = 1.5 RU/cell for each virus), or buffer-treated (mock).Total TGF-β amounts present in the cell supernatants were determined using the MLEC-PAI/L bioassay. Results are shown as mean of triplicates from one representative experiment and error bars represent the standard deviation. Luciferase activity is reported as relative light units (RLU) and TGF-β amounts are normalized per cell number. Statistical analysis was performed using Student's t test (*=$p<0.01$, **=$p<0.001$ versus mock; °=$p<0.01$; °°=$p<0.001$ versus Chi-MVMp/Δ800).

TGF-β secretion by infected GL261 was significantly reduced in all groups compared to mock-infected cell. Similarly to the results obtained at the mRNA level, GL261 infection with Chi-MVMp/Δ800 and MVMp moderately reduced TGF-β production compared to mock-treated cells, whereas the inhibition was greater after infection with cytokine-encoding vectors. The most potent inhibitions were observed after infection with Chi-MVMp/TNF-α and its combination with Chi-MVMp/IP-10, which were statistically significant compared to Chi-MVMp/IP-10 used alone ($p<0.01$).

Taken together, these results show that the infection of GL261 cells with wt and MVMp-derived vectors inhibits the production of TGF-β in GL261 at the mRNA (TGF-β3) as well as at the protein level. This effect is particularly striking for cytokine-encoding parvoviruses while the virus alone has only a moderate effect.

Interestingly, the pattern of TGF-β expression strongly correlates with the infiltration of CD4$^+$ T cells in subcutaneously implanted GL261 tumors (see Figure 4-9 B). TGF-β was reported to induce CD4$^+$ Tregs proliferation and infiltration (Chen and Wahl, 2003; Ghiringhelli et al., 2005). The decrease of TGF-β levels observed after infection with TNF-α- and IP-10-encoding parvoviruses might thus indeed lead to a decrease in the amounts of Tregs infiltrating the tumor, and supports our hypothesis. A decrease of Tregs could contribute to the antitumor effects observed, as these cells are potent inhibitors of immune responses.

In addition, TGF-β was reported to impair the function of both CD8$^+$ cytotoxic cells and CD4$^+$ helper cells (Gorelik and Flavell, 2002; Thomas and Massague, 2005). The reduction of TGF-β expression detected in GL261 cells after infection with cytokine-encoding vectors might in turn allow CD4$^+$ helper and CD8$^+$ cytotoxic T lymphocytes to exert their functions *in vivo* while being suppressed in the control groups, becoming then the potential effector cells responsible for the antitumor effects mediated with cytokine-encoding vectors.

4.3.2.2 Increased infiltration of CD68$^+$ macrophages in subcutaneous-implanted GL261 cells treated with both Chi-MVMp/TNF-α and Chi-MVMp/IP-10

Macrophages are important components of antitumor responses. They are implied in both innate- and adaptive-mediated immunity. Their role in innate immunity implies direct killing of tumor cells through phagocytosis and production of various inflammatory proteins. Through phagocytosis, macrophages can also process tumor antigens, and present them to lymphocytes in order to activate the cellular immune response.

The infiltration of macrophages was analyzed by staining of tumor samples with antibodies against CD68, also known as microsialin in mouse. CD68 is a glycosylated lysosomal antigen restricted to cells of the macrophage lineage (Holness et al., 1993).
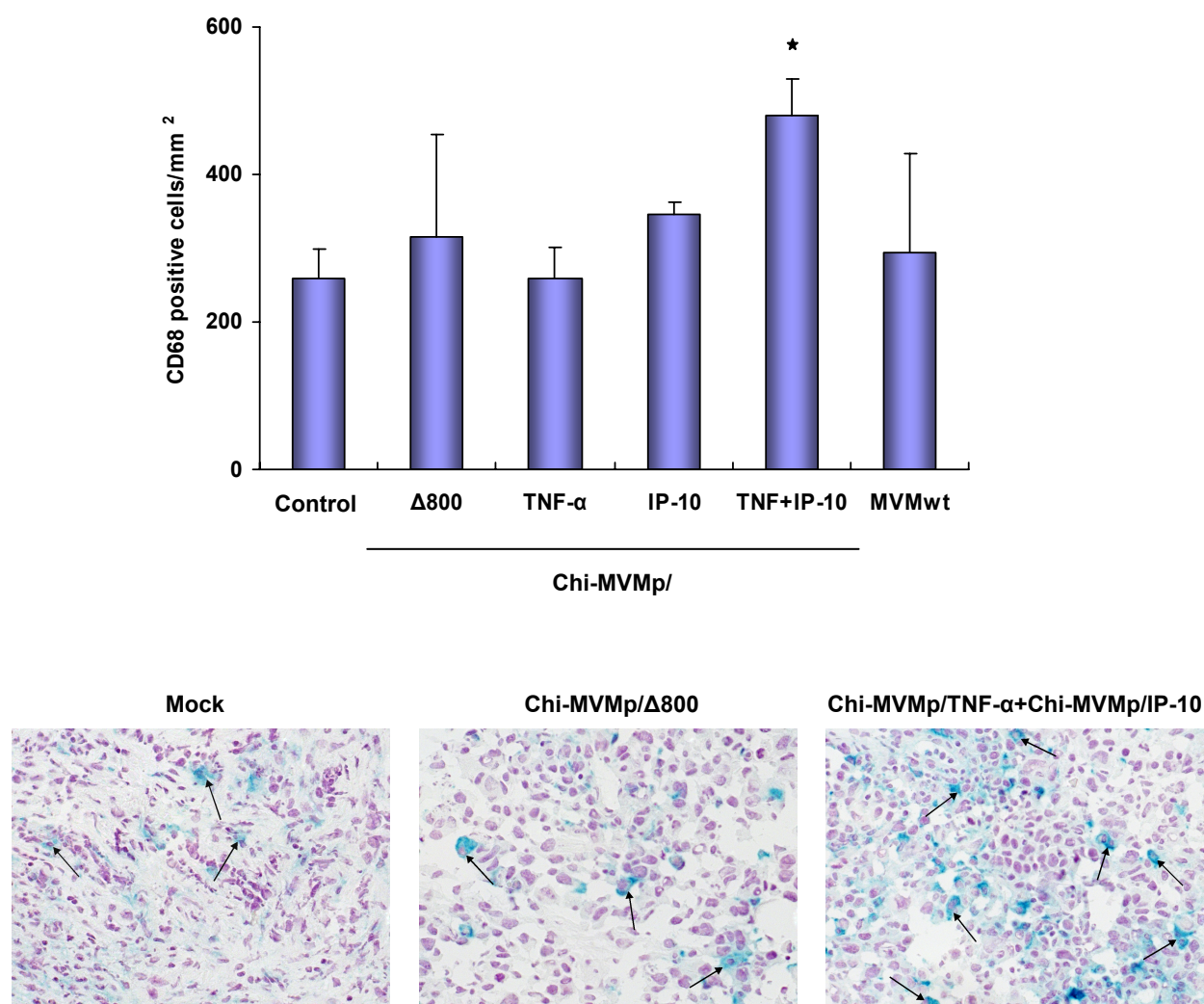
Figure 4-12: Increased infiltration of CD68^{+} macrophages in subcutaneous GL261 treated with both Chi-MVMp/TNF-α and Chi-MVMp/IP-10

1×10^6 GL261 cells were grafted subcutaneously in C57BL/6 mice. Small tumors were treated with repeated peritumoral injection (day 9 and 13 post-implantation) of Chi-MVMp/Δ800, wt MVMp, Chi-MVMp/TNF-α, Chi-MVMp/IP-10 (1×10^6 RU per injection), with both Chi-MVMp/TNF-α and Chi-MVMp/IP-10 (each at 1×10^6 RU per injection), or PBS (control) (3 mice per group). 17 days post-implantation, tumors were resected, cryofixed and macrophages were stained by immunohistochemistry using an anti-mouse CD68 rat monoclonal antibody, and counterstained with hematoxylin. Cryosections were photographed and digitalized images were processed with an imaging software to measure CD68 positive cells. The number of positive cells is given per mm^2 as mean value of three animals per treatment group and the error bars represent the standard error of the mean. Statistical analysis was performed using Student's *t* test (*=*p*<0.05 versus mock). Representative pictures are shown below.

As seen on Figure 4-12, tumor infiltrating macrophages, identified as CD68$^+$ cells, were found in all tumor samples, irrespective of the group. Whereas no significant differences were observed in tumors treated with TNF-α- or IP-10-encoding viruses, compared to Chi-MVMp/Δ800, MVMp wt, or buffer-treated tumors (control), an increased number of macrophages was detected in tumors treated with the combination of both cytokine-transducing vectors, statistically significant compared to buffer-treated tumors (control), but not to vector-infected groups.

Considering the variability between the different groups and the fact that the treatment of established GL261 tumors with parvoviral vectors encoding TNF-α, IP-10, or both vectors resulted in similar antitumor responses (Enderlin et al., 2008), the increase of macrophages observed when using both vectors might not be relevant for the antitumor effects observed.

4.3.2.3 No detectable infiltration of dendritic cells or natural killer cells

Natural killer cells and dendritic cells are also important components of antitumor responses. Whereas natural killer cells are involved in the innate immune response and can mediate direct killing of tumor cells, dendritic cells are known as the most efficient antigen presenting cells, able to activate both the humoral and cellular adaptative responses. The infiltration of natural killer cells and dendritic cells was investigated using NKG2D and 33D1 antibodies respectively. Yet, we could not detect any of these two types of cells in subcutaneous tumor samples, irrespective of the group. Thus, it seems that natural killer cells do not play a key role in the antitumor response in this system. Concerning dendritic cells, one possibility may be that at the time point analyzed, they may have already left the tumor to the draining lymph nodes.

4.3.2.4 Effects of MVMp wt and derived vectors on cell proliferation and apoptosis

The tumor growth of established GL261 tumors treated with peritumoral injections of cytokine-encoding parvoviruses was reduced compared to the control groups (Enderlin et al., 2008). In addition, parvoviral infection with MVMp wt and derived vectors impaired the cellular growth of GL261 cells *in vitro* (see section 4.2.2). Furthermore, TNF-α is a known potent pro-apoptotic factor. This prompted us to investigate whether these viruses had an effect on subcutaneous intratumoral cell proliferation or apoptosis. For this, tumor cryosections were histomorphometrically examined after staining either for

Ki67, used as a marker of cell proliferation, or after staining by terminal deoxynucleotidyl transferase Biotin-dUTP nick end labeling (TUNEL) assay to detect apoptotic cells.

Treatment group	% Ki67 positive cells	% TUNEL positive cells
Control	33.0 ± 6.5	7.5 ± 1.3
Chi-MVMp/Δ800	33.0 ± 1.5	6.0 ± 2.5
Chi-MVMp/TNF-α	30.5 ± 4.4	7.3 ± 1.8
Chi-MVMp/IP-10	29.5 ± 2.3	7.0 ± 1.2
Chi-MVMp/TNF-α + Chi-MVMp/IP-10	32.5 ± 1.5	6.0 ± 2.2
wt MVMp	30.3 ± 1.8	6.4 ± 1.5

Ki67

TUNEL
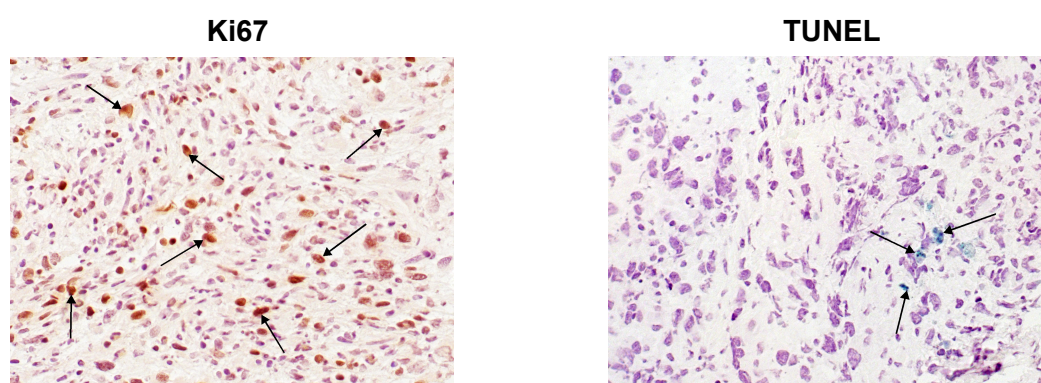
Table 4-1: Effect of MVMp wt and derived vectors on cell proliferation and apoptosis

1×10^6 GL261 cells were grafted subcutaneously in C57BL/6 mice. Small tumors were treated with two peritumoral injections (day 9 and 13 post-implantation) of Chi-MVMp/Δ800, wt MVMp, Chi-MVMp/TNF-α, Chi-MVMp/IP-10 (1×10^6 RU per injection), with both Chi-MVMp/TNF-α and Chi-MVMp/IP-10 (each at 1×10^6 RU per injection), or PBS (control) (3 mice per group). 17 days post-implantation, tumors were resected, and cryofixed. Proliferating cells were stained by immunohistochemistry with an antibody against Ki67 and apoptotic cells were detected by TUNEL assay. Cryosections were photographed and digitalized images were processed with an imaging software to measure Ki67 and TUNEL positive cells and counterstained with hematoxylin to quantify the total amount of cells. The percentage of Ki67 and TUNEL positive cells are given as mean value of three animals per treatment group ± standard error of the mean. The difference between the treated groups was not statistically significant (Student's *t* test). One representative picture for each stain is shown below.

As shown in Table 4-1, no significant differences could be observed in the proliferation or apoptosis rate between the treated groups. Thus at this time point, the infection of GL261 cells with parvoviral vectors did not affect the proliferation nor the apoptosis of intratumoral cells *in vivo*. However, one should point out that these results were obtained at only one time point and may perhaps not be representative of the situation on a long-term follow up.

4.4. Analysis of the antitumor effects of cytokine-transducing parvoviral vectors on GL261 implanted intracranially in syngeneic C57BL/6 mice

The CNS has long been considered as an immune-privileged site. However, growing evidence indicates that the CNS has a significant but tightly regulated capability to induce immune responses and many immunotherapeutic approaches, including the use of immunostimulatory genes, have already been tried in the treatment of malignant brain tumors. This prompted us to investigate the antitumor effects of cytokine-transducing parvoviruses on mouse glioma tumor growth and animal survival when glioma cells are implanted intracranially in syngeneic immunocompetent mice.

4.4.1. Establishment of GL261 cells intracranial implantation

The GL261 glioma model is widely used as subcutaneous but also as intracranial tumor model. Of interest, several reports demonstrate that GL261 cells grow well after intracerebral implantation in syngeneic C57BL/6 mice and with a highly reproducible disease progression (Cha et al., 2003; Szatmari et al., 2006; Zagzag et al., 2000).

Thus, we decided to test the antitumor effects of cytokine-encoding parvoviral vectors on mouse GL261 glioma implanted intracranially. Since this model was not established in our laboratory at the time I started, I contributed with S. Paschek (Vet. Med.) to implement it in our laboratory. Briefly, mice to be injected intracranially were anesthetized, mounted in a stereotactic frame (Figure 4-13 A) and a midline scalp incision was made to expose the surface of the skull. The point of junction of the coronal and sagittal sutures of the skull, termed bregma, served as reference point for stereotactic injections (Figure 4-13 B). A small hole was made at the define position of the caudate putamen (2.5 mm lateral to the bregma) and the needle was stereotactically introduced into the left striatum (3 mm deep) (Figure 4-13 C). 1×10^5 GL261 cells suspended in 4 µl of phosphate buffer (DPBS) were then injected over 16 min with an injection rate of 250 nl/min using a microinjection unit (Figure 4-13 A). Following injection, the needle was left in place for an additional 5 min to minimize any back-flow and the skin was sutured with non-absorbable nylon thread.
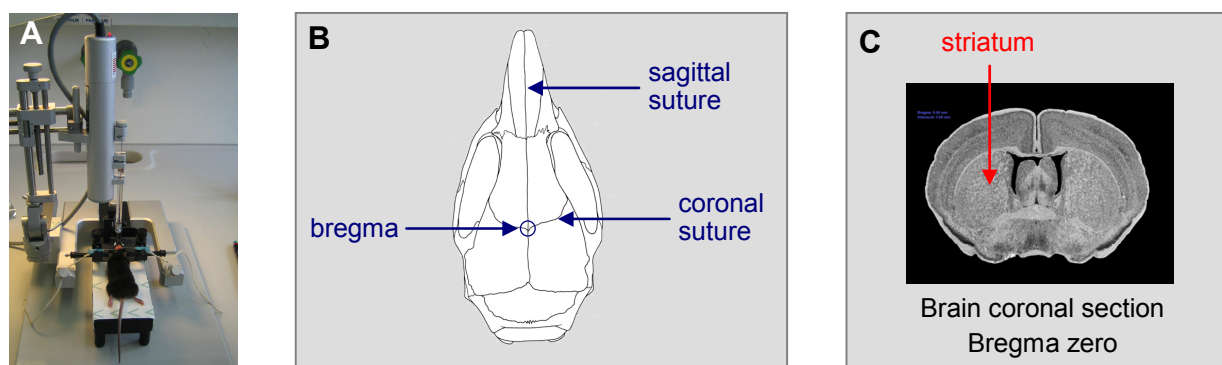
Figure 4-13: Stereotactic injection of mice in the left striatum

A: Stereotactic frame with microinjection unit; **B**: schematic representation of the skull adapted from (Cook, 1965); **C**: Coronal section of the brain adapted from the mouse brain library.

We first investigated the intracranial tumor growth of buffer-treated GL261 cells compared to cells infected with MVM wt and the empty parvoviral vector Chi-MVMp/Δ800, which had only marginal effects on tumor growth and survival in the GL261 subcutaneous model (Enderlin et al., 2008).
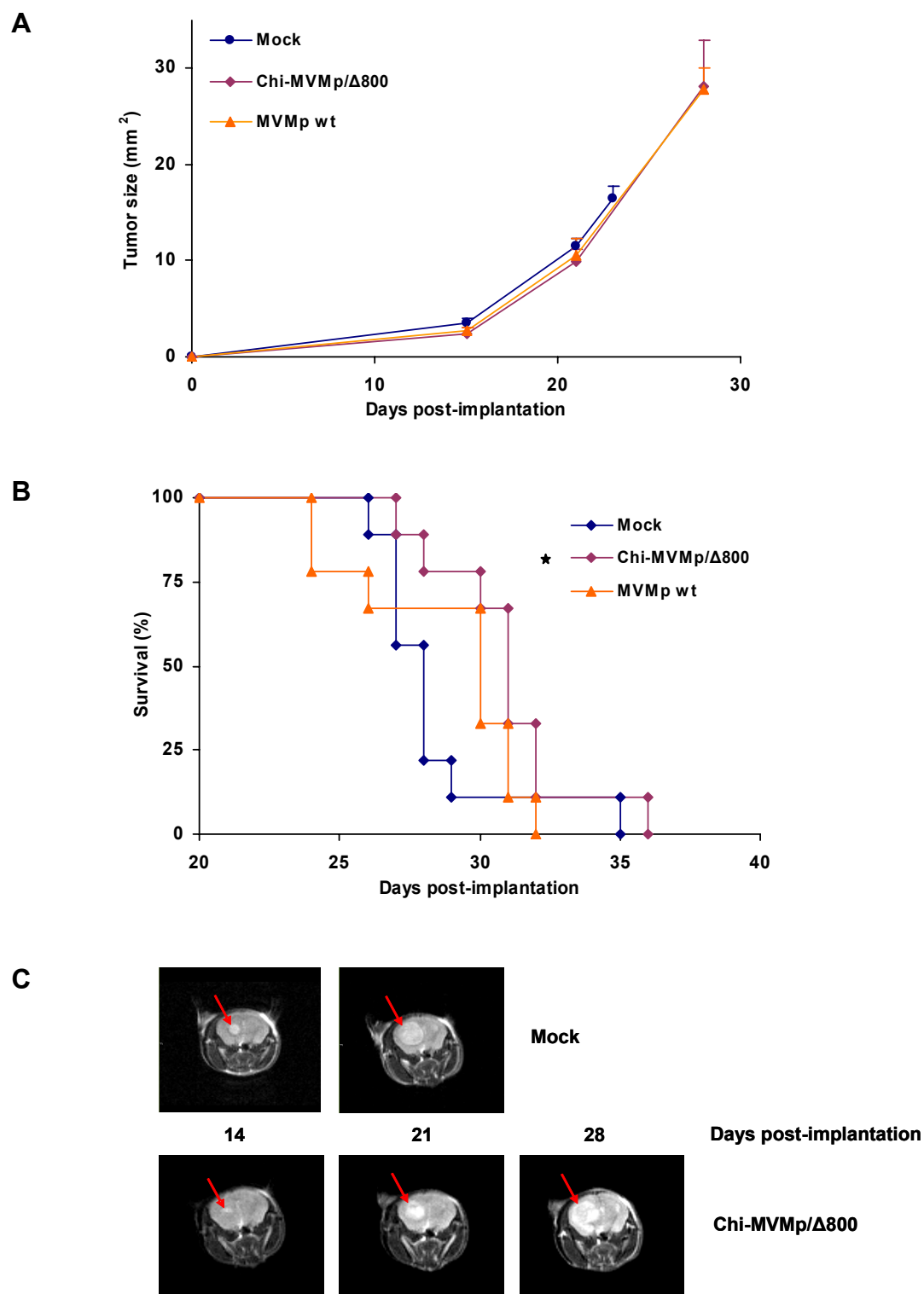
To this end, GL261 cells were infected *in vitro* with either MVMp wt, Chi-MVMp/Δ800 at an MOI of 3 RU per cell, or buffer-treated (mock). 1×10^5 cells were stereotactically implanted into the left brain hemisphere of C57BL/6 mice (9 animals per group). After intracranial tumor inoculation, tumor growth was monitored weekly by magnetic resonance imaging (MRI) and the percentage of surviving mice in the different groups was recorded daily. Tumor growth and animal survival are illustrated in Figure 4-14.

In agreement with the literature, almost all mice implanted with buffer-treated cells died within four weeks (Szatmari et al., 2006; Zagzag et al., 2000) (Figure 4-14 B).

Infection of GL261 cells prior implantation with Chi-MVMp/Δ800 or MVMp wt did not affect the intracranial tumor growth of GL261 cells up to 23 days post-implantation as shown by the similar growth compared with buffer-treated cells (mock) (Figure 4-14 A).

While the animal survival of mice implanted with Chi-MVMp/Δ800 infected cells was slightly, but statistically significantly, prolonged compared to mice implanted with buffer-treated cells ($p<0.05$), there was no statistically significant difference between MVMp wt and mock groups. The median survival of mice implanted with Chi-MVMp/Δ800- (31 days) or MVMp wt- (30 days) infected cells was only slightly prolonged compared to mice implanted with mock-infected cells (28 days) (Figure 4-14 B).

These results are in agreement with the marginal effects of parvoviral infection on the GL261 subcutaneous tumor growth and survival of mice (Enderlin et al., 2008).

A

B

C

Figure 4-14: Tumor growth and survival of mice intracranially implanted with GL261 cells infected with MVMp wt or the empty parvoviral vector Chi-MVMp/Δ800

GL261 cells were infected *in vitro* with MVMp wt, Chi-MVMp/Δ800 (MOI = 3 RU/cell) or buffer-treated, and 1 x 10^5 cells were intracranially implanted in the left striatum of C57BL/6 mice (9 per group). Tumor development and animal survival were monitored over time. The tumor growth (A) and the percentage of surviving animals per group (B) are plotted as a function of time post-implantation. The tumor size is given as mm^2 + SEM. Statistical analysis was performed using the Wilcoxon Rank Sum Test. (*=*p*<0.05 versus mock). (C) Representative MRI scans of one mice implanted with buffer-treated cells and one mice implanted with Chi-MVMp/Δ800 over time.

4.4.2. Inhibition of tumor growth and prolonged survival of mice implanted intracranially with GL261 transducing TNF-α or both TNF-α and IP-10, but not IP-10 alone

TNF-α- and IP-10-transducing parvoviral vectors were recently shown to inhibit the growth of subcutaneously grafted GL261 glioma cells in syngeneic recipient animals. The tumor growth of GL261 cells infected *in vitro* with TNF-α- and IP-10-encoding parvoviruses and subsequently implanted subcutaneously in C57BL/6 mice was significantly delayed compared to the controls and complete tumor regression was observed when glioma were coinfected with both vectors (Enderlin et al., 2008).

This prompted us to investigate the antitumor effects of TNF-α- and IP-10-transducing parvoviruses and their combination on glioma tumor growth and animal survival when GL261 cells are implanted intracranially.

To this end, GL261 cells were infected *in vitro* with either Chi-MVMp/TNF-α, or Chi-MVMp/IP-10 at an MOI of 3 RU per cell, or coinfected with both vectors at an MOI of 3 RU per cell for each vector. As control, GL261 were infected with the empty vector Chi-MVMp/Δ800 at an MOI of 3 RU per cell. 1×10^5 cells were stereotactically implanted into the left brain hemisphere of C57BL/6 mice. After intracranial tumor inoculation, tumor growth was monitored weekly and the percentage of surviving mice in the different groups was recorded daily. The tumor growth is shown for one representative experiment (9 mice per group) out of two in Figure 4-15 A and the animal survival is illustrated in Figure 4-15 B based on two independent experiments (2 x 9 mice).
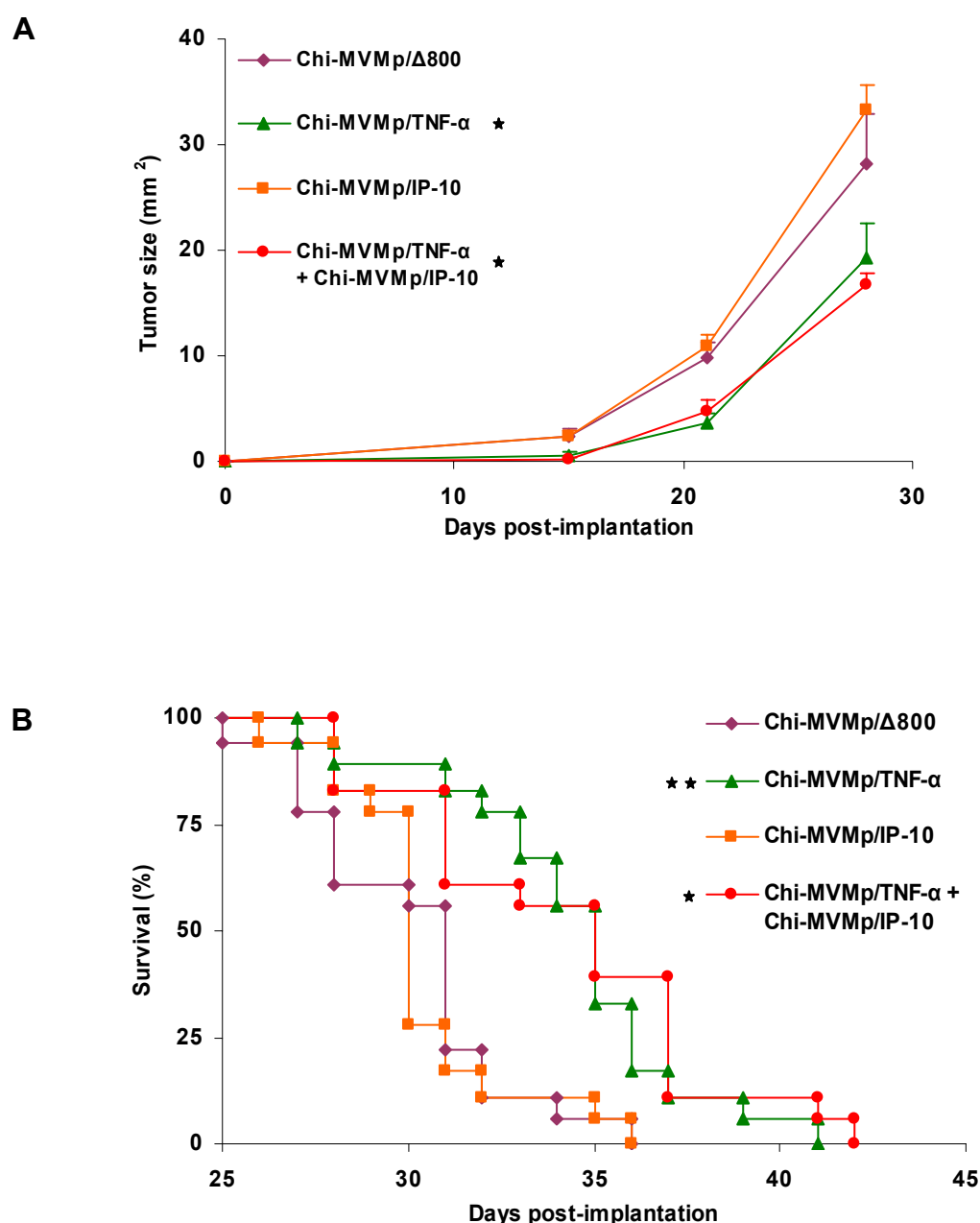
Figure 4-15: Inhibition of tumor growth and increased survival of mice implanted intracranially with GL261 transducing TNF-α or both TNF-α and IP-10, but not IP-10 alone

GL261 cells were infected *in vitro* with Chi-MVMp/TNF-α, Chi-MVMp/IP-10 (MOI = 3 RU/cell), or coinfected with Chi-MVMp/TNF-α and Chi-MVMp/IP-10 (MOI = 3 RU/cell for each vector). GL261 cells infected with Chi-MVMp/Δ800 (MOI = 3 RU/cell) served as control. 1×10^5 cells were intracranially implanted in the left striatum of C57BL/6 mice. Tumor development and animal survival was monitored over time. The tumor growth (**A**, 9 mice per group), and the percentage of surviving animals (**B**, 18 mice per group from two independent experiments) are plotted as a function of time post-implantation. The tumor size is given as mm^2 + SEM. Statistical analysis was performed using the using the Koziol test for the tumor growth (*=$p<0.05$ versus delta) and the Wilcoxon Rank Sum Test for the animal survival (*=$p<0.05$, **=$p<0.001$ versus delta).

The intracranial tumor growth was significantly delayed in animals implanted with Chi-MVMp/TNF-α-infected GL261 cells or with cells coinfected with Chi-MVMp/TNF-α and Chi-MVMp/IP-10. This tumor inhibition was statistically significant compared to the empty vector Chi-MVMp/Δ800 ($p<0.05$). Surprisingly, the growth of GL261 cells infected with Chi-MVMp/IP-10 alone was similar to the empty vector and there was no significant differences in tumor growth between parvoviral infections delivering TNF-α or both TNF-α and IP-10 (Figure 4-15 A). Furthermore, the survival of mice implanted with GL261 cells transducing TNF-α alone ($p<0.001$) or with both TNF-α and IP-10 ($p<0.05$) was statistically significantly prolonged (median survival: 35 days for both groups) compared to mice implanted with Chi-MVMp/Δ800-infected cells (median survival: 31 days). In contrast, the survival of mice implanted with GL261 cells transducing IP-10 (median survival: 30 days) was not significantly different from the control. No statistically significant differences could be observed between the survival of mice implanted with GL261 cells transducing either TNF-α alone or both TNF-α and IP-10 (Figure 4-15 B).

These results differ from the data previously obtained in the subcutaneous model, as TNF-α- and IP-10-transducing parvoviral vectors alone were shown to inhibit the growth of subcutaneous GL261 and complete tumor regression was achieved when glioma were coinfected with both vectors, showing synergistical antitumor effects. Moreover, the survival of mice implanted subcutaneously with TNF-α- or IP-10-transducing GL261 cells was quite similar and prolonged compared to the control (Chi-MVMp/Δ800), while all mice implanted with GL261 cells coinfected with Chi-MVMp/TNF-α and Chi-MVMp/IP-10 were long-term survivors (Enderlin et al., 2008).

Thus, in contrast to the results obtained subcutaneously, treatment with the IP-10-encoding vector did not reduce the GL261 intracranial tumor growth, and consequently did not increase the survival of the animals compared to the control group. No synergy between TNF-α and IP-10 could be observed in this setting. In this model, TNF-α alone was the most potent antitumor cytokine.

4.4.3. Analysis of the mechanisms sustaining the antitumor effects of parvoviral vectors transducing TNF-α alone or together with IP-10 in the GL261 intracranial model

In order to investigate the mechanisms sustaining the antitumor effects of parvoviral vectors expressing TNF-α and to elucidate the lack of effects of IP-10-encoding vectors, we analyzed tumor microvascularization, the recruitment of the major types of leukocytes involved in immune responses, as well as intratumoral cell proliferation and apoptosis by immunohistochemistry on tumors samples from infected GL261 cells implanted intracranially.

For this, GL261 cells infected *in vitro* with either Chi-MVMp/TNF-α, or Chi-MVMp/IP-10, at an MOI of 3 RU per cell, or coinfected with Chi-MVMp/TNF-α and Chi-MVMp/IP-10 at an MOI of 3 RU per cell for each virus and 1×10^5 cells were intracranially implanted in the left striatum of C57BL/6 mice (3 mice per group). Cells infected with MVMp wt, Chi-MVMp/Δ800, or buffer-treated (mock) were used as controls. 21 days post-infection, the brains were resected, cryofixed, and tumors sections were stained with specific antibodies by immunohistochemistry. Cryosections were photographed and digitalized images were processed with an imaging software to quantify positive cells or surface area.

4.4.3.1 Inhibition of tumor angiogenesis in TNF-α-transduced GL261 tumors

The cytokines used in this model are known to have both immunostimulating functions but also to potentially inhibit tumor angiogenesis. Indeed, IP-10 is known for its chemoattractive properties and also as a potent angiostatic molecule. TNF-α induces immune stimulation and was also reported to inhibit tumor angiogenesis. Therefore, we investigated the effects of parvoviral vectors delivering these transgenes on the intracranial GL261 tumor microvascularization. For this, tumor cryosections were histomorphometrically examined after staining for CD31, used as a marker of endothelial cells and microvascularization. The results are illustrated in Figure 4-16.
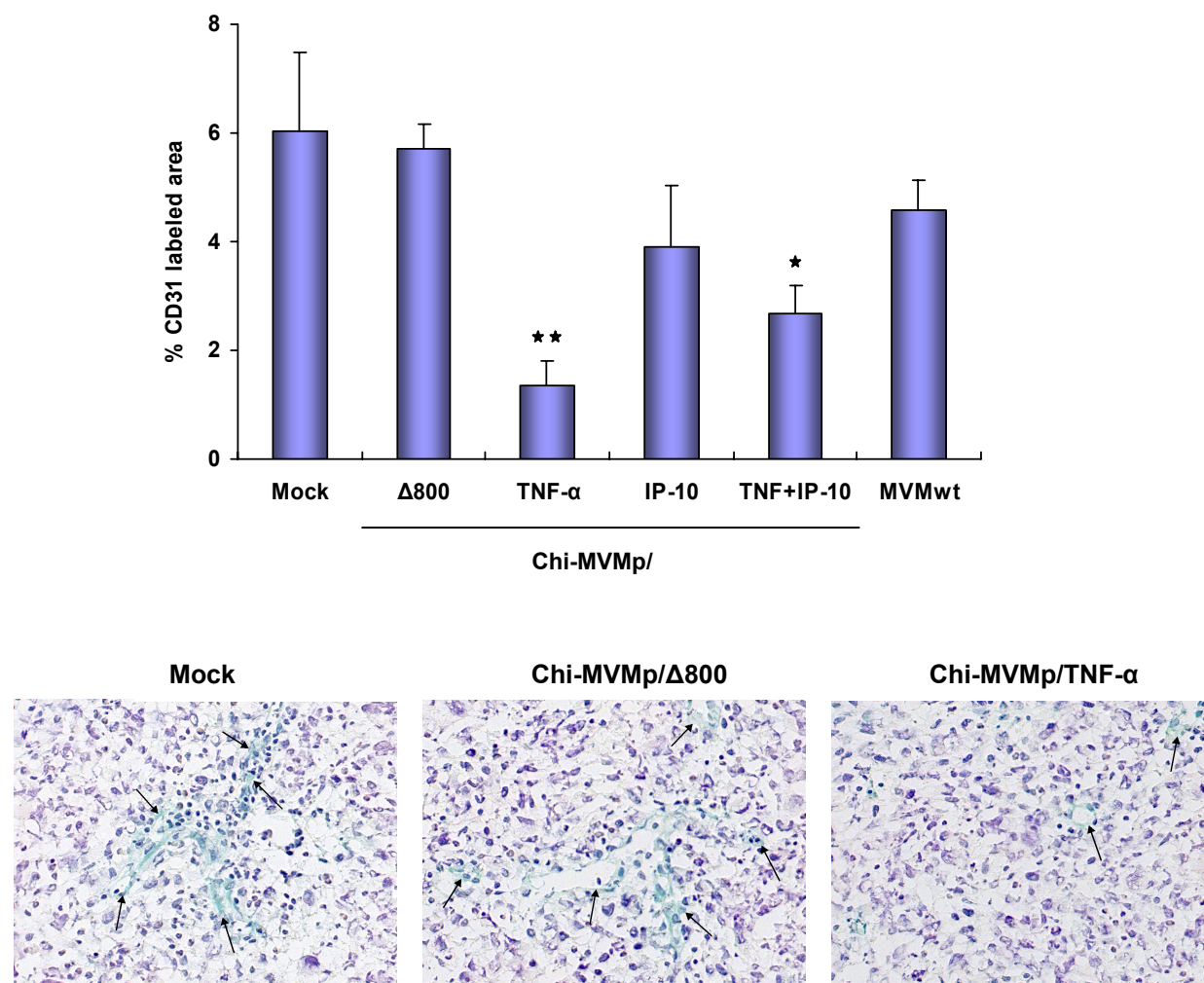
Figure 4-16: Decreased percentage of CD31$^+$ labeled area after infection with TNF-α-encoding MVMp-based vector

GL261 cells were infected *in vitro* with Chi-MVMp/TNF-α, Chi-MVMp/IP-10 (MOI = 3 RU/cell), or coinfected with both vectors (MOI = 3 for each vector). GL261 infected with wt MVMp, Chi-MVMp/Δ800 (MOI = 3 RU/cell) or buffer-treated (mock) were used as controls. 1 x 105 cells were intracranially implanted in the left brain hemisphere of C57BL/6 mice (3 per group). 21 days post-infection, brains were resected, cryofixed and tumors sections were stained with an antibody against CD31 by immunohistochemistry, and counterstained with hematoxylin. Cryosections were photographed and digitalized images were processed with an imaging software to quantify CD31$^+$ labeled area. The percentage of CD31$^+$ labeled area within the tumor is given as mean value of three animals per treatment group. Error bars represent standard deviations. Statistical analysis versus buffer-treated cells (mock) was performed using Student's t test (*=$p<0.05$, **=$p<0.01$). Representative pictures are showed below.

The microvascularization, as shown by CD31 labeling, was significantly decreased in tumors derived from GL261 cells infected with Chi-MVMp/TNF-α alone ($p<0.01$) or coinfected with Chi-MVMp/TNF-α and Chi-MVMp/IP-10 ($p<0.05$) compared to the control group (mock). TNF-α-transducing parvovirus had the most potent effect with less than 2 % of CD31$^+$ labeled area compared with 6 % in the control (mock). In contrast, the effects of Chi-MVMp/IP-10, Chi-MVMp/Δ800 or MVMp wt on tumor microvascularization were not statistically significant compared to the control (mock).

These results indicate that TNF-α has an antiangiogenic effect on intracranial GL261 tumor microvascularization while IP-10 has no significant effect.

The effects of parvoviruses encoding TNF-α or its combination with IP-10 on microvascularization correlate with the increased survival of mice and suggest that inhibition of tumor angiogenesis by TNF-α may contribute to the antitumor mechanisms.

4.4.3.2 Increased infiltration of CD8^{+} and CD4^{+} lymphocytes in mice intracranially implanted with parvovirus-infected GL261 cells

To investigate the effect of parvoviral vectors on the recruitment of T cells in intracranial GL261 cells, we analyzed the infiltration of lymphocytes in tumor samples, using anti-CD4 and CD8, antibodies respectively. The results are illustrated in Figure 4-17.

B
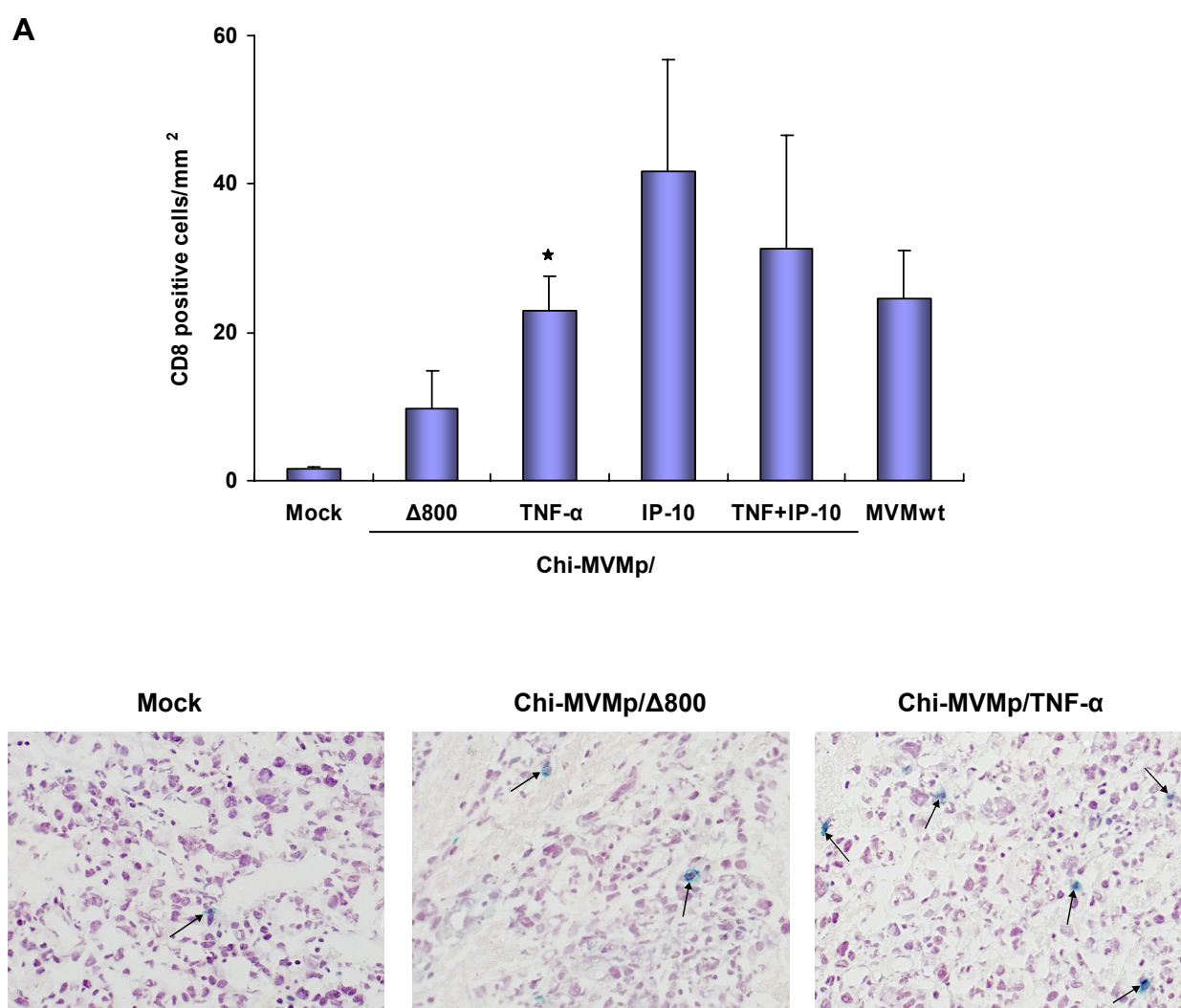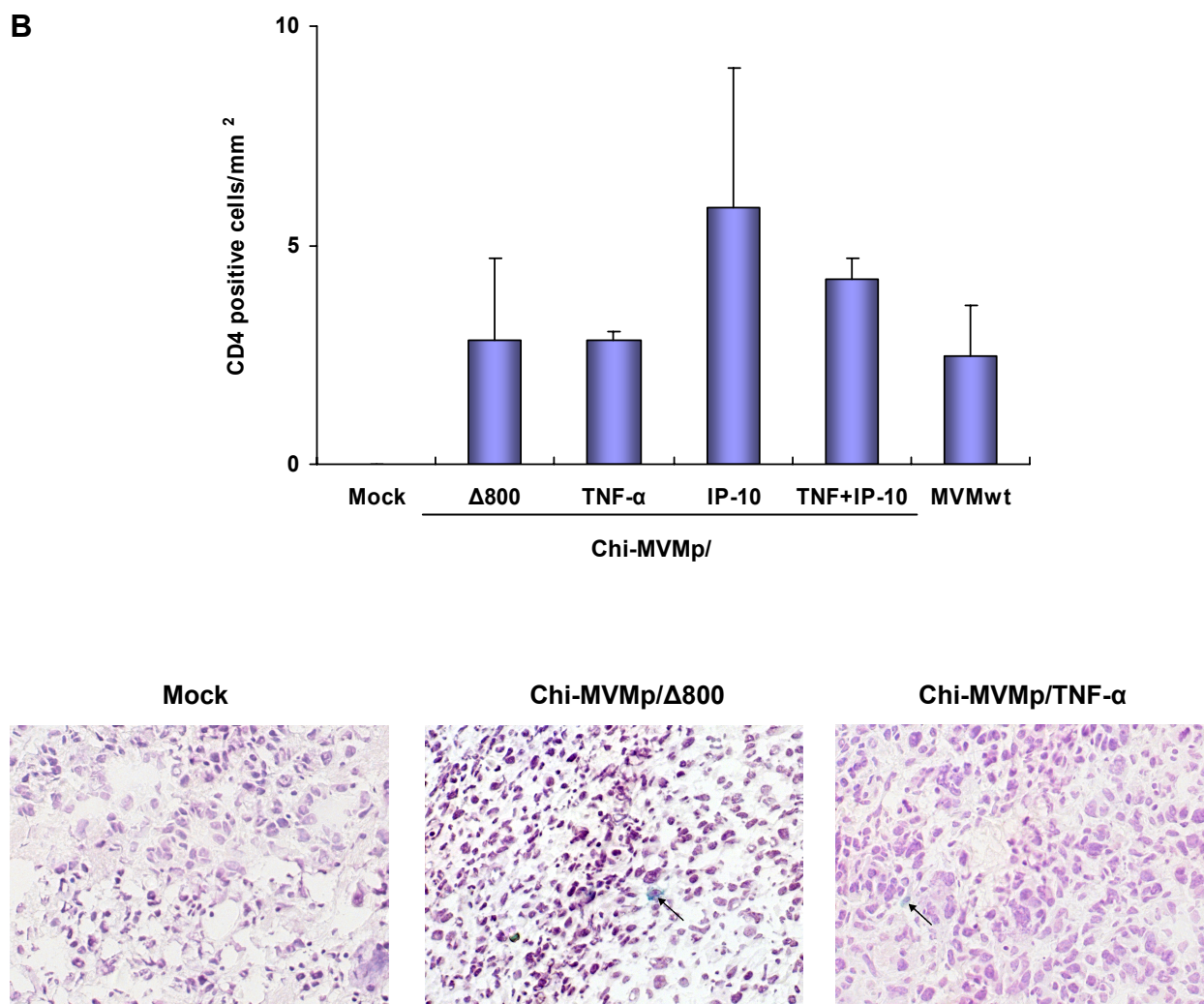
Figure 4-17: Increased infiltration of CD8^{+} and CD4^{+} lymphocytes in mice intracranially implanted with parvovirus-infected GL261

GL261 cells were infected *in vitro* with Chi-MVMp/TNF-α, Chi-MVMp/IP-10 (MOI = 3 RU/cell), or coinfected with both vectors (MOI = 3 RU/cell for each vector). GL261 infected with wt MVMp, Chi-MVMp/Δ800 (MOI = 3 RU/cell) or buffer-treated (mock) were used as controls. 1 x 10^{5} cells were intracranially implanted in C57BL/6 mice (3 per group). 21 days post-infection, tumors were resected, cryofixed and T lymphocytes were stained by immunohistochemistry using anti-mouse CD8^{+} (**A**) and CD4^{+} (**B**) rat monoclonal antibodies, and counterstained with hematoxylin. Cryosections were photographed and digitalized images were processed with an imaging software to measure CD4^{+} and CD8^{+} positive cells. The number of positive cells is given per mm[2] as mean value of three animals per treatment group and the error bars represent the SEM. Statistical analysis was performed using Student's *t* test (*=$p < 0.05$ versus mock). Representative pictures are showed below.

Whereas very low numbers of CD8^{+} lymphocytes and no CD4^{+} could be detected in tumors derived from buffer-treated GL261 cells, a significant, yet limited, infiltration of both types of lymphocytes could be observed in all tumors derived from parvoviral infected GL261 cells. The lymphocyte infiltration into intracranial GL261 control tumors was much less than of the subcutaneous tumors, which is in agreement with the literature (Badie et al., 2001).

The increase in lymphocyte numbers was statistically significant for CD8$^+$ lymphocytes in the case of tumors derived from GL261 infected with Chi-MVMp/TNF-α ($p<0.05$) compared to the mock, but not between the different parvoviral-treated groups, due to the large standard deviations observed for all other groups. Similarly the difference of infiltration of CD4$^+$ lymphocytes between the different parvoviral-treated groups was not statistically significant.

Thus, the parvoviral infection alone is able to induce the intracranial infiltration of CD4$^+$ and CD8$^+$ lymphocytes, but we could not observe a significant effect of any of the transgenes on the attraction of these leukocytes.

Yet, it is worth noting that, as shown in section 4.3.2.1, independently of the numbers of infiltrating lymphocytes, the cells might be differentially activated depending on the treatment. Indeed, we could show a decrease of TGF-β in GL261 cells infected with parvoviral vectors transducing transgenes. Thus, CD4$^+$ and CD8$^+$ might be activated in tumors derived from GL261 cells infected with cytokine-encoding parvoviral vectors while being suppressed in the control groups (Chi-MVMp/Δ800, MVM wt).

4.4.3.3 Decreased infiltration of macrophages and/or microglia in mice intracranially implanted with parvovirus-infected GL261 cells.

Both human and animal brain tumors have been shown to be significantly infiltrated by blood derived-macrophages and/or by microglia, the latter known as the brain resident macrophages (Badie and Schartner, 2000; Roggendorf et al., 1996). Once activated, microglial cells acquire morphological and immunophenotypical features similar to peripheral macrophages. Hence, it is difficult to distinguish between these two types of cells and they are often designated as macrophage/microglial cells (Stoll and Jander, 1999). The role of glioma-infiltrating macrophages/microglia remains controversial, as they were shown to have both pro- and antitumor activities (Badie and Schartner, 2001).

In order to analyze the effect of parvoviral vectors on the infiltration of activated macrophages/microglia in intracranially-implanted GL261, tumor cryosections were histomorphometrically examined after staining with anti-CD68 antibodies, specific for cells of the macrophage lineage.
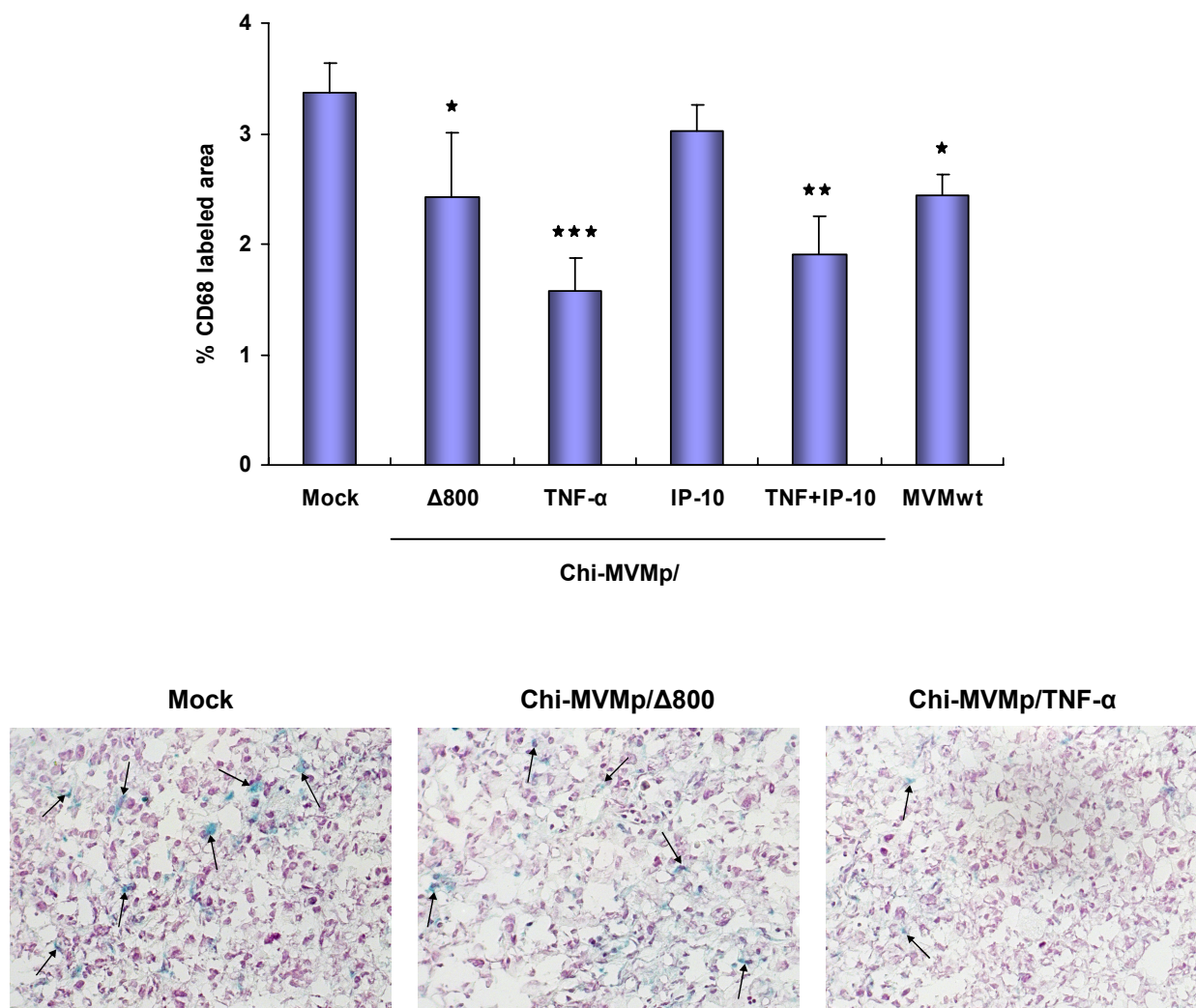
Figure 4-18: Decreased infiltration of macrophages and/or microglia in mice intracranially implanted with parvovirus-infected GL261

GL261 cells were infected *in vitro* with Chi-MVMp/TNF-α, Chi-MVMp/IP-10 (MOI = 3 RU/cell), or coinfected with both vectors (MOI = 3 RU/cell for each vector). GL261 infected with wt MVMp, Chi-MVMp/Δ800 (MOI = 3 RU/cell) or buffer-treated (mock) were used as controls. 1×10^5 cells were intracranially implanted in C57BL/6 mice (3 per group). 21 days post-infection, brains were resected, cryofixed and tumors sections were stained for macrophages/microglia using a CD68-specific antibody. Cryosections were photographed and digitalized images were processed with an imaging software to quantify CD68 labeled area. The percentage of CD68 positive labeled area within the tumor is given as mean value of three animals per treatment group. Error bars represent standard deviations. Statistical analysis versus buffer-treated cells was performed using Student's *t* test (*=$p<0.05$, **=$p<0.01$, ***=$p<0.001$). Representative pictures are showed below.

As shown in Figure 4-18, the infiltration of CD68$^+$ macrophages/microglia was statistically decreased in all parvovirus-infected cells compared to the control (Mock), except for GL261 transducing IP-10. However, the difference between GL261 cells infected with Chi-MVMp/IP-10 or Chi-MVMp/Δ800 was not statistically significant.

The macrophages/microglia numbers were minimal in GL261 cells infected with Chi-MVMp/TNF-α ($p<0.001$) or with both Chi-MVMp/TNF-α and Chi-MVMp/IP-10

(p<0.01), suggesting an effect of the transduced TNF-α on the infiltration of macrophages. This could be owing to a decreased invasion into the tumor, but also to a decreased proliferation or induced cell death within the tumor of macrophages/microglia upon treatment with TNF-α-transducing parvoviral vector.

The degree of macrophages/microglia infiltration inversely correlates with the tumor growth and survival *in vivo* and indicates that these cells might have rather tumor promoting features in our experimental setting. Indeed, brain microglia/macrophages were reported to secrete many factors including cytokines and matrix proteases which directly or indirectly promote glioma proliferation, migration, and angiogenesis (Rao, 2003; Watters et al., 2005). Thus, this might also be related to the reduced vascularization observed in TNF-α-transducing tumors (see section 4.4.3.1).

4.4.3.4 No detectable infiltration of dendritic cells or natural killer cells

The infiltration of natural killer cells and dendritic cells was analyzed using anti-NKG2D and 33D1 antibodies respectively. At the time point analyzed, we could not detect any of these two immune cells in GL261 intracranial tumors, irrespective of the group, similarly to the situation in subcutaneous tumors.

4.4.3.5 No effect of MVMp-derived vectors on cell proliferation and apoptosis

In order to determine whether parvoviral vectors may affect the intratumoral cell proliferation and apoptosis, intracranial tumor cryosections were histomorphometrically examined after staining for Ki67 (cell proliferation marker), or after TUNEL assay to detect apoptotic cells.

As shown in Table 4-2, the proliferation rate of tumors was comparable in all groups, with about 30% of proliferating cells. The difference between the treatment groups was not statistically significant, similarly to what was observed subcutaneously. This suggests that at the time point analyzed (21 days post-implantation) neither the infection of GL261 cells with parvoviral vectors nor the transduced cytokines did affect the proliferation of intracranial GL261 or non tumoral cells.

Intratumoral apoptosis was evaluated using the TUNEL assay (data not shown). The rate of positively stained cells in both cases were very variable between the three individual of each group and no significant differences could be observed. Therefore no clear effect could be seen on intratumoral apoptosis.

Treatment group	% Ki67 positive cells
Mock	29 ± 1.4
Chi-MVMp/Δ800	31 ± 1.8
Chi-MVMp/TNF-α	32 ± 4.2
Chi-MVMp/IP-10	31 ± 5.1
Chi-MVMp/TNF-α + Chi-MVMp/IP-10	28 ± 5.6
wt MVMp	29 ± 3.8

Table 4-2: No effect of MVMp-derived vectors on intracranial tumor cell proliferation

GL261 cells were infected *in vitro* with Chi-MVMp/TNF-α, Chi-MVMp/IP-10 (MOI = 3 RU/cell), or coinfected with both vectors (MOI = 3 RU/cell for each vector). GL261 infected with wt MVMp, Chi-MVMp/Δ800 (MOI = 3 RU/cell) or buffer-treated (mock) were used as controls. 1×10^5 cells were intracranially implanted in C57BL/6 mice (3 per group). 21 days post-infection, brains were resected, cryofixed and tumors sections were stained with an antibody against KI67 by immunohistochemistry, and counterstained with hematoxylin. Cryosections were photographed using a and digitalized images were processed with an imaging software to measure Ki67 positive cells and counterstained with hematoxylin to quantify the total amount of cells. The percentage of KI67 positive cells is given as mean value of three animals per treatment group ± standard deviation. The difference between the treatment groups was not statistically significant (Student's *t* test).

Thus, at the time point analyzed, the infection of GL261 cells with parvoviral vectors did not significantly affect the proliferation nor the apoptosis of intratumoral cells *in vivo*. However, one should point out that these results were obtained at only one time point and may perhaps not be representative of the situation on a long-term follow up.

4.4.4. Analysis of the antitumor effects of MCP-2- and MCP-3-transducing parvoviral vectors on GL261 implanted intracranially in C57BL/6 mice

Monocyte chemotactic proteins MCP-2 and MCP-3 are known to be potent immunoactive cytokines, recruiting a broad range of leukocytes. Their chemotaxis for NK cells, T cells and DCs, known to play a critical role in antitumor immunity, makes them attractive candidate as antitumor agents. Parvoviral vectors delivering MCP-3 were previously demonstrated to inhibit the tumor growth of human Hela grafted in nude mice (Wetzel et al., 2001) and mouse melanoma implanted subcutaneously in syngeneic mice (Wetzel et al., 2007). This prompted us to investigate the antitumor effects of parvoviruses delivering MCP-2 and MCP-3 in the GL261 intracranial glioma model.

For this, GL261 cells were infected *in vitro* with Chi-MVMp/MCP-2, Chi-MVMp/MCP-3 at an MOI of 3 RU per cell. As control, GL261 cells were infected with Chi-MVMp/Δ800 at

an MOI of 3 RU per cell or buffer-treated. 1 x 10^5 cells were stereotactically implanted into the left brain hemisphere of C57BL/6 mice (8 mice per group) and tumor growth was monitored weekly by magnetic resonance imaging (MRI). The percentage of surviving mice in the different groups was recorded daily. The tumor growth and the animal survival are illustrated in Figure 4-19.
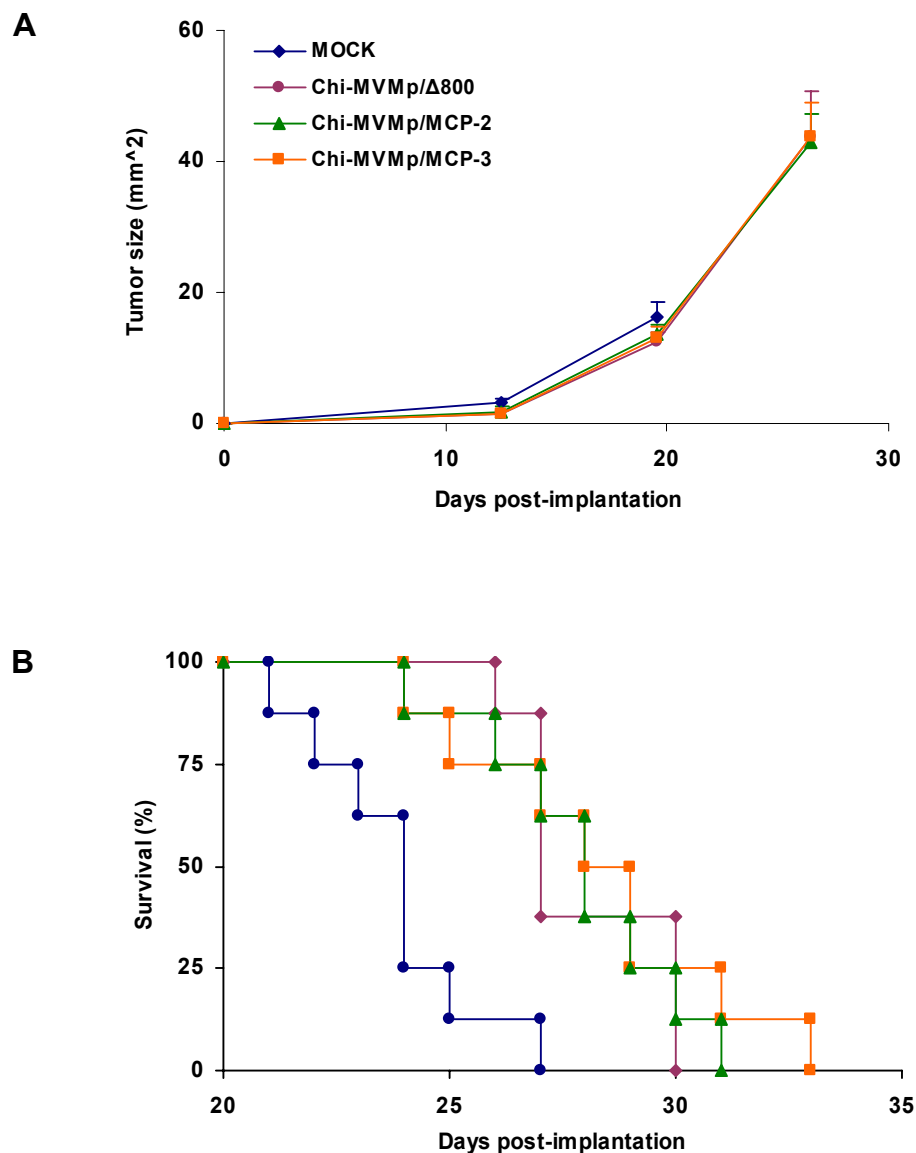
Figure 4-19: Tumor growth and animal survival of mice intracranially implanted with GL261 cells transducing MCP-2 or MCP-3

GL261 cells were infected *in vitro* with Chi-MVMp/MCP-2, or Chi-MVMp/MCP-3 (MOI = 3 RU/cell). Chi-MVMp/Δ800-infected cells (MOI = 3 RU/cell) and buffer-treated cells (mock) served as control. 1 x 10^5 cells were intracranially implanted in the left striatum of C57BL/6 mice (9 per group). Tumor development and animal survival were monitored over time. The tumor growth (A) and the percentage of surviving animals per group (B) are plotted as a function of time post-implantation. The tumor size is given as mm^2 + SEM.

As observed in Figure 4-19, whereas the tumor growth of GL261 infected with Chi-MVMp/Δ800 or buffer-treated was comparable up to 20 days post-implantation, the median survival of mice implanted with GL261 infected with Chi-MVMp/Δ800 (27 days) was slightly increased compared to mice implanted with buffer-treated cells (24 days). The intracranial tumor growth of GL261 cells infected with parvoviral vectors transducing MCP-2 or MCP-3 and the corresponding survival (median survival: 28 days for MCP-2, and 28.5 days for MCP-3) was similar to that of the empty vector (median survival: 27 days). This indicates that the effect observed can be attributed to the parvoviral vector alone rather than to the inflammatory cytokines. It might be that these two cytokines are processed when produced by GL261, leading to their inactivation by cleavage, as it was shown for MCP-2 delivered by parvoviral-derived vectors in melanomas (Struyf et al., in press).

5. DISCUSSION

5.1. Mechanisms sustaining tumor inhibition by TNF-α- and IP-10-expressing parvoviral vectors in the GL261 subcutaneous model

Parvoviral vectors transducing hIP-10 and mTNF-α were recently shown to strongly inhibit the growth of GL261 glioma, especially when GL261 cells were coinfected *in vitro* with TNF-α- and IP-10-transducing parvoviruses, and subcutaneously implanted in syngeneic mice. A synergistic antitumor activity of these cytokines was demonstrated. The treatment of established tumors with peritumoral injections of cytokine-encoding parvoviruses also inhibited the tumor growth compared to tumors treated with the controls but to a lesser extend than in the *in vitro* setting and the antitumor effects of TNF-α- and IP-10-transducing vectors or the combination of both were comparable (Enderlin et al., 2008).

5.1.1. Implication of T lymphocytes and the possible roles of Tregs and TGF-β

The immunohistochemical analysis of CD4$^+$ lymphocytes infiltrating established GL261 subcutaneous tumors treated with parvoviral vectors showed a dramatically decreased infiltration that inversely correlated with the tumor growth *in vivo*. Thus, we hypothesized that the antitumor response might be related to a decreased tumor invasion and/or proliferation of CD4$^+$ Tregs, known to suppress immune responses. Supporting this possibility, the depletion of Tregs was shown to prolong the survival of C57BL/6 mice bearing intracranial GL261 tumors (El Andaloussi et al., 2006; Grauer et al., 2007).

This hypothesis would need to be confirmed through the analysis of Treg specific markers. Up to now, the most specific marker for mouse Tregs is FoxP3, a member of the forkhead transcription factor family. FoxP3 is highly expressed in CD4$^+$ Tregs and was shown to be linked to their suppressive activity (Fontenot et al., 2003; Hori et al., 2003). Other molecules are constitutively expressed on Tregs such as the IL-2 receptor α-chain (CD25) and the cytotoxic lymphocyte-associated antigen-4 (CTLA-4), and are alternatively used to identify Tregs. However, these molecules can also be found temporarily on conventional CD4$^+$ T cells upon activation and are thus not highly specific for Tregs (Furtado et al., 2002; Takahashi et al., 2000). Hence, to confirm a

decrease of CD4$^+$ Tregs upon infection with recombinant parvoviruses, a double staining for CD4 and FoxP3 could be performed by immunohistochemistry or fluorescence-activated cell sorting (FACS) analysis. Furthermore, we could verify that anti-CD25 antibodies-mediated depletion of Tregs reduces the growth of virus-infected GL261 implanted subcutaneously.

Moreover, our results revealed that the decrease in CD4$^+$ lymphocytes correlated with decreased expression of TGF-β, which is known to induce Treg infiltration and proliferation (Chen and Wahl, 2003; Ghiringhelli et al., 2005). To confirm the effect of TGF-β on CD4$^+$ Tregs, we could block TGF-β *in vivo* by means of TGF-β blocking antibodies and study its effect on the proportion of CD4$^+$ Tregs infiltrating tumors.

We showed a decreased expression of TGF-β *in vitro* in GL261 cells infected with cytokine-encoding vectors compared to cells infected with the controls (MVMp wt, empty vector or buffer-treated cells). Interestingly, TGF-β was also reported to impair the function of both CD4$^+$ and CD8$^+$ lymphocytes (Gorelik and Flavell, 2002; Thomas and Massague, 2005). This prompted us to consider that the lymphocyte activity might be impaired by TGF-β in the controls but not in cytokine-treated tumors. To verify this hypothesis, we could test in our experimental setting the activation status of CD4$^+$ and CD8$^+$ tumor infiltrating lymphocytes by FACS analysis for lymphocyte activation markers such as CD25, CD69 or CD44^{high}. As for cytotoxic CD8$^+$ T lymphocytes (CTL), we could also perform RT-PCR on tumors samples for the expression of markers of CTL-mediated cytotoxicity such as perforin, granzyme A and B, IFN-γ, and Fas ligand (Russell and Ley, 2002).

5.1.2. Implication of macrophages

The analysis of the macrophage infiltration in established subcutaneous GL261 tumor revealed a slight increase in tumors treated with the combination of parvoviral vectors encoding TNF-α and IP-10 compared to the control. Since the treatment of established tumors with parvoviral vectors transducing TNF-α, IP-10 or both had similar antitumor effects, we assume that the contribution of macrophages is only marginal in this setting. However, it would be interesting to verify the contribution of macrophages when *in vitro* infected GL261 cells are subsequently grafted subcutaneously, as in this setting, the combination of parvoviral vectors encoding TNF-α and IP-10 had the most potent effect. This could be tested by depletion of macrophages using anti-CD68 antibodies.

5.2. Inhibition of tumor growth and increased survival of mice implanted intracranially with GL261 cells transducing TNF-α alone or in combination with IP-10, but not IP-10 alone

We showed that the infection of GL261 cells prior implantation with Chi-MVMp/Δ800 and MVMp wt did not significantly affect the intracranial tumor growth of GL261 cells compared with buffer-treated cells, and only slightly prolonged the survival of mice. These results are in agreement with the marginal effects of parvoviral infection in the GL261 subcutaneous model (Enderlin et al., 2008).

The intracranial tumor growth was significantly delayed and the survival prolonged in animals implanted with Chi-MVMp/TNF-α-infected GL261 cells or with cells coinfected with Chi-MVMp/TNF-α and Chi-MVMp/IP-10 compared to the empty vector Chi-MVMp/Δ800. Surprisingly, in contrast to the data obtained subcutaneously, the growth of GL261 cells infected with Chi-MVMp/IP-10 alone and the survival of recipient mice was similar to the empty vector. Moreover, there were no significant differences in tumor growth and survival between mice implanted with parvoviral vectors delivering TNF-α alone or together with IP-10.

Thus, in contrast to the subcutaneous setting, when the glioma cells are implanted intracranially, the most potent antitumor effects were obtained with TNF-α-transducing parvoviral vector. The effects of TNF-α are in agreement with those of Ehtesham et al., who observed a prolonged survival of mice implanted with GL26 glioma cells treated with an adenoviral vector encoding TNF-α compared to mice treated with a control vector encoding LacZ (Ehtesham et al., 2002).

The lack of antitumor effect of the recombinant parvovirus encoding human IP-10 (hIP-10) prompted us to investigate the possibility that hIP-10 transduced in GL261 cells could be degraded or inactivated. To verify this, hIP-10 produced by parvovirus-infected GL261 cells was purified until homogeneity from cell supernatants and was analyzed by mass spectrometry in collaboration with S. Struyf (Rega Institute, University of Leuven, Belgium). Preliminary results indicate that several forms of hIP-10 are produced by infected GL261 cells, some of which might be inactive.

Yet, Chi-MVMp/IP-10 was shown to be effective as antitumor agent subcutaneously when used alone. This suggests that the levels of active hIP-10 transduced are sufficient to induce an antitumor response subcutaneously. In the brain, hIP-10 might be further modified or degraded due to the presence of modifying enzymes or proteases in

the tumor environment. Alternatively, some brain cells might bind and/or trap (decoy receptors) IP-10, thus diminishing its availability to attract leukocytes. Indeed, CXCR3 expression was found to be constitutively expressed *in vivo* in astrocytes and neurons (Goldberg et al., 2001; Xia et al., 2000).

Moreover, the fact that hIP-10 produced by infected GL261 cells might be partly degraded or inactivated supports the hypothesis that the synergistical antitumor effects observed subcutaneously, when using both vectors encoding mTNF-α and hIP-10, could indeed be related to the increased mIP-10 secretion in GL261 cells infected with TNF-α-transducing parvovirus.

Our hypothesis is that in the brain, but not subcutaneously, the levels of intact hIP-10 produced by recombinant parvovirus-infected GL261 cells are further processed so that only endogenous mIP-10, induced by TNF-α, may be produced in an active form, yet at too low levels to be effective.

To test this, it appears thus relevant to produce a Chi-MVMp-based parvoviral vector delivering mouse IP-10 and to evaluate its antitumor effects intracranially, alone or in combination with the TNF-α-transducing vector.

5.3. Mechanisms sustaining the antitumor effects of TNF-α-transducing parvoviral vectors in the GL261 intracranial tumor model

The above mentioned observations prompted us to study the mechanisms responsible for the antitumor effects of TNF-α-transducing parvoviral vector. TNF-α is a pluripotent cytokine, known for its immunostimulatory properties, but also as a potent inhibitor of angiogenesis (Lejeune et al., 1998; Mocellin et al., 2005). In addition, it is also able to induce direct killing of tumor cells through necrosis or apoptosis (Ashkenazi and Dixit, 1998; Carswell et al., 1975). Here, we showed an effect of parvoviral TNF-α on intracranial tumor vascularization and on the infiltration of macrophages. We also investigated the apoptosis of intratumoral cells but could not see any significant differences between the different groups. This suggest that at least at the time point studied, TNF-α did not induce direct killing of tumor cells, although GL261 cells express TNF-α receptors.

5.3.1. Parvoviral-transduced TNF-α inhibits GL261 tumor microvascularization

We observed that parvoviral-transduced TNF-α significantly decreased the microvascularization of intracranial GL261 tumors, as shown by reduced CD31 labeling. TNF-α was reported to inhibit tumor neovascularization as well as to induce endothelial cell death (Lejeune et al., 2006; Mocellin et al., 2005; Polunovsky et al., 1994; Sato et al., 1987). Whether inhibition of angiogenesis and/or endothelial cell death contribute to the decrease of microvascularization in our system remains to be elucidated.

The angiogenesis was previously also investigated in the subcutaneous tumor model by CD31 labeling but no effect could be detected neither with parvoviruses encoding TNF-α, IP-10, or the combination of both. However, this analysis was performed on subcutaneous established tumors that were treated *in vivo* with parvoviruses. Therefore, the cytokine levels achieved might have been too low, due to loss of the virus in non-tumoral cells. Yet, tumor necrosis was shown to be enhanced in the groups treated with parvoviral vector encoding TNF-α (Enderlin et al., 2008). Whether this was due to direct killing of GL261 cells or to vascular damage remains to ne determined.

5.3.2. Parvoviral-transduced TNF-α decreases the infiltration of macrophages and/or microglia in GL261 brain tumors

We showed lower numbers of macrophages/microglia in GL261 tumors transducing TNF-α. The reduced infiltration with microglia/macrophages correlated with the reduced tumor growth and increased survival of mice. These results are in agreement with clinical studies indicating that the extend of glioma-associated macrophages/microglia positively correlates with poor prognosis (Leung et al., 1997; Roggendorf et al., 1996; Rossi et al., 1988). These data are also in accordance with those of Engel et al., who showed that inhibition of C6 rat glioma growth correlated with decreased macrophages/microglial infiltration (Engel et al., 1999), and of Platten et al., who showed that macrophages/microglia infiltration induced by MCP-1-transducing CNS-1 glioma tumors inversely correlated with animal survival (Platten et al., 2003). Macropages/micoglia may indeed contribute to tumor development by secreting growth signals, angiogenic factors, matrix-degrading proteinases, and immunosuppressors (Badie and Schartner, 2001; Bingle et al., 2002; Graeber et al., 2002).

Both peripheral macrophages and microglia are CD68$^+$. Thus, we cannot discriminate between the relative contribution of both types of cells in our system by means of this marker. So far, no specific markers have been identified to differentiate microglia and

macrophages. Yet, some markers are differentially expressed on both types of cells in the mouse, such as CD45 which is highly expressed on macrophages (CD45^{high}) and less on microglia (CD45$^+$) (Sedgwick et al., 1991). We could thus consider using such a marker to discriminate both cell types by FACS analysis.

The reduced numbers of macrophages/microglia in TNF-α-transduced intracranial GL261 tumors could be due to reduced invasion in the tumor, reduced proliferation, or increased cell death within the tumor. Indeed, TNFR-1 and TNFR-2 expression was reported on macrophages/microglia (Dopp et al., 1997) and TNF-α could thus directly kill these cells. Both types of cells are known to produce TNF-α upon activation (Waterston and Bower, 2004; Watters et al., 2005) and have thus evolved to be resistant to TNF-α-mediated apoptosis. For instance, macrophages were shown to constitutively express NF-κB, and its inhibition induced macrophages apoptosis (Liu et al., 2004). It might be that macrophages/microglia are sensitized to TNF-α-induced cell death in the glioma microenvironment through inhibition of NF-κB. Alternatively, TNF-α may act indirectly by inducing or inhibiting the production of other proteins that would lead to macrophages/microglia cell death or decrease their infiltration and/or proliferation.

5.3.3. Slight increased infiltration of lymphocyte in parvovirus-infected brain tumors

We showed a mild increase of CD4$^+$ and CD8$^+$ lymphocytes in parvovirus-infected GL261 intracranial tumors compared to the control (mock), but no significant attraction due to the cytokines expressed by parvoviral vectors. Yet, as mentioned before, it might be that the activation of lymphocytes is higher in tumors transducing cytokines than in the controls (MVMp wt and the empty vector) as a result of the decreased TGF-β secretion in GL261 transducing cytokines. In agreement with this, inhibition of TGF-β signaling using an inhibitor of the TGF-βRI kinase was shown to restore immune surveillance and to improve the survival of mice implanted intracranially with SMA-560 glioma (Tran et al., 2007). Furthermore, the eradication of established intracranial 9L rat gliomas was reported after subcutaneous immunizations with 9L cells expressing a TGF-β antisense construct (Fakhrai et al., 1996). Thus, it would be interesting to test the expression of TGF-β *in vivo* in our system, for example by RT-PCR on tumor samples.

5.4. Potential of cytokine-transducing parvoviral vectors for glioma therapy

Our findings illustrate the efficacy of TNF-α-encoding parvoviral vectors as antitumor agent in a mouse syngeneic intracranial glioma model. Further studies should be performed to exploit the therapeutic potential of cytokine-encoding parvoviral vectors and their possible application to malignant gliomas. This would include the injection of parvoviral vectors *in vivo* in established brain tumors or the use cytokine-secreting autologous glioma vaccines. As the adult brain is composed of low proliferating glial cells and post-mitotic neurons, the application of parvoviral vectors *in vivo* should selectively target glioma tumor cells, as the parvoviral life cycle is strictly dependent on host cell proliferation. In agreement with this, preclinical studies showed that normal mouse astrocytes and microglia sustain an abortive viral life cycle upon MVMp infection (Abschuetz et al., 2006).

Cytokine-transducing parvoviral vectors, like all emerging immunotherapeutic agents, should be considered to be applied as adjuvant to the conventional treatment strategy, involving surgery, radiation and chemotherapy, to eradicate residual brain tumor cells. Of interest, several reports showed that the combination of radiation with intratumoral administration of TNF-α-encoding vectors substantially reduced glioma tumor progression (Li et al., 1998; Staba et al., 1998).

Thus, the use of TNF-α-encoding parvoviral vectors in combination with radiotherapy and/or chemotherapy appears as a promising therapeutic approach for the treatment of malignant gliomas. Whether TNF-α can be combined with IP-10 to increase its efficacy in the brain remains to be further investigated.

6. REFERENCES

Abe, M., Harpel, J.G., Metz, C.N., Nunes, I., Loskutoff, D.J., and Rifkin, D.B. (1994). An assay for transforming growth factor-beta using cells transfected with a plasminogen activator inhibitor-1 promoter-luciferase construct. Anal Biochem *216*, 276-284.

Abschuetz, A., Kehl, T., Geibig, R., Leuchs, B., Rommelaere, J., and Regnier-Vigouroux, A. (2006). Oncolytic murine autonomous parvovirus, a candidate vector for glioma gene therapy, is innocuous to normal and immunocompetent mouse glial cells. Cell and tissue research *325*, 423-436.

Aggarwal, B.B. (2003). Signalling pathways of the TNF superfamily: a double-edged sword. Nat Rev Immunol *3*, 745-756.

Aghi, M., and Chiocca, E.A. (2006). Gene therapy for glioblastoma. Neurosurgical focus *20*, E18.

Anderson, L.J. (2007). Human bocavirus: a new viral pathogen. Clin Infect Dis *44*, 911-912.

Anderson, M.J., Jones, S.E., Fisher-Hoch, S.P., Lewis, E., Hall, S.M., Bartlett, C.L., Cohen, B.J., Mortimer, P.P., and Pereira, M.S. (1983). Human parvovirus, the cause of erythema infectiosum (fifth disease)? Lancet *1*, 1378.

Andreansky, S.S., He, B., Gillespie, G.Y., Soroceanu, L., Markert, J., Chou, J., Roizman, B., and Whitley, R.J. (1996). The application of genetically engineered herpes simplex viruses to the treatment of experimental brain tumors. Proceedings of the National Academy of Sciences of the United States of America *93*, 11313-11318.

Angiolillo, A.L., Sgadari, C., Taub, D.D., Liao, F., Farber, J.M., Maheshwari, S., Kleinman, H.K., Reaman, G.H., and Tosato, G. (1995). Human interferon-inducible protein 10 is a potent inhibitor of angiogenesis in vivo. The Journal of experimental medicine *182*, 155-162.

Arenberg, D.A., Kunkel, S.L., Polverini, P.J., Morris, S.B., Burdick, M.D., Glass, M.C., Taub, D.T., Iannettoni, M.D., Whyte, R.I., and Strieter, R.M. (1996). Interferon-gamma-inducible protein 10 (IP-10) is an angiostatic factor that inhibits human non-small cell lung cancer (NSCLC) tumorigenesis and spontaneous metastases. The Journal of experimental medicine *184*, 981-992.

Ashkenazi, A., and Dixit, V.M. (1998). Death receptors: signaling and modulation. Science (New York, NY *281*, 1305-1308.

Badie, B., and Schartner, J. (2001). Role of microglia in glioma biology. Microscopy research and technique *54*, 106-113.

Badie, B., Schartner, J., Prabakaran, S., Paul, J., and Vorpahl, J. (2001). Expression of Fas ligand by microglia: possible role in glioma immune evasion. Journal of neuroimmunology *120*, 19-24.

Badie, B., and Schartner, J.M. (2000). Flow cytometric characterization of tumor-associated macrophages in experimental gliomas. Neurosurgery *46*, 957-961; discussion 961-952.

Balkwill, F. (1998). The molecular and cellular biology of the chemokines. Journal of viral hepatitis *5*, 1-14.

Balkwill, F. (2006). TNF-alpha in promotion and progression of cancer. Cancer metastasis reviews *25*, 409-416.

Ball-Goodrich, L.J., Leland, S.E., Johnson, E.A., Paturzo, F.X., and Jacoby, R.O. (1998). Rat parvovirus type 1: the prototype for a new rodent parvovirus serogroup. Journal of virology *72*, 3289-3299.

REFERENCES

Barzon, L., Zanusso, M., Colombo, F., and Palu, G. (2006). Clinical trials of gene therapy, virotherapy, and immunotherapy for malignant gliomas. Cancer gene therapy *13*, 539-554.

Bashir, T., Rommelaere, J., and Cziepluch, C. (2001). In vivo accumulation of cyclin A and cellular replication factors in autonomous parvovirus minute virus of mice-associated replication bodies. Journal of virology *75*, 4394-4398.

Belperio, J.A., Keane, M.P., Arenberg, D.A., Addison, C.L., Ehlert, J.E., Burdick, M.D., and Strieter, R.M. (2000). CXC chemokines in angiogenesis. Journal of leukocyte biology *68*, 1-8.

Bemelmans, M.H., van Tits, L.J., and Buurman, W.A. (1996). Tumor necrosis factor: function, release and clearance. Critical reviews in immunology *16*, 1-11.

Benitez, J.A., Dominguez-Monzon, G., and Segovia, J. (2008). Conventional and gene therapy strategies for the treatment of brain tumors. Current medicinal chemistry *15*, 729-742.

Berns, K.I. (1996). Parvoviridae: the viruses and their replication. In Fields virology, Kerr JR, Cotmore SF, Bloom ME, Linden RM, Parrish, CR Lippincot-Raven: Philadelphia 2173-2197.

Berns, K.I., Bergoin, M.B., M., Muzyczka, N., Tal, J., and Tattersall, P. (2000). Family Parvoviridae. In Virus Taxonomy. Seventh Report of the International Committee on Taxonomy of Viruses, pp 311–323 Edited by M H V van Regenmortel, C M Fauquet, D H L Bishop & 8 others San Diego: Academic Press.

Bikfalvi, A. (2004). Recent developments in the inhibition of angiogenesis: examples from studies on platelet factor-4 and the VEGF/VEGFR system. Biochemical pharmacology *68*, 1017-1021.

Bingle, L., Brown, N.J., and Lewis, C.E. (2002). The role of tumour-associated macrophages in tumour progression: implications for new anticancer therapies. The Journal of pathology *196*, 254-265.

Bodendorf, U., Cziepluch, C., Jauniaux, J.C., Rommelaere, J., and Salome, N. (1999). Nuclear export factor CRM1 interacts with nonstructural proteins NS2 from parvovirus minute virus of mice. Journal of virology *73*, 7769-7779.

Bonecchi, R., Bianchi, G., Bordignon, P.P., D'Ambrosio, D., Lang, R., Borsatti, A., Sozzani, S., Allavena, P., Gray, P.A., Mantovani, A*., et al.* (1998). Differential expression of chemokine receptors and chemotactic responsiveness of type 1 T helper cells (Th1s) and Th2s. The Journal of experimental medicine *187*, 129-134.

Brada, M. (2006). Radiotherapy in malignant glioma. Ann Oncol *17 Suppl 10*, x183-185.

Brandenburger, A., Coessens, E., El Bakkouri, K., and Velu, T. (1999). Influence of sequence and size of DNA on packaging efficiency of parvovirus MVM-based vectors. Human gene therapy *10*, 1229-1238.

Brandenburger, A., Legendre, D., Avalosse, B., and Rommelaere, J. (1990). NS-1 and NS-2 proteins may act synergistically in the cytopathogenicity of parvovirus MVMp. Virology *174*, 576-584.

Brandes, A.A., Tosoni, A., Franceschi, E., Reni, M., Gatta, G., and Vecht, C. (2008). Glioblastoma in adults. Critical reviews in oncology/hematology *67*, 139-152.

Brockhaus, K., Plaza, S., Pintel, D.J., Rommelaere, J., and Salome, N. (1996). Nonstructural proteins NS2 of minute virus of mice associate in vivo with 14-3-3 protein family members. Journal of virology *70*, 7527-7534.

Brown, C.S., DiSumma, F.M., Rommelaere, J., Dege, A.Y., Cornelis, J.J., Dinsart, C., and Spaan, W.J. (2002). Production of recombinant H1 parvovirus stocks devoid of replication-competent viruses. Human gene therapy *13*, 2135-2145.

Brown, K.E., Anderson, S.M., and Young, N.S. (1993). Erythrocyte P antigen: cellular receptor for B19 parvovirus. Science (New York, NY *262*, 114-117.

Buttmann, M., Berberich-Siebelt, F., Serfling, E., and Rieckmann, P. (2007). Interferon-beta is a potent inducer of interferon regulatory factor-1/2-dependent IP-10/CXCL10 expression in primary human endothelial cells. Journal of vascular research *44*, 51-60.

Caillet-Fauquet, P., Perros, M., Brandenburger, A., Spegelaere, P., and Rommelaere, J. (1990). Programmed killing of human cells by means of an inducible clone of parvoviral genes encoding non-structural proteins. The EMBO journal *9*, 2989-2995.

Carswell, E.A., Old, L.J., Kassel, R.L., Green, S., Fiore, N., and Williamson, B. (1975). An endotoxin-induced serum factor that causes necrosis of tumors. Proceedings of the National Academy of Sciences of the United States of America *72*, 3666-3670.

CBTRUS (2004). Statistical report: Primary brain tumors in the United States, 1997-2001. Hinsdale, IL, Central Brain Tumor Registry of the United States.

Cervantes-Barragan, L., Zust, R., Weber, F., Spiegel, M., Lang, K.S., Akira, S., Thiel, V., and Ludewig, B. (2007). Control of coronavirus infection through plasmacytoid dendritic-cell-derived type I interferon. Blood *109*, 1131-1137.

Cha, S., Johnson, G., Wadghiri, Y.Z., Jin, O., Babb, J., Zagzag, D., and Turnbull, D.H. (2003). Dynamic, contrast-enhanced perfusion MRI in mouse gliomas: correlation with histopathology. Magn Reson Med *49*, 848-855.

Chen, G., and Goeddel, D.V. (2002). TNF-R1 signaling: a beautiful pathway. Science (New York, NY *296*, 1634-1635.

Chen, W., and Wahl, S.M. (2003). TGF-beta: the missing link in CD4+CD25+ regulatory T cell-mediated immunosuppression. Cytokine & growth factor reviews *14*, 85-89.

Chintala, S.K., Fueyo, J., Gomez-Manzano, C., Venkaiah, B., Bjerkvig, R., Yung, W.K., Sawaya, R., Kyritsis, A.P., and Rao, J.S. (1997). Adenovirus-mediated p16/CDKN2 gene transfer suppresses glioma invasion in vitro. Oncogene *15*, 2049-2057.

Chiocca, E.A., Abbed, K.M., Tatter, S., Louis, D.N., Hochberg, F.H., Barker, F., Kracher, J., Grossman, S.A., Fisher, J.D., Carson, K.*, et al.* (2004). A phase I open-label, dose-escalation, multi-institutional trial of injection with an E1B-Attenuated adenovirus, ONYX-015, into the peritumoral region of recurrent malignant gliomas, in the adjuvant setting. Mol Ther *10*, 958-966*.*

Chomczynski, P., and Sacchi, N. (1987). Single-step method of RNA isolation by acid guanidinium thiocyanate-phenol-chloroform extraction. Anal Biochem *162*, 156-159.

Clemens, K.E., and Pintel, D. (1987). Minute virus of mice (MVM) mRNAs predominantly polyadenylate at a single site. Virology *160*, 511-514.

Cole, K.E., Strick, C.A., Paradis, T.J., Ogborne, K.T., Loetscher, M., Gladue, R.P., Lin, W., Boyd, J.G., Moser, B., Wood, D.E.*, et al.* (1998). Interferon-inducible T cell alpha chemoattractant (I-TAC): a novel non-ELR CXC chemokine with potent activity on activated T cells through selective high affinity binding to CXCR3. The Journal of experimental medicine *187*, 2009-2021.

Cook, M. (1965). The anatomy of the laboratory mouse. Academic Press Inc, US*.*

Corbau, R., Duverger, V., Rommelaere, J., and Nuesch, J.P. (2000). Regulation of MVM NS1 by protein kinase C: impact of mutagenesis at consensus phosphorylation sites on replicative functions and cytopathic effects. Virology *278*, 151-167.

Cornelis, J.J., Becquart, P., Duponchel, N., Salome, N., Avalosse, B.L., Namba, M., and Rommelaere, J. (1988). Transformation of human fibroblasts by ionizing radiation, a chemical carcinogen, or simian virus 40 correlates with an increase in susceptibility to the autonomous parvoviruses H-1 virus and minute virus of mice. Journal of virology *62*, 1679-1686.

Cornelis, J.J., Lang, S.I., Stroh-Dege, A.Y., Balboni, G., Dinsart, C., and Rommelaere, J. (2004a). Cancer gene therapy through autonomous parvovirus--mediated gene transfer. Current gene therapy *4*, 249-261.

Cornelis, J.J., Salome, N., Dinsart, C., and Rommelaere, J. (2004b). Vectors based on autonomous parvoviruses: novel tools to treat cancer? The journal of gene medicine *6 Suppl 1*, S193-202.

Cotmore, S.F., Christensen, J., Nuesch, J.P., and Tattersall, P. (1995). The NS1 polypeptide of the murine parvovirus minute virus of mice binds to DNA sequences containing the motif [ACCA]2-3. Journal of virology *69*, 1652-1660.

Cotmore, S.F., D'Abramo, A.M., Jr., Carbonell, L.F., Bratton, J., and Tattersall, P. (1997). The NS2 polypeptide of parvovirus MVM is required for capsid assembly in murine cells. Virology *231*, 267-280.

Cotmore, S.F., and Tattersall, P. (1987). The autonomously replicating parvoviruses of vertebrates. Advances in virus research *33*, 91-174.

Cotmore, S.F., and Tattersall, P. (2007). Parvoviral host range and cell entry mechanisms. Advances in virus research *70*, 183-232.

Creagan, E.T., Kovach, J.S., Moertel, C.G., Frytak, S., and Kvols, L.K. (1988). A phase I clinical trial of recombinant human tumor necrosis factor. Cancer *62*, 2467-2471.

Deleu, L., Pujol, A., Faisst, S., and Rommelaere, J. (1999). Activation of promoter P4 of the autonomous parvovirus minute virus of mice at early S phase is required for productive infection. Journal of virology *73*, 3877-3885.

Dopp, J.M., Mackenzie-Graham, A., Otero, G.C., and Merrill, J.E. (1997). Differential expression, cytokine modulation, and specific functions of type-1 and type-2 tumor necrosis factor receptors in rat glia. Journal of neuroimmunology *75*, 104-112.

Dupont, F., Avalosse, B., Karim, A., Mine, N., Bosseler, M., Maron, A., Van den Broeke, A.V., Ghanem, G.E., Burny, A., and Zeicher, M. (2000). Tumor-selective gene transduction and cell killing with an oncotropic autonomous parvovirus-based vector. Gene therapy *7*, 790-796.

Dupont, F., Karim, A., Dumon, J.C., Mine, N., and Avalosse, B. (2001). A novel MVMp-based vector system specifically designed to reduce the risk of replication-competent virus generation by homologous recombination. Gene therapy *8*, 921-929.

Dupont, F., Tenenbaum, L., Guo, L.P., Spegelaere, P., Zeicher, M., and Rommelaere, J. (1994). Use of an autonomous parvovirus vector for selective transfer of a foreign gene into transformed human cells of different tissue origins and its expression therein. Journal of virology *68*, 1397-1406.

Dupressoir, T., Vanacker, J.M., Cornelis, J.J., Duponchel, N., and Rommelaere, J. (1989). Inhibition by parvovirus H-1 of the formation of tumors in nude mice and colonies in vitro by transformed human mammary epithelial cells. Cancer research *49*, 3203-3208.

Ehtesham, M., Samoto, K., Kabos, P., Acosta, F.L., Gutierrez, M.A., Black, K.L., and Yu, J.S. (2002). Treatment of intracranial glioma with in situ interferon-gamma and tumor necrosis factor-alpha gene transfer. Cancer gene therapy *9*, 925-934.

Eichwald, V., Daeffler, L., Klein, M., Rommelaere, J., and Salome, N. (2002). The NS2 proteins of parvovirus minute virus of mice are required for efficient nuclear egress of progeny virions in mouse cells. Journal of virology *76*, 10307-10319.

El Andaloussi, A., Han, Y., and Lesniak, M.S. (2006). Prolongation of survival following depletion of CD4+CD25+ regulatory T cells in mice with experimental brain tumors. Journal of neurosurgery *105*, 430-437.

El Bakkouri, K., Servais, C., Clement, N., Cheong, S.C., Franssen, J.D., Velu, T., and Brandenburger, A. (2005). In vivo anti-tumour activity of recombinant MVM parvoviral vectors carrying the human interleukin-2 cDNA. The journal of gene medicine *7*, 189-197.

Enderlin, M. (2004). Evaluation of IP-10 and TNF-α transducing parvoviral vectors as antitumoral agents in animal glioblastoma models. PhD thesis.

Enderlin, M., Kleinmann, E.V., Struyf, S., Buracchi, C., Vecchi, A., Kinscherf, R., Kiessling, F., Paschek, S., Sozzani, S., Rommelaere, J*., et al.* (2008). TNF-alpha and the IFN-gamma-inducible protein 10 (IP-10/CXCL-10) delivered by parvoviral vectors act in synergy to induce antitumor effects in mouse glioblastoma. Cancer gene therapy.

Engel, S., Isenmann, S., Stander, M., Rieger, J., Bahr, M., and Weller, M. (1999). Inhibition of experimental rat glioma growth by decorin gene transfer is associated with decreased microglial infiltration. Journal of neuroimmunology *99*, 13-18.

Faisst, S., Guittard, D., Benner, A., Cesbron, J.Y., Schlehofer, J.R., Rommelaere, J., and Dupressoir, T. (1998). Dose-dependent regression of HeLa cell-derived tumours in SCID mice after parvovirus H-1 infection. International journal of cancer *75*, 584-589.

Fakhrai, H., Dorigo, O., Shawler, D.L., Lin, H., Mercola, D., Black, K.L., Royston, I., and Sobol, R.E. (1996). Eradication of established intracranial rat gliomas by transforming growth factor beta antisense gene therapy. Proceedings of the National Academy of Sciences of the United States of America *93*, 2909-2914.

Feldman, A.L., Friedl, J., Lans, T.E., Libutti, S.K., Lorang, D., Miller, M.S., Turner, E.M., Hewitt, S.M., and Alexander, H.R. (2002). Retroviral gene transfer of interferon-inducible protein 10 inhibits growth of human melanoma xenografts. International journal of cancer *99*, 149-153.

Feldman, E.D., Weinreich, D.M., Carroll, N.M., Burness, M.L., Feldman, A.L., Turner, E., Xu, H., and Alexander, H.R., Jr. (2006). Interferon gamma-inducible protein 10 selectively inhibits proliferation and induces apoptosis in endothelial cells. Annals of surgical oncology *13*, 125-133.

Fioretti, F., Fradelizi, D., Stoppacciaro, A., Ramponi, S., Ruco, L., Minty, A., Sozzani, S., Garlanda, C., Vecchi, A., and Mantovani, A. (1998). Reduced tumorigenicity and augmented leukocyte infiltration after monocyte chemotactic protein-3 (MCP-3) gene transfer: perivascular accumulation of dendritic cells in peritumoral tissue and neutrophil recruitment within the tumor. J Immunol *161*, 342-346.

Fiveash, J.B., and Spencer, S.A. (2003). Role of radiation therapy and radiosurgery in glioblastoma multiforme. Cancer journal (Sudbury, Mass *9*, 222-229.

Fontenot, J.D., Gavin, M.A., and Rudensky, A.Y. (2003). Foxp3 programs the development and function of CD4+CD25+ regulatory T cells. Nature immunology *4*, 330-336.

Fueyo, J., Gomez-Manzano, C., Alemany, R., Lee, P.S., McDonnell, T.J., Mitlianga, P., Shi, Y.X., Levin, V.A., Yung, W.K., and Kyritsis, A.P. (2000). A mutant oncolytic adenovirus targeting the Rb pathway produces anti-glioma effect in vivo. Oncogene *19*, 2-12.

Furtado, G.C., Curotto de Lafaille, M.A., Kutchukhidze, N., and Lafaille, J.J. (2002). Interleukin 2 signaling is required for CD4(+) regulatory T cell function. The Journal of experimental medicine *196*, 851-857.

Gattass, C.R., King, L.B., Luster, A.D., and Ashwell, J.D. (1994). Constitutive expression of interferon gamma-inducible protein 10 in lymphoid organs and inducible expression in T cells and thymocytes. The Journal of experimental medicine *179*, 1373-1378.

Ghiringhelli, F., Puig, P.E., Roux, S., Parcellier, A., Schmitt, E., Solary, E., Kroemer, G., Martin, F., Chauffert, B., and Zitvogel, L. (2005). Tumor cells convert immature myeloid dendritic cells into TGF-beta-secreting cells inducing CD4+CD25+ regulatory T cell proliferation. The Journal of experimental medicine *202*, 919-929.

Giese, N.A., Raykov, Z., DeMartino, L., Vecchi, A., Sozzani, S., Dinsart, C., Cornelis, J.J., and Rommelaere, J. (2002). Suppression of metastatic hemangiosarcoma by a parvovirus MVMp vector transducing the IP-10 chemokine into immunocompetent mice. Cancer gene therapy *9*, 432-442.

Goldberg, S.H., van der Meer, P., Hesselgesser, J., Jaffer, S., Kolson, D.L., Albright, A.V., Gonzalez-Scarano, F., and Lavi, E. (2001). CXCR3 expression in human central nervous system diseases. Neuropathology and applied neurobiology *27*, 127-138.

REFERENCES

Gorelik, L., and Flavell, R.A. (2002). Transforming growth factor-beta in T-cell biology. Nat Rev Immunol *2*, 46-53.

Graeber, M.B., Scheithauer, B.W., and Kreutzberg, G.W. (2002). Microglia in brain tumors. Glia *40*, 252-259.

Graham, F.L., Smiley, J., Russell, W.C., and Nairn, R. (1977). Characteristics of a human cell line transformed by DNA from human adenovirus type 5. The Journal of general virology *36*, 59-74.

Grauer, O.M., Nierkens, S., Bennink, E., Toonen, L.W., Boon, L., Wesseling, P., Sutmuller, R.P., and Adema, G.J. (2007). CD4+FoxP3+ regulatory T cells gradually accumulate in gliomas during tumor growth and efficiently suppress antiglioma immune responses in vivo. International journal of cancer *121*, 95-105.

Graycar, J.L., Miller, D.A., Arrick, B.A., Lyons, R.M., Moses, H.L., and Derynck, R. (1989). Human transforming growth factor-beta 3: recombinant expression, purification, and biological activities in comparison with transforming growth factors-beta 1 and -beta 2. Molecular endocrinology (Baltimore, Md *3*, 1977-1986.

Greener, A. (1990). E. coli SURE™ strain: Clone 'unclonable' DNA. Strategies *3*, 5–6.

Haag, A., Menten, P., Van Damme, J., Dinsart, C., Rommelaere, J., and Cornelis, J.J. (2000). Highly efficient transduction and expression of cytokine genes in human tumor cells by means of autonomous parvovirus vectors; generation of antitumor responses in recipient mice. Human gene therapy *11*, 597-609.

Harrow, S., Papanastassiou, V., Harland, J., Mabbs, R., Petty, R., Fraser, M., Hadley, D., Patterson, J., Brown, S.M., and Rampling, R. (2004). HSV1716 injection into the brain adjacent to tumour following surgical resection of high-grade glioma: safety data and long-term survival. Gene therapy *11*, 1648-1658.

Heise, C., Sampson-Johannes, A., Williams, A., McCormick, F., Von Hoff, D.D., and Kirn, D.H. (1997). ONYX-015, an E1B gene-attenuated adenovirus, causes tumor-specific cytolysis and antitumoral efficacy that can be augmented by standard chemotherapeutic agents. Nature medicine *3*, 639-645.

Herrero, Y.C.M., Cornelis, J.J., Herold-Mende, C., Rommelaere, J., Schlehofer, J.R., and Geletneky, K. (2004). Parvovirus H-1 infection of human glioma cells leads to complete viral replication and efficient cell killing. International journal of cancer *109*, 76-84.

Herrlinger, U., Aulwurm, S., Strik, H., Weit, S., Naumann, U., and Weller, M. (2004). MIP-1alpha antagonizes the effect of a GM-CSF-enhanced subcutaneous vaccine in a mouse glioma model. Journal of neuro-oncology *66*, 147-154.

Holness, C.L., da Silva, R.P., Fawcett, J., Gordon, S., and Simmons, D.L. (1993). Macrosialin, a mouse macrophage-restricted glycoprotein, is a member of the lamp/lgp family. The Journal of biological chemistry *268*, 9661-9666.

Hori, S., Nomura, T., and Sakaguchi, S. (2003). Control of regulatory T cell development by the transcription factor Foxp3. Science (New York, NY *299*, 1057-1061.

Horuk, R. (1998). Chemokines beyond inflammation. Nature *393*, 524-525.

Hsieh, J.C., and Lesniak, M.S. (2005). Surgical management of high-grade gliomas. Expert review of neurotherapeutics *5*, S33-39.

Jacoby, R.O., Ball-Goodrich, L.J., Besselsen, D.G., McKisic, M.D., Riley, L.K., and Smith, A.L. (1996). Rodent parvovirus infections. Laboratory animal science *46*, 370-380.

Kaplan, E.L., and Meier, P. (1958). Nonparametric estimation from incomplete observations. J Amer Statist Assoc *53*, 457-481.

Kato, A., Homma, T., Batchelor, J., Hashimoto, N., Imai, S., Wakiguchi, H., Saito, H., and Matsumoto, K. (2003). Interferon-alpha/beta receptor-mediated selective induction of a gene cluster by CpG oligodeoxynucleotide 2006. BMC Immunol *4*, 8.

Kerr, J.R., Cotmore, S.F., Bloom, M.E., Linden, R.M., and Parrish, C.R. (2006). Parvoviruses. Hodder Arnold Publication.

Kestler, J., Neeb, B., Struyf, S., Van Damme, J., Cotmore, S.F., D'Abramo, A., Tattersall, P., Rommelaere, J., Dinsart, C., and Cornelis, J.J. (1999). cis requirements for the efficient production of recombinant DNA vectors based on autonomous parvoviruses. Human gene therapy *10*, 1619-1632.

Keyser, J., Schultz, J., Ladell, K., Elzaouk, L., Heinzerling, L., Pavlovic, J., and Moelling, K. (2004). IP-10-encoding plasmid DNA therapy exhibits anti-tumor and anti-metastatic efficiency. Experimental dermatology *13*, 380-390.

Kilham, L., and Olivier, L.J. (1959). A latent virus of rats isolated in tissue culture. Virology *7*, 428-437.

Kim, C.H., Johnston, B., and Butcher, E.C. (2002). Trafficking machinery of NKT cells: shared and differential chemokine receptor expression among V alpha 24(+)V beta 11(+) NKT cell subsets with distinct cytokine-producing capacity. Blood *100*, 11-16.

Kimsey, P.B., Engers, H.D., Hirt, B., and Jongeneel, C.V. (1986). Pathogenicity of fibroblast- and lymphocyte-specific variants of minute virus of mice. Journal of virology *59*, 8-13.

Kleihues, P., and Ohgaki, H. (1999). Primary and secondary glioblastomas: from concept to clinical diagnosis. Neuro-oncology *1*, 44-51.

Kock, H., Harris, M.P., Anderson, S.C., Machemer, T., Hancock, W., Sutjipto, S., Wills, K.N., Gregory, R.J., Shepard, H.M., Westphal, M.*, et al.* (1996). Adenovirus-mediated p53 gene transfer suppresses growth of human glioblastoma cells in vitro and in vivo. International journal of cancer *67*, 808-815.

Koziol, J.A., Maxwell, D.A., Fukushima, M., Colmerauer, M.E., and Pilch, Y.H. (1981). A distribution-free test for tumor-growth curve analyses with application to an animal tumor immunotherapy experiment. Biometrics *37*, 383-390.

Kunsch, C., Ruben, S.M., and Rosen, C.A. (1992). Selection of optimal kappa B/Rel DNA-binding motifs: interaction of both subunits of NF-kappa B with DNA is required for transcriptional activation. Molecular and cellular biology *12*, 4412-4421.

Laing, K.J., and Secombes, C.J. (2004). Chemokines. Developmental and comparative immunology *28*, 443-460.

Lang, F.F., Bruner, J.M., Fuller, G.N., Aldape, K., Prados, M.D., Chang, S., Berger, M.S., McDermott, M.W., Kunwar, S.M., Junck, L.R.*, et al.* (2003). Phase I trial of adenovirus-mediated p53 gene therapy for recurrent glioma: biological and clinical results. J Clin Oncol *21*, 2508-2518.

Lang, S.I., Giese, N.A., Rommelaere, J., Dinsart, C., and Cornelis, J.J. (2006). Humoral immune responses against minute virus of mice vectors. The journal of gene medicine *8*, 1141-1150.

Laperriere, N., Zuraw, L., and Cairncross, G. (2002). Radiotherapy for newly diagnosed malignant glioma in adults: a systematic review. Radiother Oncol *64*, 259-273.

Le Cesne, A., Dupressoir, T., Janin, N., Spielmann, M., Le Chevalier, T., Sancho-Garnier, H., Paoletti, C., Rommelaere, J., Stehelin, D., and Tursz, T. (1993). Intra-lesionaladministration of a live virus, parvovirus H-1 (PVH-1) in cancer patients: A feasibility study. Proc Annu Meet Am Soc Clin Oncol *12*, 297.

Lejeune, F., Lienard, D., Eggermont, A., Schraffordt Koops, H., Kroon, B., Gerain, J., Rosenkaimer, F., and Schmitz, P. (1994). Clinical experience with high-dose tumor necrosis factor alpha in regional therapy of advanced melanoma. Circulatory shock *43*, 191-197.

Lejeune, F.J., Lienard, D., Matter, M., and Ruegg, C. (2006). Efficiency of recombinant human TNF in human cancer therapy. Cancer Immun *6*, 6.

REFERENCES

Lejeune, F.J., Ruegg, C., and Lienard, D. (1998). Clinical applications of TNF-alpha in cancer. Current opinion in immunology *10*, 573-580.

Leung, S.Y., Wong, M.P., Chung, L.P., Chan, A.S., and Yuen, S.T. (1997). Monocyte chemoattractant protein-1 expression and macrophage infiltration in gliomas. Acta neuropathologica *93*, 518-527.

Li, J., Andres, M.L., Fodor, I., Nelson, G.A., and Gridley, D.S. (1998). Evaluation of pGL1-TNF-alpha therapy in combination with radiation. Oncology research *10*, 379-387.

Li, X., and Rhode, S.L., 3rd (1990). Mutation of lysine 405 to serine in the parvovirus H-1 NS1 abolishes its functions for viral DNA replication, late promoter trans activation, and cytotoxicity. Journal of virology *64*, 4654-4660.

Littlefield, J.W. (1964). Three Degrees of Guanylic Acid--Inosinic Acid Pyrophosphorylase Deficiency in Mouse Fibroblasts. Nature *203*, 1142-1144.

Liu, H., Ma, Y., Pagliari, L.J., Perlman, H., Yu, C., Lin, A., and Pope, R.M. (2004). TNF-alpha-induced apoptosis of macrophages following inhibition of NF-kappa B: a central role for disruption of mitochondria. J Immunol *172*, 1907-1915.

Loetscher, M., Gerber, B., Loetscher, P., Jones, S.A., Piali, L., Clark-Lewis, I., Baggiolini, M., and Moser, B. (1996). Chemokine receptor specific for IP10 and mig: structure, function, and expression in activated T-lymphocytes. The Journal of experimental medicine *184*, 963-969.

Lombardo, E., Ramirez, J.C., Garcia, J., and Almendral, J.M. (2002). Complementary roles of multiple nuclear targeting signals in the capsid proteins of the parvovirus minute virus of mice during assembly and onset of infection. Journal of virology *76*, 7049-7059.

Lonardi, S., Tosoni, A., and Brandes, A.A. (2005). Adjuvant chemotherapy in the treatment of high grade gliomas. Cancer treatment reviews *31*, 79-89.

Louis, D.N., Ohgaki, H., Wiestler, O.D., Cavenee, W.K., Burger, P.C., Jouvet, A., Scheithauer, B.W., and Kleihues, P. (2007). The 2007 WHO classification of tumours of the central nervous system. Acta neuropathologica *114*, 97-109.

Louis, D.N., Pomeroy, S.L., and Cairncross, J.G. (2002). Focus on central nervous system neoplasia. Cancer cell *1*, 125-128.

Luster, A.D. (1998). Chemokines--chemotactic cytokines that mediate inflammation. The New England journal of medicine *338*, 436-445.

Luster, A.D., Greenberg, S.M., and Leder, P. (1995). The IP-10 chemokine binds to a specific cell surface heparan sulfate site shared with platelet factor 4 and inhibits endothelial cell proliferation. The Journal of experimental medicine *182*, 219-231.

Luster, A.D., and Leder, P. (1993). IP-10, a -C-X-C- chemokine, elicits a potent thymus-dependent antitumor response in vivo. The Journal of experimental medicine *178*, 1057-1065.

Luster, A.D., Unkeless, J.C., and Ravetch, J.V. (1985). Gamma-interferon transcriptionally regulates an early-response gene containing homology to platelet proteins. Nature *315*, 672-676.

Ma, H.I., Lin, S.Z., Chiang, Y.H., Li, J., Chen, S.L., Tsao, Y.P., and Xiao, X. (2002). Intratumoral gene therapy of malignant brain tumor in a rat model with angiostatin delivered by adeno-associated viral (AAV) vector. Gene therapy *9*, 2-11.

Majumder, S., Zhou, L.Z., Chaturvedi, P., Babcock, G., Aras, S., and Ransohoff, R.M. (1998). Regulation of human IP-10 gene expression in astrocytoma cells by inflammatory cytokines. Journal of neuroscience research *54*, 169-180.

Majumder, S., Zhou, L.Z., and Ransohoff, R.M. (1996). Transcriptional regulation of chemokine gene expression in astrocytes. Journal of neuroscience research *45*, 758-769.

Mani, B., Baltzer, C., Valle, N., Almendral, J.M., Kempf, C., and Ros, C. (2006). Low pH-dependent endosomal processing of the incoming parvovirus minute virus of mice virion leads to externalization of the VP1 N-terminal sequence (N-VP1), N-VP2 cleavage, and uncoating of the full-length genome. Journal of virology *80*, 1015-1024.

Manusama, E.R., Nooijen, P.T., Stavast, J., Durante, N.M., Marquet, R.L., and Eggermont, A.M. (1996). Synergistic antitumour effect of recombinant human tumour necrosis factor alpha with melphalan in isolated limb perfusion in the rat. The British journal of surgery *83*, 551-555.

Markert, J.M., Medlock, M.D., Rabkin, S.D., Gillespie, G.Y., Todo, T., Hunter, W.D., Palmer, C.A., Feigenbaum, F., Tornatore, C., Tufaro, F.*, et al.* (2000). Conditionally replicating herpes simplex virus mutant, G207 for the treatment of malignant glioma: results of a phase I trial. Gene therapy *7*, 867-874.

Maroto, B., Valle, N., Saffrich, R., and Almendral, J.M. (2004). Nuclear export of the nonenveloped parvovirus virion is directed by an unordered protein signal exposed on the capsid surface. Journal of virology *78*, 10685-10694.

Matikainen, S., Pirhonen, J., Miettinen, M., Lehtonen, A., Govenius-Vintola, C., Sareneva, T., and Julkunen, I. (2000). Influenza A and sendai viruses induce differential chemokine gene expression and transcription factor activation in human macrophages. Virology *276*, 138-147.

Maxwell, I.H., Maxwell, F., Rhode, S.L., 3rd, Corsini, J., and Carlson, J.O. (1993). Recombinant LuIII autonomous parvovirus as a transient transducing vector for human cells. Human gene therapy *4*, 441-450.

Maxwell, I.H., Spitzer, A.L., Long, C.J., and Maxwell, F. (1996). Autonomous parvovirus transduction of a gene under control of tissue-specific or inducible promoters. Gene therapy *3*, 28-36.

Menten, P., Wuyts, A., and Van Damme, J. (2001). Monocyte chemotactic protein-3. European cytokine network *12*, 554-560.

Miller, C.L., and Pintel, D.J. (2002). Interaction between parvovirus NS2 protein and nuclear export factor Crm1 is important for viral egress from the nucleus of murine cells. Journal of virology *76*, 3257-3266.

Mocellin, S., and Nitti, D. (2008). TNF and cancer: the two sides of the coin. Front Biosci *13*, 2774-2783.

Mocellin, S., Rossi, C.R., Pilati, P., and Nitti, D. (2005). Tumor necrosis factor, cancer and anticancer therapy. Cytokine & growth factor reviews *16*, 35-53.

Muppidi, J.R., Tschopp, J., and Siegel, R.M. (2004). Life and death decisions: secondary complexes and lipid rafts in TNF receptor family signal transduction. Immunity *21*, 461-465.

Murphy, P.M. (2002). International Union of Pharmacology. XXX. Update on chemokine receptor nomenclature. Pharmacological reviews *54*, 227-229.

Naeger, L.K., Cater, J., and Pintel, D.J. (1990). The small nonstructural protein (NS2) of the parvovirus minute virus of mice is required for efficient DNA replication and infectious virus production in a cell-type-specific manner. Journal of virology *64*, 6166-6175.

Narvaiza, I., Mazzolini, G., Barajas, M., Duarte, M., Zaratiegui, M., Qian, C., Melero, I., and Prieto, J. (2000). Intratumoral coinjection of two adenoviruses, one encoding the chemokine IFN-gamma-inducible protein-10 and another encoding IL-12, results in marked antitumoral synergy. J Immunol *164*, 3112-3122.

Nathan, C., and Sporn, M. (1991). Cytokines in context. The Journal of cell biology *113*, 981-986.

Nuesch, J.P., Dettwiler, S., Corbau, R., and Rommelaere, J. (1998). Replicative functions of minute virus of mice NS1 protein are regulated in vitro by phosphorylation through protein kinase C. Journal of virology *72*, 9966-9977.

Ohmori, Y., and Hamilton, T.A. (1992). Ca2+ and calmodulin selectively regulate lipopolysaccharide-inducible cytokine mRNA expression in murine peritoneal macrophages. J Immunol *148*, 538-545.

REFERENCES

Ohmori, Y., and Hamilton, T.A. (1993). Cooperative interaction between interferon (IFN) stimulus response element and kappa B sequence motifs controls IFN gamma- and lipopolysaccharide-stimulated transcription from the murine IP-10 promoter. The Journal of biological chemistry *268*, 6677-6688.

Okada, H., and Pollack, I.F. (2004). Cytokine gene therapy for malignant glioma. Expert opinion on biological therapy *4*, 1609-1620.

Oppenheimer, J., and Feldmann, M. (2000). Cytokine reference. San Diego:Academic Press.

Palmer, G.A., and Tattersall, P. (2000). MVM-based vectors for transducing human and murine T cells. 8th Parvovirus Workshop, Mont-Tremblant, Canada, pp 70-1.

Papanastassiou, V., Rampling, R., Fraser, M., Petty, R., Hadley, D., Nicoll, J., Harland, J., Mabbs, R., and Brown, M. (2002). The potential for efficacy of the modified (ICP 34.5(-)) herpes simplex virus HSV1716 following intratumoural injection into human malignant glioma: a proof of principle study. Gene therapy *9*, 398-406.

Parker, J.S., Murphy, W.J., Wang, D., O'Brien, S.J., and Parrish, C.R. (2001). Canine and feline parvoviruses can use human or feline transferrin receptors to bind, enter, and infect cells. Journal of virology *75*, 3896-3902.

Paulukat, J., Bosmann, M., Nold, M., Garkisch, S., Kampfer, H., Frank, S., Raedle, J., Zeuzem, S., Pfeilschifter, J., and Muhl, H. (2001). Expression and release of IL-18 binding protein in response to IFN-gamma. J Immunol *167*, 7038-7043.

Penna, G., Sozzani, S., and Adorini, L. (2001). Cutting edge: selective usage of chemokine receptors by plasmacytoid dendritic cells. J Immunol *167*, 1862-1866.

Peroulis, I., Jonas, N., and Saleh, M. (2002). Antiangiogenic activity of endostatin inhibits C6 glioma growth. International journal of cancer *97*, 839-845.

Pestka, S., Krause, C.D., and Walter, M.R. (2004). Interferons, interferon-like cytokines, and their receptors. Immunol Rev *202*, 8-32.

Petry, H., Cashion, L., Szymanski, P., Ast, O., Orme, A., Gross, C., Bauzon, M., Brooks, A., Schaefer, C., Gibson, H.*, et al.* (2006). Mx1 and IP-10: biomarkers to measure IFN-beta activity in mice following gene-based delivery. J Interferon Cytokine Res *26*, 699-705.

Pintel, D., Dadachanji, D., Astell, C.R., and Ward, D.C. (1983). The genome of minute virus of mice, an autonomous parvovirus, encodes two overlapping transcription units. Nucleic acids research *11*, 1019-1038.

Platten, M., Kretz, A., Naumann, U., Aulwurm, S., Egashira, K., Isenmann, S., and Weller, M. (2003). Monocyte chemoattractant protein-1 increases microglial infiltration and aggressiveness of gliomas. Ann Neurol *54*, 388-392.

Platten, M., Wick, W., and Weller, M. (2001). Malignant glioma biology: role for TGF-beta in growth, motility, angiogenesis, and immune escape. Microscopy research and technique *52*, 401-410.

Polunovsky, V.A., Wendt, C.H., Ingbar, D.H., Peterson, M.S., and Bitterman, P.B. (1994). Induction of endothelial cell apoptosis by TNF alpha: modulation by inhibitors of protein synthesis. Experimental cell research *214*, 584-594.

Rampling, R., Cruickshank, G., Papanastassiou, V., Nicoll, J., Hadley, D., Brennan, D., Petty, R., MacLean, A., Harland, J., McKie, E.*, et al.* (2000). Toxicity evaluation of replication-competent herpes simplex virus (ICP 34.5 null mutant 1716) in patients with recurrent malignant glioma. Gene therapy *7*, 859-866.

Ransohoff, R.M., Hamilton, T.A., Tani, M., Stoler, M.H., Shick, H.E., Major, J.A., Estes, M.L., Thomas, D.M., and Tuohy, V.K. (1993). Astrocyte expression of mRNA encoding cytokines IP-10 and JE/MCP-1 in experimental autoimmune encephalomyelitis. Faseb J *7*, 592-600.

Rao, J.S. (2003). Molecular mechanisms of glioma invasiveness: the role of proteases. Nat Rev Cancer *3*, 489-501.

Rhode, S.L., 3rd (1985). trans-Activation of parvovirus P38 promoter by the 76K noncapsid protein. Journal of virology *55*, 886-889.

Roggendorf, W., Strupp, S., and Paulus, W. (1996). Distribution and characterization of microglia/macrophages in human brain tumors. Acta neuropathologica *92*, 288-293.

Rommelaere, J., and Cornelis, J.J. (1991). Antineoplastic activity of parvoviruses. Journal of virological methods *33*, 233-251.

Ros, C., Burckhardt, C.J., and Kempf, C. (2002). Cytoplasmic trafficking of minute virus of mice: low-pH requirement, routing to late endosomes, and proteasome interaction. Journal of virology *76*, 12634-12645.

Rossi, D., and Zlotnik, A. (2000). The biology of chemokines and their receptors. Annual review of immunology *18*, 217-242.

Rossi, M.L., Cruz-Sanchez, F., Hughes, J.T., Esiri, M.M., Coakham, H.B., and Moss, T.H. (1988). Mononuclear cell infiltrate and HLA-DR expression in low grade astrocytomas. An immunohistological study of 23 cases. Acta neuropathologica *76*, 281-286.

Russell, J.H., and Ley, T.J. (2002). Lymphocyte-mediated cytotoxicity. Annual review of immunology *20*, 323-370.

Russell, S.J., Brandenburger, A., Flemming, C.L., Collins, M.K., and Rommelaere, J. (1992). Transformation-dependent expression of interleukin genes delivered by a recombinant parvovirus. Journal of virology *66*, 2821-2828.

Sahli, R., McMaster, G.K., and Hirt, B. (1985). DNA sequence comparison between two tissue-specific variants of the autonomous parvovirus, minute virus of mice. Nucleic acids research *13*, 3617-3633.

Sallusto, F., Lenig, D., Mackay, C.R., and Lanzavecchia, A. (1998). Flexible programs of chemokine receptor expression on human polarized T helper 1 and 2 lymphocytes. The Journal of experimental medicine *187*, 875-883.

Salmaggi, A., Gelati, M., Dufour, A., Corsini, E., Pagano, S., Baccalini, R., Ferrero, E., Scabini, S., Silei, V., Ciusani, E.*, et al.* (2002). Expression and modulation of IFN-gamma-inducible chemokines (IP-10, Mig, and I-TAC) in human brain endothelium and astrocytes: possible relevance for the immune invasion of the central nervous system and the pathogenesis of multiple sclerosis. J Interferon Cytokine Res *22*, 631-640.

Salome, N., van Hille, B., Duponchel, N., Meneguzzi, G., Cuzin, F., Rommelaere, J., and Cornelis, J.J. (1990). Sensitization of transformed rat cells to parvovirus MVMp is restricted to specific oncogenes. Oncogene *5*, 123-130.

Sandmair, A.M., Loimas, S., Puranen, P., Immonen, A., Kossila, M., Puranen, M., Hurskainen, H., Tyynela, K., Turunen, M., Vanninen, R.*, et al.* (2000). Thymidine kinase gene therapy for human malignant glioma, using replication-deficient retroviruses or adenoviruses. Human gene therapy *11*, 2197-2205.

Sato, N., Fukuda, K., Nariuchi, H., and Sagara, N. (1987). Tumor necrosis factor inhibiting angiogenesis in vitro. Journal of the National Cancer Institute *79*, 1383-1391.

Schramm, C., Huber, S., Protschka, M., Czochra, P., Burg, J., Schmitt, E., Lohse, A.W., Galle, P.R., and Blessing, M. (2004). TGFbeta regulates the CD4+CD25+ T-cell pool and the expression of Foxp3 in vivo. International immunology *16*, 1241-1249.

Sedgwick, J.D., Schwender, S., Imrich, H., Dorries, R., Butcher, G.W., and ter Meulen, V. (1991). Isolation and direct characterization of resident microglial cells from the normal and inflamed central

nervous system. Proceedings of the National Academy of Sciences of the United States of America *88*, 7438-7442.

Segovia, J.C., Real, A., Bueren, J.A., and Almendral, J.M. (1991). In vitro myelosuppressive effects of the parvovirus minute virus of mice (MVMi) on hematopoietic stem and committed progenitor cells. Blood *77*, 980-988.

Seligman, A.M., and Shear, M.J. (1939). Studies in carcinogenesis. VIII. Experimental production of brain tumors in mice with methylcholanthrene. Am J Cancer *37*, 364–395.

Sgadari, C., Angiolillo, A.L., Cherney, B.W., Pike, S.E., Farber, J.M., Koniaris, L.G., Vanguri, P., Burd, P.R., Sheikh, N., Gupta, G.*, et al.* (1996). Interferon-inducible protein-10 identified as a mediator of tumor necrosis in vivo. Proceedings of the National Academy of Sciences of the United States of America *93*, 13791-13796.

Sheng, W.S., Hu, S., Ni, H.T., Rowen, T.N., Lokensgard, J.R., and Peterson, P.K. (2005). TNF-alpha-induced chemokine production and apoptosis in human neural precursor cells. Journal of leukocyte biology *78*, 1233-1241.

Siegl, G. (1984). Biology and pathogenesis of autonomous parvoviruses. in Berns KI (ed): The Parvoviruses New York, Plenum Press, 297-362.

Staba, M.J., Mauceri, H.J., Kufe, D.W., Hallahan, D.E., and Weichselbaum, R.R. (1998). Adenoviral TNF-alpha gene therapy and radiation damage tumor vasculature in a human malignant glioma xenograft. Gene therapy *5*, 293-300.

Stoll, G., and Jander, S. (1999). The role of microglia and macrophages in the pathophysiology of the CNS. Progress in neurobiology *58*, 233-247.

Strieter, R.M., Polverini, P.J., Kunkel, S.L., Arenberg, D.A., Burdick, M.D., Kasper, J., Dzuiba, J., Van Damme, J., Walz, A., Marriott, D.*, et al.* (1995). The functional role of the ELR motif in CXC chemokine-mediated angiogenesis. The Journal of biological chemistry *270*, 27348-27357.

Stupp, R., Mason, W.P., van den Bent, M.J., Weller, M., Fisher, B., Taphoorn, M.J., Belanger, K., Brandes, A.A., Marosi, C., Bogdahn, U.*, et al.* (2005a). Radiotherapy plus concomitant and adjuvant temozolomide for glioblastoma. The New England journal of medicine *352*, 987-996.

Stupp, R., Pavlidis, N., and Jelic, S. (2005b). ESMO Minimum Clinical Recommendations for diagnosis, treatment and follow-up of malignant glioma. Ann Oncol *16 Suppl 1*, i64-65.

Suikkanen, S., Saajarvi, K., Hirsimaki, J., Valilehto, O., Reunanen, H., Vihinen-Ranta, M., and Vuento, M. (2002). Role of recycling endosomes and lysosomes in dynein-dependent entry of canine parvovirus. Journal of virology *76*, 4401-4411.

Sun, Y., Finger, C., Alvarez-Vallina, L., Cichutek, K., and Buchholz, C.J. (2005). Chronic gene delivery of interferon-inducible protein 10 through replication-competent retrovirus vectors suppresses tumor growth. Cancer gene therapy *12*, 900-912.

Szatmari, T., Lumniczky, K., Desaknai, S., Trajcevski, S., Hidvegi, E.J., Hamada, H., and Safrany, G. (2006). Detailed characterization of the mouse glioma 261 tumor model for experimental glioblastoma therapy. Cancer science *97*, 546-553.

Takahashi, T., Tagami, T., Yamazaki, S., Uede, T., Shimizu, J., Sakaguchi, N., Mak, T.W., and Sakaguchi, S. (2000). Immunologic self-tolerance maintained by CD25(+)CD4(+) regulatory T cells constitutively expressing cytotoxic T lymphocyte-associated antigen 4. The Journal of experimental medicine *192*, 303-310.

Taub, D.D., Lloyd, A.R., Conlon, K., Wang, J.M., Ortaldo, J.R., Harada, A., Matsushima, K., Kelvin, D.J., and Oppenheim, J.J. (1993). Recombinant human interferon-inducible protein 10 is a chemoattractant for human monocytes and T lymphocytes and promotes T cell adhesion to endothelial cells. The Journal of experimental medicine *177*, 1809-1814.

Taub, D.D., Sayers, T.J., Carter, C.R., and Ortaldo, J.R. (1995). Alpha and beta chemokines induce NK cell migration and enhance NK-mediated cytolysis. J Immunol *155*, 3877-3888.

Thelen, M. (2001). Dancing to the tune of chemokines. Nature immunology *2*, 129-134.

Thomas, D.A., and Massague, J. (2005). TGF-beta directly targets cytotoxic T cell functions during tumor evasion of immune surveillance. Cancer cell *8*, 369-380.

Tominaga, M., Iwashita, Y., Ohta, M., Shibata, K., Ishio, T., Ohmori, N., Goto, T., Sato, S., and Kitano, S. (2007). Antitumor effects of the MIG and IP-10 genes transferred with poly [D,L-2,4-diaminobutyric acid] on murine neuroblastoma. Cancer gene therapy *14*, 696-705.

Toolan, H.W., Buttle, G.A.H., and Kay, H.E.M. (1962). Isolation of the H-1 and H-3 viruses directly from human embryos. Proc Am Assoc Cancer Res *3*, 368.

Toolan, H.W., Rhode, S.L., 3rd, and Gierthy, J.F. (1982). Inhibition of 7,12-dimethylbenz(a)anthracene-induced tumors in Syrian hamsters by prior infection with H-1 parvovirus. Cancer research *42*, 2552-2555.

Toolan, H.W., Saunders, E.L., Southam, C.M., Moore, A.E., and Levin, A.G. (1965). H-1 Virus Viremia in the Human. Proceedings of the Society for Experimental Biology and Medicine Society for Experimental Biology and Medicine (New York, NY *119*, 711-715.

Tran, T.T., Uhl, M., Ma, J.Y., Janssen, L., Sriram, V., Aulwurm, S., Kerr, I., Lam, A., Webb, H.K., Kapoun, A.M.*, et al.* (2007). Inhibiting TGF-beta signaling restores immune surveillance in the SMA-560 glioma model. Neuro-oncology *9*, 259-270.

Trevejo, J.M., Marino, M.W., Philpott, N., Josien, R., Richards, E.C., Elkon, K.B., and Falck-Pedersen, E. (2001). TNF-alpha -dependent maturation of local dendritic cells is critical for activating the adaptive immune response to virus infection. Proceedings of the National Academy of Sciences of the United States of America *98*, 12162-12167.

Tuettenberg, J., Friedel, C., and Vajkoczy, P. (2006). Angiogenesis in malignant glioma--a target for antitumor therapy? Critical reviews in oncology/hematology *59*, 181-193.

Tullis, G.E., Burger, L.R., and Pintel, D.J. (1993). The minor capsid protein VP1 of the autonomous parvovirus minute virus of mice is dispensable for encapsidation of progeny single-stranded DNA but is required for infectivity. Journal of virology *67*, 131-141.

Van Coillie, E., Van Damme, J., and Opdenakker, G. (1999). The MCP/eotaxin subfamily of CC chemokines. Cytokine & growth factor reviews *10*, 61-86.

Van Damme, J., Proost, P., Lenaerts, J.P., and Opdenakker, G. (1992). Structural and functional identification of two human, tumor-derived monocyte chemotactic proteins (MCP-2 and MCP-3) belonging to the chemokine family. The Journal of experimental medicine *176*, 59-65.

Van Horssen, R., Ten Hagen, T.L., and Eggermont, A.M. (2006). TNF-alpha in cancer treatment: molecular insights, antitumor effects, and clinical utility. The oncologist *11*, 397-408.

Vihinen-Ranta, M., Suikkanen, S., and Parrish, C.R. (2004). Pathways of cell infection by parvoviruses and adeno-associated viruses. Journal of virology *78*, 6709-6714.

Wajant, H., Pfizenmaier, K., and Scheurich, P. (2003). Tumor necrosis factor signaling. Cell death and differentiation *10*, 45-65.

Waterston, A., and Bower, M. (2004). TNF and cancer: good or bad? Cancer therapy *2*, 131-148.

Watters, J.J., Schartner, J.M., and Badie, B. (2005). Microglia function in brain tumors. Journal of neuroscience research *81*, 447-455.

Wetzel, K., Menten, P., Opdenakker, G., Van Damme, J., Grone, H.J., Giese, N., Vecchi, A., Sozzani, S., Cornelis, J.J., Rommelaere, J.*, et al.* (2001). Transduction of human MCP-3 by a parvoviral vector

induces leukocyte infiltration and reduces growth of human cervical carcinoma cell xenografts. The journal of gene medicine *3*, 326-337.

Wetzel, K., Struyf, S., Van Damme, J., Kayser, T., Vecchi, A., Sozzani, S., Rommelaere, J., Cornelis, J.J., and Dinsart, C. (2007). MCP-3 (CCL7) delivered by parvovirus MVMp reduces tumorigenicity of mouse melanoma cells through activation of T lymphocytes and NK cells. International journal of cancer *120*, 1364-1371.

Wilson, G.M., Jindal, H.K., Yeung, D.E., Chen, W., and Astell, C.R. (1991). Expression of minute virus of mice major nonstructural protein in insect cells: purification and identification of ATPase and helicase activities. Virology *185*, 90-98.

Wollmann, G., Tattersall, P., and van den Pol, A.N. (2005). Targeting human glioblastoma cells: comparison of nine viruses with oncolytic potential. Journal of virology *79*, 6005-6022.

Wrzesinski, C., Tesfay, L., Salome, N., Jauniaux, J.C., Rommelaere, J., Cornelis, J., and Dinsart, C. (2003). Chimeric and pseudotyped parvoviruses minimize the contamination of recombinant stocks with replication-competent viruses and identify a DNA sequence that restricts parvovirus H-1 in mouse cells. Journal of virology *77*, 3851-3858.

Xia, M.Q., Bacskai, B.J., Knowles, R.B., Qin, S.X., and Hyman, B.T. (2000). Expression of the chemokine receptor CXCR3 on neurons and the elevated expression of its ligand IP-10 in reactive astrocytes: in vitro ERK1/2 activation and role in Alzheimer's disease. Journal of neuroimmunology *108*, 227-235.

Yanagawa, Y., Iijima, N., Iwabuchi, K., and Onoe, K. (2002). Activation of extracellular signal-related kinase by TNF-alpha controls the maturation and function of murine dendritic cells. Journal of leukocyte biology *71*, 125-132.

Yang, J., Choi, I., Kim, S.D., Kim, E.S., Cho, B., Kim, J.Y., and Ahn, C. (2007). Molecular characterization of cDNA encoding porcine IP-10 and induction of porcine endothelial IP-10 in response to human TNF-alpha. Veterinary immunology and immunopathology *117*, 124-128.

Yanisch-Perron, C., Vieira, J., and Messing, J. (1985). Improved M13 phage cloning vectors and host strains: nucleotide sequences of the M13mp18 and pUC19 vectors. Gene *33*, 103-119.

Young, P.J., Jensen, K.T., Burger, L.R., Pintel, D.J., and Lorson, C.L. (2002). Minute virus of mice small nonstructural protein NS2 interacts and colocalizes with the Smn protein. Journal of virology *76*, 6364-6369.

Zadori, Z., Szelei, J., Lacoste, M.C., Li, Y., Gariepy, S., Raymond, P., Allaire, M., Nabi, I.R., and Tijssen, P. (2001). A viral phospholipase A2 is required for parvovirus infectivity. Developmental cell *1*, 291-302.

Zadori, Z., Szelei, J., and Tijssen, P. (2005). SAT: a late NS protein of porcine parvovirus. Journal of virology *79*, 13129-13138.

Zagzag, D., Amirnovin, R., Greco, M.A., Yee, H., Holash, J., Wiegand, S.J., Zabski, S., Yancopoulos, G.D., and Grumet, M. (2000). Vascular apoptosis and involution in gliomas precede neovascularization: a novel concept for glioma growth and angiogenesis. Lab Invest *80*, 837-849.

Zlotnik, A., and Yoshie, O. (2000). Chemokines: a new classification system and their role in immunity. Immunity *12*, 121-127.

Zlotnik, A., Yoshie, O., and Nomiyama, H. (2006). The chemokine and chemokine receptor superfamilies and their molecular evolution. Genome biology *7*, 243.

Zolotukhin, S., Byrne, B.J., Mason, E., Zolotukhin, I., Potter, M., Chesnut, K., Summerford, C., Samulski, R.J., and Muzyczka, N. (1999). Recombinant adeno-associated virus purification using novel methods improves infectious titer and yield. Gene therapy *6*, 973-985.

7. LIST OF FIGURES AND TABLES

7.1. List of figures

7.2. List of tables

8. LIST OF ABBREVIATIONS

8.1. Terms

Amp	ampicillin
ATPase	adenosine triphosphatase
BBB	blood brain barrier
BSA	bovine serum albumine
CD	cluster of differentiation
cDNA	complementary DNA
CNS	central nervous system
CO_2	carbone dioxyde
CMV	human cytomegalovirus
CMR1	chromosome region maintenance protein 1
DAB	diamino-benzidine
DC	dendritic cell
dCTP	Deoxycytidine triphosphate
DMEM	Dulbecco's modified Eagle medium
DMEMc	DMEM complete
DMSO	dimethyl sulfoxide
DNA	deoxyribonucleic acid
Dnase	deoxyribonuclease
dNTP	deoxynucleotide triphosphate
DPBS	Dulbecco phosphate buffered saline
ds DNA	double stranded DNA
DTT	dithiothreitol
E. Coli	*Escherichia Coli*
EDTA	ethylenediaminetetraacetic acid
EGF	epidermal growth factor
ELISA	enzyme linked immunosorbent assay
ER	endoplasmic reticulum
FACS	fluorescence-activated cell sorting
FBS	fetal bovine serum
FGF	fibroblast growth factor
GAPDH	glyceraldehyde-3-phosphate dehydrogenase
GBM	glioblastoma multiforme
h	human
HBSS	Hanks' balanced salt solution
HRP	horseradish peroxidase
HSV	herpes simplex virus
i.c.	intracranial

IFN	interferon
Ig	immunoglobulin
IHC	immunohistochemistry
IL	interleukin
IP-10	interferon-γ inducible protein 10
JNK	Jun kinase
Kan	kanamycin
LB	Luria-Bertani
LPS	lipopolysaccharide
Luc	luciferase
m	mouse
MCP	monocyte chemotactic protein
M-MLV RT	Moloney murine leukemia virus reverse transcriptase
MCS	multiple cloning site
MEM	minimum essential medium Eagle
MEMc	MEM complete
MHC	major histocompatibility complex
MLEC	mink lung epithelial cells
MOI	multiplicity of infection
MPV-1	mouse parvovirus 1
MRI	magnetic resonance imaging
mRNA	messenger RNA
MVM	minute virus of mice
MVMi	MVM immunosuppressive strain
MVMp	MVM prototype strain
NF-κB	nuclear factor kappa B
NK	natural killer
NS	viral non-structural proteins
O/N	over night
OCT	optimum cutting temperature
ORF	open reading frame
^{32}P	Phosphorus 32
PBS	phosphate buffered saline
PAI	plasminogen activator inhibitor
PCR	polymerase chain reaction
PFA	paraformaldehyde
PFU	plaque forming unit
p.i.	post-infection
PLA$_2$	phospholipase A$_2$
PV	parvovirus
RCV	replication-dependent virus
RLU	relative light unit
RNA	ribonucleic acid
Rnase	ribonuclease
RT	room temperature
RT-PCR	reverse transcription-PCR

RU	replication unit
s.c.	subcutaneous
SAT	small alternatively translated protein
SD	standard deviation
SDS	sodium dodecyl sulfate
SEM	standard error of the mean
SMN	survival motor neuron protein
SSC	saline-sodium citrate
TAE	tris-acetate/EDTA
TAR	transactivating region
TE	tris-EDTA
Tet	tetracyclin
TGF	transforming growth factor
TK	thymidine kinase
TNF	tumor necrosis factor
TNFR	TNF receptor
TUNEL	terminal deoxynucleotidyl transferase biotin-dUTP nick end labeling
UV	ultraviolet
VEGF	vascular endothelial growth factor
VP	viral capsid proteins
V-TE	viral TE
v/v	volume per volume
w/v	weight per volume
wt	wild-type
WHO	world health organization
x	fold, times

8.2. Units

bp	base pair
°C	degree Celsius
Ci	Curie
cm	centimeter
CPM	counts per minute
g	gram
h	hours
kg	kilogram
l	liter
µ	micro
M	molar
m	milli
mm	millimeter
min	minute
n	nano

LIST OF ABBREVIATIONS

nt	nucleotide
p	pico
rpm	revolution per minute
s	second
V	volt
U	units